The Thesis Committee for Travis Evans Lowe
Certifies that this is the approved version of the following thesis:

An Investigative Study on Physical Sulfate Attack and Alkali-Silica Reaction Test Methods

APPROVED BY
SUPERVISING COMMITTEE:

Supervisor:

Kevin Folliard

Thano Drimalas

An Investigative Study on Physical Sulfate Attack and Alkali-Silica Reaction Test Methods

by

Travis Evans Lowe, B.S.C.E.

Thesis

Presented to the Faculty of the Graduate School of

The University of Texas at Austin

in Partial Fulfillment

of the Requirements

for the Degree of

Master of Science in Engineering

The University of Texas at Austin

May 2011

Dedication

To my grandmother: Jane Connell DiMambro,

And my parents: Candy Connell and Keith Lowe.

Without your love and support I would have never made it this far.

Acknowledgements

The work presented in this thesis would not have been possible without the help from the following individuals. The support given by each of these people is greatly appreciated.

I would first like to thank my supervisor, Dr. Kevin Folliard, for giving me the opportunity to be involved in these research projects. Thank you for providing me with this wonderful opportunity to attend graduate school. The experiences and skills I have learned at the Concrete Durability Center will prove useful for the rest of my life.

I want to acknowledge Dr. Thano Drimalas for being a mentor throughout my projects. Without your insight and guidance I would have been lost at times. Also, I am thankful for Dr. Mike Thomas and Dr. Kyle Riding's assistance and recommendations through the course of these projects.

I would like to express my appreciation for Dr. Maria Juenger. Without your kind heart, I would have never realized the opportunity for working in such an interesting field.

I would like to thank the staff of the Concrete Durability Center, Sherian Williams and Mike Rung. The daily tasks at the research lab could not have happened without the skill, experience, and patience of each of you.

Also, I would like to express my appreciation and thank all of my fellow graduate and undergraduate researchers. During these projects, Chris Clement, Evan Wehrle, Anthony Bentivegna, Philip Pesek, Alex Garde, and Brenden Adams helped me for countless hours above and beyond the call of duty as fellow researchers. Chris Clement and Evan Wehrle thank you allowing me to visit my family over the holidays. Without

your assistance on countless days, including Christmas Day, I would not have been able to take the much needed time off to visit with my family. Chris Clement thank you for being a peer mentor and help with guiding me into and through graduate school. I wouldn't have made it this far without you. I can't thank everyone enough for giving me a helping hand throughout my projects. Alex Garde and Mitchel Dornak thank you for being dedicated enough to help me take measurements at 6AM. Michelle Wilkinson and Karla Kruse thank you for your steady hands and elegant engraving for my exposure block tags. I am grateful for Andy Jasso, Mitchell Dornak, Alex Garde, Chris Clement, Evan Wehrle, and Brian Hanson for making mixing and demolding days far less difficult and time consuming. Also, I want to thank Dr. Jason Ideker, Anthony Bentivegna, Chris Clement, Eric Gianni, Katy Gustashaw, Dongyeop Han, Marc Rached, and Irvin Chen for guidance over the years I spent at the Concrete Durability Center. Finally, I am thankful for everyone for being a friend inside and outside of the lab.

To close, I want to thank my entire family, to whom I owe all of my success. Without your unwavering love and support, I would have never made it this far. Grammy, you have always been there to support me; thank you for being the best grandmother anyone could ask for. Mom, thank you for lifting me up when I was down and teaching me to enjoy life. Pop, you let me know if I ever need help to just call. Alice, thank you for being patient with me and for the professional advice I have received. Zach, thank you for being the older brother that is always there for me. Kevin, thank you for being patient with me when I was not the supportive older brother that I should have been.

May 3, 2011

Abstract

An Investigative Study on Physical Sulfate Attack and Alkali-Silica Reaction Test Methods

Travis Evans Lowe, M.S.E.

The University of Texas at Austin, 2011

Supervisor: Kevin J. Folliard

This thesis is unique in that it investigated two completely different forms of concrete deterioration: physical sulfate attack and the alkali-silica reaction (ASR). Research was undertaken to better understand physical sulfate attack in order to provide much needed guidance on how to prevent durable this form of deterioration. A testing regime was designed to evaluate and analyze different concrete mixtures with varying water to cementitious material ratios (w/cm), cement types (Type I and V), and use of supplementary cementing materials (SCMs) in accelerated laboratory exposure and outdoor exposure testing. The accelerated laboratory testing evaluated the performance of concrete cylinder segments fully submerged in 30% (by mass of solution) sodium sulfate solution exposed to a temperature and humidity cycle that would promote cycles of alternative conversion between anhydrous sodium sulfate (thenardite) and decahydrate

sodium sulfate (mirabilite). In the outdoor exposure site, two different sized concrete cylinders per mixture proportion were partially submerged in 5% (33,000 ppm) sodium sulfate solution and exposed to alternative wetting and drying conditions, along with, temperature fluctuations that would promote conversion between thenardite (Na_2SO_4) and mirabilite ($Na_2SO_4 \cdot 10H_2O$).

With regard to ASR test methods, it has been shown with past research that it is not possible to evaluate "job mixtures" or determine alkali thresholds using ASTM C 1293 (Concrete Prism Test) with evaluating aggregates and concrete mixture proportions for the susceptibility of ASR when testing job mixtures. The most commonly cited issue with the concrete prism test is excessive leaching of alkalis during the course of the test, which may not be a major issue when using the standard, high-alkali concrete mixtures as per ASTM C 1293 but is clearly an issue when testing lower-alkali concrete mixtures. For low-alkali mixtures, alkali leaching can reduce the internal alkali content below the threshold that triggers expansion for a given aggregate. A comprehensive study was initiated that evaluated various modifications to ASTM C 1293, with the intention of developing a testing regime better suited to testing "job mixes" and/or low-alkali concrete mixtures.

Table of Contents

List of Tables

List of Figures

Chapter 1: Introduction

1.1 BACKGROUND

The research described in this thesis is unique in that it involved two completely different forms of concrete deterioration: physical sulfate attack and the alkali-silica reaction (ASR). Research was undertaken to better understand physical sulfate attack in order to provide much needed guidance on durable concrete mixtures for this form of concrete deterioration. After the discovery of ASR by Stanton in the late 1930s, much research has been completed on the mechanisms of ASR. Also, test methods have been developed over the decades for predicting an aggregates level of reactivity; however, faults still lie in the evaluation of "job mixtures", especially low-alkali concrete mixtures.

Physical sulfate attack, which has been recently referred to as physical salt attack due to the attacking mechanism, has only been recently recognized as a concrete durability issue. In 2008, the American Concrete Institute (ACI) acknowledged this form of concrete deterioration by including it in the Chemical Attack chapter of the ACI 201 document, which is ACI's Guide to Durable Concrete. Insufficient research has been carried out to fully encompass the attacking mechanisms and subsequent concrete materials mixture proportions that will be durable to this aggressive form of attack on concrete. This research described herein investigated what the effects of materials and mixture proportions on physical sulfate attack, both in the laboratory and in the field.

ASR has been significantly researched but testing methods for evaluating an aggregate's level of reactivity have not advanced enough through prior research. Since Stanton developed the first method for evaluating an aggregate's reactivity level in 1940, many improvements and advancements in testing methods has occurred. However, all of

the testing methods have significant flaws in efficiency, practicality, and/or validity of accurately evaluating an aggregate and concrete mixture for ASR susceptibility. In particular, ASR test methods have deficiencies in evaluating an aggregate in low-alkali concrete mixtures. Currently, only field testing has been able to determine alkali thresholds above which ASR is a concern for a given aggregate. Currently, ASTM C1293 is the preferred accelerated laboratory test in the United States for evaluating an aggregate and concrete mixture for suppressing ASR. Research was initiated to investigate accelerated laboratory testing methods, in order to obtain failure in low-alkali concrete mixtures that have previously only had failure observed in the field.

Since the testing regimes associated with this study require more time, data presented will encompass measurements to date. The remaining measurements will continue and be available upon completion of testing.

1.2 RESEARCH OBJECTIVES

The following objectives were identified for the basis of these two different studies.

Physical sulfate attack objectives:

- Evaluate different concrete mixtures in accelerated laboratory testing.
- Correlate laboratory data of concrete mixtures to outdoor exposure testing.
- Ultimately, provide guidance on how to mitigate this newly recognized form of attack.

ASR testing methods objectives:

- Evaluate accelerated testing methods for better classifying low-alkali concrete mixtures' alkali-silica reactivity.
- Determine an accelerated laboratory testing method that will cause a low-alkali mixture that has been observed to fail in field exposure blocks but has previously passed the ASTM C1293's 0.04% expansion limit to reach this expansion limit criterion within one year.

1.3 OUTLINE OF THESIS

The remainder of this thesis is organized into the following chapters, with additional detailed information included as appendices:

- *Chapter 2* describes a comprehensive laboratory study on the resistance of concrete mixtures to physical sulfate attack.
- *Chapter 3* describes a study on the resistance of concrete mixtures to physical sulfate attack at the outdoor exposure site developed in Austin, TX.
- *Chapter 4* describes a study focusing on accelerated laboratory tests aimed at evaluating the resistance to alkali-silica reaction of low-alkali concrete mixtures.
- *Chapter 5* briefly summarizes the main conclusions from these three different studies to date, describes additional research in progress, and identifies additional research needs for future work.

Chapter 2: Laboratory Evaluations of Physical Sulfate Attack

2.1 INTRODUCTION

Physical sulfate attack (or salt hydration distress) involves phase changes of salt solution as temperature and relative humidity changes. The distress mechanism is caused by crystallization pressures of supersaturated salts in the pores at or near the evaporation surface of concrete (Scherer 2004). Sodium sulfate is the most common culprit. This physical attacking mechanism used to be characterized as chemical sulfate attack; however, chemical reactions are not involved in this physical distress mechanism (Stark 2002). Physical sulfate attack can happen in poor quality, porous concrete and occurrences have been documented in the field and by laboratory research (Stark 1984, 1989, 2002; O'Neill 1992; Folliard and Sandberg 1994; Haynes et al. 1996, 2008, 2010; Nehdi and Hayek 2005).

Research is needed to evaluate aspects of physical sulfate attack that are not fully understood. Currently, there are no standard test methods for evaluating a concrete mixture's resistance to physical sulfate attack. A testing regime was designed to evaluate and analyze key aspects of physical sulfate attack and to attempt to identify materials and mixture proportions that provide the highest level of protection against this form of attack. The laboratory evaluation of physical sulfate attack involved accelerated exposure testing in an environmental chamber. Also, a parallel evaluation of some of the same mixtures used in the laboratory testing was conducted through exposed outdoors to sodium sulfate will be presented in the next chapter. It was desired to develop a correlation between the laboratory and field performances of the different concrete mixture designs. This chapter presents the first phase of the study, which evaluated the

laboratory performance of concrete cylinder segments fully submerged in 30% (300,000 ppm) sodium sulfate solution and exposed to a temperature cycle that would promote alternate cycles of conversion between anhydrous sodium sulfate (thenardite) and decahydrate sodium sulfate (mirabilite). A discussion of results from this study will also be presented.

2.1.1 Research Significance

Further research is needed to fully understand the mechanisms underlying physical sulfate attack. The testing regime evaluated the resistance of various portland cement concretes, supplementary cementing materials (SCM), and mixture proportions to the physical attack caused by sodium sulfate (Na_2SO_4). When all phases are completed, it is anticipated that guidance will be developed on how best to produce durable concrete in severe sulfate exposure conditions.

2.1.2 Literature Review: Physical Sulfate Attack

The literature review herein pertains to this chapter, as well as, Chapter 3, which presents the field evaluation on physical sulfate attack. A detailed literature review related to sulfate attack was previously compiled by Drimalas (2007) and is not repeated herein. Possible damage related to sulfate attack includes: decreased alkalinity, expansion, increased porosity, softening of paste matrix, loss of binding capacity, paste microcracking, loss of engineering properties, spalling and delamination (Skalny et al. 2002). Sulfate attack can be classified as internal or external (based on source of sulfates) and chemical or physical (based on mechanisms of deterioration). Although these variants of sulfate attack are discussed separately, it is possible for concrete to suffer

from both internal and external sulfate attack, with both chemical and physical forms of distress.

2.1.2.1 Sulfate Attack

Sulfate attack can be caused by both internal and external sources of sulfates. For internal sulfate attack, sulfates in excessive quantity originate from the mix components. In example, sulfates can come from over sulfated cement, gypsum-contaminated aggregates, and high-sulfate fly ash. In addition, exposure to elevated temperature above 158°F (70°C) at early ages leads to DEF. For external sulfate attack, sulfate salts must be present in a solution to have the ability to ingress into the concrete specimen; soil and groundwater generally provides the means for sulfate salt ingress. Sulfates can also be found in seawater, pyritic soils and fill, sewer water, atmospheric pollution, industrial or agricultural waste waters, and mine drainage. Sulfates can concentrate in concrete due to moisture gradients or wetting and drying cycles.

In chemical sulfate attack, sulfates chemically react with the cement hydration products which can form ettringite, gypsum, and thaumasite (Skalny et al. 2002). This delayed formation of ettringite results in an increased volume of the hardened concrete as the ettringite crystals follow the Oswalt ripening process, in which, the ettringite crystals grow larger and larger at the expense of the smaller crystals. In addition, late formation of calcium sulfate (gypsum) causes loss in concrete strength from softening of the concrete matrix. More recently, sulfate attack has been defined to have both a chemical and physical mechanism of concrete deterioration. The American Concrete Institute's (ACI) Guide to Durable Concrete lists physical salt (sulfate) attack under the chapter on

chemical attack, however recent work has confirmed that it is a physical distress mechanism (ACI 201.2R 2001).

2.1.2.2 Mechanisms

The chemical mechanism of sulfate attack involves chemical changes resulting in calcium hydroxide consumption, excessive ettringite formation, gypsum formation, thaumasite formation, calcium silicate hydrate decomposition, decomposition of unhydated clinker, and formation of Mg-compounds (Skalny et al. 2002). In traditional chemical sulfate attack, chemical reactions involving the sulfate ion, SO_4^{2-}, and cement hydration products deleteriously alter the hydration products. First, tricalcium aluminates, C_3A, are attacked by the sulfate ions to form ettringite, $C_6A\bar{S}_3H_{32}$. Then, with the depletion of tricalcium aluminate hydration products, the sulfate ion attacks calcium hydroxide, CH, to form gypsum. Gypsum formation causes a loss of cohesion in concrete. Finally, the sulfate ions degrade calcium silicate hydrates, C-S-H, by decalcification, which is the basic binding product in concrete.

Over the years comprehensive tests have been performed to analyze causes and solutions to the chemical sulfate attack concrete durability problem. The ACI 201.2R-08 document, Guide to Durable Concrete (2008), recently recognized physical sulfate attack, which used to be classified as a form of chemical sulfate attack, as a newly emerging form of concrete deterioration; however, insufficient testing has been performed to evaluate the mechanisms and mitigation techniques of physical sulfate attack. In physical sulfate attack dissolved salt ions ingress through the concrete similar to chemical sulfate attack. Then, subsequent capillary rise of the salt ions from diffusion through the concrete matrix leads to an increased concentration at the exposed surface of the concrete (Haynes

et al. 1996). Evaporation from the exposed surface causes the salt ion concentrations to increase as more salt ions precipitate from the evaporating water molecules (Haynes et al. 1996). Recent work by Haynes found that as the relative humidity decreases, the height of the evaporation front also decreases (Haynes 2008). As the salt ions continue to build up in the concrete pores and the temperature cycles, the salt ions change phases, thus resulting in a volume change. Crystallization from a supersaturated thenardite (Na_2SO_4) solution to mirabilite ($Na_2SO_4 \cdot 10H_2O$) conversion is triggered by a temperature drop and/or relative humidity increase, resulting in the sodium sulfate ion absorbing ten water molecules and thus increasing by 314% in volume (Hime et al. 2001). With sufficient temperature cycles and as salt ion concentrations increase at the evaporation front, surface distress occurs similar to that of freeze-thaw scaling (Folliard and Sandberg 1994). A study by Nehdi and Hayek (2004) on concrete partially submerged in sodium sulfate solution showed that the sodium sulfate increased in concentration at the evaporation front right above the solution line. In addition, the study showed that sodium sulfate formed at higher levels on specimens when the relative humidity cycled between 32% to 95%, rather than a static relative humidity condition at 32% (Nehdi and Hayek 2004). Rodriguez-Navarro et al. (2000) also showed that cycling between thenardite and mirabilite caused the most aggressive environment. Chemical alterations of the hydrated cement products do not occur in the physical manifestation of sulfate attack distress. Recent work by Scherer (2004) provides proof that crystallization pressures can cause microcracking in the concrete matrix when pressures exceed the tensile strength. The crystallization pressures impose stresses on the pore walls and these pressures increase with decreasing pore size of the matrix (Scherer 2004). Also, Scherer found (2004) that supersaturation of salts in the pore solution causes higher crystallization pressures, thus

increasing the degree of supersaturation of salts near the evaporation front can lead to more damage.

2.1.2.3 Prevention

ACI 201.2R-08 recommends lowering the w/cm for improving concrete's resistance to external, chemical sulfate attack by reducing the ingress and movement of water in concrete. It is also recommended that the C_3A content of the portland cement be reduced and that supplementary cementing materials be used to provide for increased chemical resistance to sulfate attack. Table 1 highlights the guidance provided in the ACI 318-08 building code with regard to external, chemical sulfate. In ACI 201.2R-08, the degree of sulfate protection is determined by the severity of potential exposure. Guidelines are given for w/cm by mass of 0.50, 0.45, or 0.40 and cementitious material requirements of Type II, Type V, or Type V plus a pozzolan or slag as the severity of potential exposure increases, respectively (2001). The recommended proportion of fly ash is between 20 to 35% by mass of total cementitious material and the recommended proportion of slag is between 40 to 70% by mass of total cementitious material (2001). To determine the classification of sulfate exposure, it is ncessary to first analyze the given environment's water and/or soil. Analyzing the sulfate content in soil can be complicated and controversial due to extraction ratios, which are based on a mass of water to mass of soil in the ASTM standard.

Table 1: Additional Requirements as Determined by ACI 318-08

Exposure Class	Max. *w/cm**	Min. f'_c, psi	Cementitious materials†—types			Calcium chloride admixture
			ASTM C150	ASTM C595	ASTM C1157	
S0	N/A	2500	No Type restriction	No Type restriction	No Type restriction	No restriction
S1	0.50	4000	II‡	IP(MS), IS (<70) (MS)	MS	No restriction
S2	0.45	4500	V§	IP (HS) IS (<70) (HS)	HS	Not permitted
S3	0.45	4500	V + pozzolan or slag‖	IP (HS) + pozzolan or slag‖ or IS (<70) (HS) + pozzolan or slag‖	HS + pozzolan or slag‖	Not permitted

The mechanism of physical sulfate attack is not fully understood. Traditionally, Type V sulfate-resisting cement is required for environments that have higher tendency of potential exposure. Recent work performed by Folliard and Drimalas (unpublished) has shown that Type V cement does not provide protection against physical sulfate attack as it is essentially a chemical solution to a physical problem. Also, research by both Haynes (1996) and Stark (2002) supports the notion that a sulfate-resisting cement does not alleviate the physical mechanism of sulfate distress. There are no current guidelines for recognizing, mitigating, and preventing this form of attack on concrete. However, preliminary ACI guidelines for physical sulfate attack recommend a low w/cm along with a pozzolan to improve durability by reducing the concrete's permeability to retard the ingress of the sulfate salts. Higher concrete permeability allows sulfates to wick to the exposed surface of the concrete, which leads to higher concentrations near the surface and subsequent spalling of the concrete. Minimizing the salt ingress can be effective in controlling both physical and chemical sulfate attack. Recent work in the Middle East suggests that capillary absorption may be more important than permeability as absorption

may have a larger impact on wicking action and salt crystallization. Given the above discussions, there is clearly a need to better understand the mechanisms of physical sulfate attack and to develop guidance for practitioners on how to avoid physical sulfate attack.

2.1.2.4 Test Methods and Specifications

The most common test method for determining the sulfate resistance of a cementitious system is ASTM C1012, which evaluates the performance of mortar exposed to a sodium sulfate solution. However, there are no standardized tests for physical sulfate attack.

2.1.2.5 Field Studies

A long-term field and laboratory test program at the PCA's sodium sulfate soils test facility in Sacramento, California has provided evidence of the physical deterioration process of salt crystallization by repeated wetting and drying cycles in sodium sulfate solution. The field exposure site subjected concrete specimens to alternative wetting and drying cycles in a 6.5% (65,000 ppm) sulfate concentration for up to 16 years (Stark 2002). Companion specimens were fully submerged in the same solution in a static laboratory environment. Stark (2002) reported that only field specimens deteriorated and concluded that the w/cm and its subsequent permeability were the primary factors governing the durability of the specimens in the outdoor exposure conditions. Lowering the w/cm improved the performance of the specimens (Stark 2002). In addition, Stark (2002) established that cement composition had little importance to the specimen's

performance in the cyclical exposure. The field study used ASTM Type I, Type II, and Type V portland cements in the PCA testing regime.

Drimalas (2007) and Clement (2009) evaluated various concentrations of sodium sulfate, magnesium sulfate, and calcium sulfate in an exposure site at the Concrete Durability Center (CDC) at the University of Texas at Austin. The research showed that sodium sulfate was the most aggressive of the salt solutions tested. Drimalas (2007) evaluated 30 concrete mixtures in S3 exposure of sodium sulfate in Phase I of an external sulfate attack study, which is the most severe class listed in Table 2 from ACI 318-08. Drimalas (2007) used a 0.40 and 0.70 w/cm. In Phase II of this study, Clement (2009) simulated ACI 318-08's S1 and S2 exposure classifications, which also incorporated a w/cm of 0.45 and 0.50 in addition to the previous w/cm used by Drimalas (2007). Both phases of the external sulfate attack study used concrete prisms with dimensions of 3 in x 3 in x 11.25 in (75 mm x 75 mm x 285 mm) exposed in an outdoor sulfate exposure site in Austin, TX. Expansion measurements and mass loss were recorded over the life of these studies and continues to date. Each mixture contained two completely submerged samples and three vertically stored samples with 6 in (150 mm) of the prism submerged in the sulfate-bearing soil (Clement 2009). Clement (2009) also stored three more concrete prisms in a static modified ASTM C1012 storage condition in the same concentration of sodium sulfate as the outdoor exposure. Drimalas (2007) and Clement's (2009) prior research concluded that:

- The rate of distress to the prisms increased with increasing w/cm.
- Concrete prisms in S3 conditions expanded more than concrete prisms exposed to S1 and S2 conditions.
- Concrete prisms experienced increased damage above the soil line due to physical sulfate attack rather than because of external sulfate attack below the soil line.

- The concrete prisms in sodium sulfate generally performed worse in the majority of the testing, including laboratory and field conditions.
- Sodium sulfate was the most aggressive of the solutions tested.

Concrete prisms constructed with Type V cement at a 0.40 w/cm in a ternary blend of Class C fly ash and silica fume or having used Class F fly ash performed superior.

Table 2: Sulfate Exposure Classification as Determined by ACI 318-08

Category	Severity	Class	Condition	
			Water-soluble sulfate (SO_4) in soil, percent by weight	Dissolved sulfate (SO_4) in water, ppm
S Sulfate	Not applicable	S0	$SO_4 < 0.10$	$SO_4 < 150$
	Moderate	S1	$0.10 \leq SO_4 < 0.20$	$150 \leq SO_4 < 1500$ Seawater
	Severe	S2	$0.20 \leq SO_4 \leq 2.00$	$1500 \leq SO_4 \leq 10,000$
	Very severe	S3	$SO_4 > 2.00$	$SO_4 > 10,000$

2.1.2.6 Research Needs

The topic of physical sulfate attack is still misunderstood. Research is still needed to understand basic mechanisms of physical sulfate attack and to provide more sound technical guidance on achieving sulfate resistance in field applications. Some of the research needs include the following:

- Guidance on how to ensure long-term durability with regard to the physical sulfate attack mechanism.
- Evaluation of Type I versus Type V cement to the physical sulfate distress mechanisms.
- Role of SCMs in refining the pore structure of concrete and the subsequent effects of permeability and absorption in sulfate-rich environments.

- Evaluation of ACI 201 sulfate resistance guidelines in concern with the physical distress mechanism.

To address these technical objectives, concrete mixtures were cast with varying w/cm ratios, portland cement types, and SCMs to evaluate the resistance to physical attack caused by sodium sulfate, both in the laboratory and in the aforementioned outdoor exposure site, as described next.

2.2 EXPERIMENTAL METHODS

2.2.1 Materials

Two portland cements were used in this study, a Type I and a Type V cement, as per ASTM C150. The coarse aggregate selected was an ASTM C33 No. 57 gradation dolomitic limestone from Georgetown, TX, USA and the fine aggregate selected was natural siliceous river sand from Austin, Texas, USA. The fine aggregate was procured from a sand and gravel pit located along the Colorado River. The coarse aggregate is considered to be non-reactive, while the fine aggregate is a low reactive aggregate. The pertinent aggregate properties are shown in Table 3. Six concrete mixtures that included SCM blends were used in the mix matrix. The SCM blends included a Grade 120 slag (meeting ASTM C1240), a Class C fly ash, and a Class F fly ash (as per ASTM C618). Table 4 contains the chemical composition (oxide analysis) of the two cements used, whereas Table 5 contains the chemical composition of the SCMs.

Table 3: Aggregate Properties

Aggregate	Bulk SG (OD)	Bulk SG (SSD)	Apparent SG	Absorption (%)	Mineralogy
C1	2.47	2.55	2.67	3.21	dolomitic limestone
F1	2.57	-	-	0.93	siliceous sand

Table 4: Cement Chemical Composition

Chemical Composition	Cement	
	Type I	Type V
SiO_2, %	19.87	20.55
Al_2O_3, %	5.53	4.19
Fe_2O_3, %	2.52	5.32
Sum of SiO_2, Al_2O_3, Fe_2O_3, %	27.92	30.06
CaO, %	63.21	63.36
MgO, %	1.19	0.83
SO_3, %	3.4	3.81
Na_2O, %	0.128	0.32
K_2O, %	0.97	-
Na_2O Eq., %	0.77	-
LOI, %	-	-
Free CaO, %	-	-
C_3S, %*	55.91	-
C_2S, %*	14.77	-
C_3A, %*	10.39	2.11
C_4AF, %*	7.66	-

Table 5: SCM's Chemical Composition

Chemical Composition	Fly Ashes		Other SCMs
	Class F	Class C	Slag
SiO_2, %	52.07	30.76	35.91
Al_2O_3, %	23.65	17.75	11.98
Fe_2O_3, %	4.55	5.98	0.94
Sum of SiO_2, Al_2O_3, Fe_2O_3, %	80.27	54.49	48.83
CaO, %	12.76	28.98	44.1
MgO, %	2.02	6.55	8.9
SO_3, %	0.78	3.64	1.63
Na_2O, %	0.31	2.15	-
K_2O, %	0.80	0.30	-
Na_2O Eq., %	0.84	2.35	0.58
LOI, %	0.95	0.44	-

The mix matrix consisted of 27 concrete mixtures with varying w/cm, cement types, and SCMs. Table 6 and 7 show the mixture proportions used in this study. Since ACI 201.2R-08 recommends a w/cm of 0.40 to 0.50 for sulfate environments, three water to cementitious materials ratios were selected in that range for the mix matrix: 0.40, 0.45, 0.50 w/cm. The mixture proportions were calculated using a typical seven sack cement proportion. Each mixture was proportioned with 658 $^{lb}/_{yd^3}$ (390 $^{kg}/_{m3}$) of cementitious materials. ACI 201.2R-08 has guidelines for cement content replacement by mass with SCMs for sulfate-resisting enhancement. It is recommended that either a fly ash proportion between 25% and 35% by mass or a slag proportion between 40% and 70% by mass be used in the mixture proportions. Based on these criteria, three SCMs were selected to improve the durability of the concrete: Class F fly ash, Class C fly ash, and Grade 120 slag. Each type of SCM had a low and high percentage replacement by cementitious mass in the testing regime. The two Class F ash mixtures were tested at a

20% and 30% replacement of the cement by mass with a specific gravity of 2.34; whereas the Class C fly ash mixtures were tested at 20% and 40% replacement of the cement by mass with a specific gravity of 2.62. The Grade 120 slag mixtures were tested at a 35% and 50% replacement of the cement by mass with a specific gravity of 2.87. These SCMs' percentage cement replacement by mass values are typical dosages in the field. A polycarboxylate-based high-range water reducer was added to mixtures as needed to obtain a two to four inch slump. Normal dosages for the admixture range from 3 to $10^{oz}/_{cwt}$ (195 to 650 $^{ml}/_{100kg}$).

Table 6: w/cm Mixture Proportions

Material	Weight, lb. (kg)		
w/c	0.40	0.45	0.50
Water	263.2 (119.4)	296.1 (134.3)	329 (149.2)
Cement	658 (298.5)	658 (298.5)	658 (298.5)
Coarse Aggregate	1790.2 (812.0)	1790.2 (812.0)	1790.2 (812.0)
Fine Aggregate	1098.38 (498.2)	1098.38 (498.2)	1098.38 (498.2)

Table 7: SCM Mixture Proportions

Ternary Blend Description	Cement, $^{lb}/_{yd^3}$ (kg/m^3)	SCMs, $^{lb}/_{yd^3}$ (kg/m^3)
20 % Welsh	526.4 (312)	131.6 (78.1)
40 % Welsh	394.8 (234)	263.2 (156)
20% Rockdale	526.4 (312)	131.6 (78.1)
30% Rockdale	460.6 (273)	197.4 (117)
35% Slag	427.7 (254)	230.3 (137)
50% Slag	329 (195)	329 (195)

2.2.1.1 Nomenclature

Given the robust mixture matrix, a labeling system was designed to simplify presentation of the data. The labeling system has three components: w/cm, cement type, and percentage of SCM replacement by mass, if any. This labeling system is presented in Table 8. For example, 0.50 - V – 30F has a w/cm of 0.50 with Type V cement that has a 30% Class F fly ash replacement by mass, calculated as percentage by mass of the total cementitious material.

Table 8: Label System for Mixture Proportions

		w/cm		
		0.40	0.45	0.50
Type I Cement	control	0.40 - I	0.45 - I	0.50 - I
	20% C fly ash	0.40 - I – 20C	0.45- I – 20C	0.50 - I – 20C
	40% C fly ash	0.40 - I – 40C	0.45 - I – 40C	0.50 - I – 40C
	20% F fly ash	0.40 - I – 20F	0.45 - I – 20F	0.50 - I – 20F
	30% F fly ash	0.40 - I – 30F	0.45 - I – 30F	0.50 - I – 30F
	35% slag	0.40 - I - 35S	0.45 - I - 35S	0.50 - I - 35S
	50% slag	0.40 - I - 50S	0.45 - I - 50S	0.50 - I - 50S
Type V Cement	control	0.40 - V	0.45 - V	0.50 - V
	20% C fly ash	-	-	-
	40% C fly ash	-	-	0.50 - V – 40C
	20% F fly ash	-	-	-
	30% F fly ash	-	-	0.50 - V – 30F
	35% slag	-	-	-
	50% slag	-	-	0.50 - V - 50S

2.2.2 Test Procedure

2.2.2.1 Specimen Procedure

All the concrete test specimens were batched, mixed, and cast at the Concrete Durability Center of the University of Texas at Austin. A revised mixture procedure, based on ASTM C192, was used for mixing the concrete. All of the materials for the concrete mixtures were placed in the mixing room at least 24 hours before mixing to ensure that all the materials reached equilibrium with the temperature of the room. The mixing room is kept at 73 ±3 °F (23 ±1.67 °C). First, the aggregates were blended in a steel drum concrete mixer, and then the first half of the mixing water was added and mixed for 30 seconds. Next, the cementitious materials were added and blended for 30 seconds before the second half of the mixing water was added. The second half of the mixing water was poured in the mixer over a 30 second time period, at the end of which is the starting time for the age of the concrete specimens. The cementitious material was mixed for a total of two minutes, including the 30 seconds of mixing water addition, after which the concrete mixture was allowed to rest for 3 minutes before it was mixed again for 2 minutes. When needed, superplasticizer was added to the fresh concrete mixture to obtain a two to four inch. Usually, any incorporation of SCMs required a minimum dosage of the superplasticizer. Then, the fresh concrete was poured into wheel barrels for casting specimens. The slump of the mixtures was measured following ASTM C143 and the corresponding unit weight was calculated using ASTM C138.

Next, 4 in x 8 in (100 mm x 200 mm) cylinder specimens were cast in two equal volume lifts with at least 25 steel roddings after each lift for consolidation, according to ASTM C192. The concrete was placed in the plastic cylinder molds using a scoop and the cylinders were tapped with a steel rod 12 to 16 times before consolidation to remove any

entrapped air. The second rodding went to a depth of at least a third into the previous lift layer. The concrete cylinders were tapped by the rubber mallet after both lifts and consolidations. After all the cylinders had been cast for the mix, the excess concrete was removed from the top of the cylinders with a wooden trowel and allowed to bleed during setting. Depending on the concrete mixtures, the concrete cylinders were allowed to set for 30 to 60 minutes before being finished first with a wooden trowel, and then with a magnesium float. Next, the freshly made concrete was capped with plastic lids to minimize water loss. Also, concrete cylinders were covered with wet burlap to further ensure adequate curing. Curing was executed on the mix matrix as specified in ASTM C192.

After casting, specimens were demolded at 24 ± 1 hour and placed in a moist-curing room at 73 ºF (23 ºC) and 100% relative humidity that meets ASTM C192 specifications for a curing environment. The 4 in x 8 in (100 mm x 200 mm) cylinder specimens were demolded with air pressure, which resulted in minor surface defects at the base of some of the specimens. Due to a shortage of plastic cylinder molds for the robust amount of specimens that were cast; the cylinder molds were re-used for this project. In order to re-use the plastic cylinder molds a hole was drilled in the bottom of the molds, so that air pressure could be used to pop off the molds from the concrete cylinders. Before casting the cylinders, painter's tape was placed in the bottom of the plastic cylinder molds to eliminate cement paste bleeding through the hole. The tape was placed on the exterior and interior of the cylinder molds. The cylinders were moist-cured for 28 days before testing began.

Five 4 in x 8 in (100 mm x 200 mm) cylinders were cast for each of the 27 concrete mixtures, along with $11^1/_2$ in x $14^1/_2$ in (300 mm x 375 mm) tapered cylinders for 14 of the concrete mixtures, including: 0.40-I-20C, 0.40-I-40C, 0.4-I-20F, 0.40-I-30F,

0.40-I-35S, 0.40-I-50S, 0.50-I, 0.50-I-40C, 0.50-I-30F, 0.50-I-50S, 0.5-V, 0.50-V-40C, 0.50-V-30F, and 0.50-V-50S. The $11^1/_2$ in x $14^1/_2$ in (300 mm x 375 mm) tapered cylinders were cast in five gallon pails and are discussed in Chapter 3 since they pertain to the field testing. Two 4 in x 8 in (100 mm x 200 mm) cylinders from each type of mixture were cut into three segments. Cuts were made horizontally to the specimens to make one 3.0 ±0.125 in (75 ±3 mm) and two 2.375 ±0.125 in (60 ±3 mm) segments. Hydraulic fluid and water were used as the cutting medium, so all the cylinder cut segments were cleaned with tap water after the cutting process. The 3.0 ±0.125 in (75 ±3 mm) segment contains the finished surface of the 4 in x 8 in (100 mm x 200 mm) cylinder. The 4 in x 8 in (100 mm x 200 mm) cylinder cuts are shown in Figure 1.

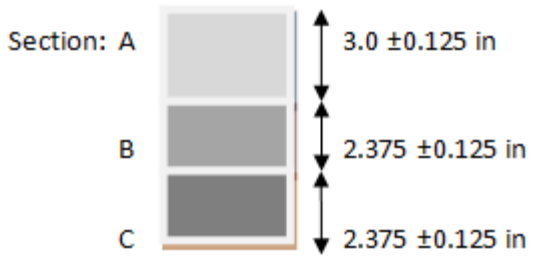

Figure 1: 4 in x 8 in Cylinder Section Cuts

The 27 different concrete mixtures were tested following the described procedure below. The bottom two pairs, Section B and C, of the 2.375 ±0.125 in (60 ±3 mm) high segments of the cut 4 in x 8 in (100 mm x 200 mm) cylinders were both placed in two plastic containers. In other words, each mixture had two plastic containers that each contained both a Section B and C cut cylinder segment. Figure 2 shows two segments in one of the plastic containers. The two containers per mixture proportion were filled with 30% (by mass of solution) sodium sulfate solution and sealed with plastic lids to limit

evaporation. The specimens were fully submerged in the solution. The pair of containers from each mix were separated into an environmental chamber for cyclical testing and the other container stored at ambient conditions for static testing. The containers for cyclical testing were stored in a Tenney Twenty environmental test chamber that cycled the temperature from 41 to 104°F (5 to 40°C). These temperatures were selected for cycling according to the sodium sulfate solubility curve to ensure the formation of mirabilite and thenardite by the sodium sulfate (Folliard and Sandberg 1994). Sodium sulfate's solubility curve is presented in Figure 3. The static testing containers were stored indoors in ambient environmental conditions at 73 ±3°F (23 ±1.67 °C) to help evaluate the potential for chemical sulfate attack on the concrete mixtures.

Figure 2: Concrete Cylinder Segment in Plastic Storage Container

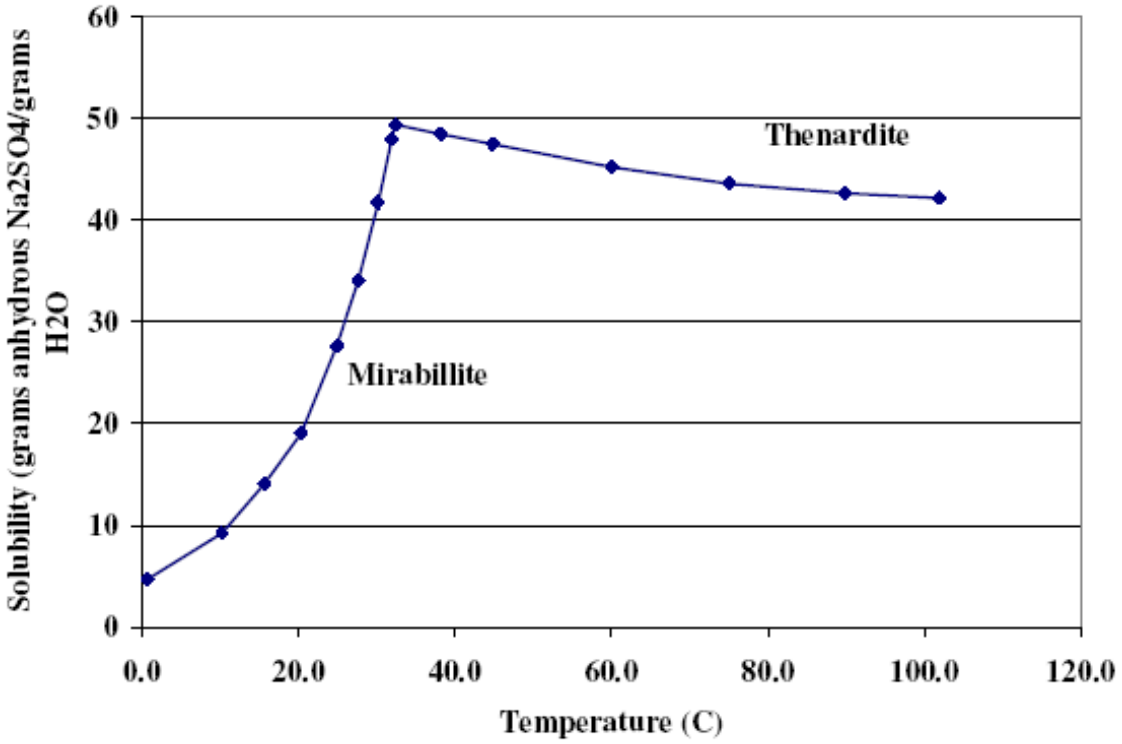

Figure 3: Solubility Curve of Sodium Sulfate (Drimalas 2007)

(Note: °F = 1.8°C + 32)

In addition to the plastic containers with 30% (by mass of solution) sodium sulfate, a Section A, the top section of the cut 4 in x 8 in (100 mm x 200 mm) cylinders for each mixture proportion was also placed fully submerged in deionized water for controls in the mix matrix. These containers containing the one 4 in x 8 in (100 mm x 200 mm) cylinder section and the deionized water were also placed in the environmental chamber with the 30% (by mass of solution) sodium sulfate containers for cyclical testing.

The temperature cycle in the environmental chamber had two phases. In Phase I a temperature cycle was selected according to Folliard and Sandberg's (1994) previous research. Then, due to insufficient sodium sulfate solubility at the peak of the temperature

cycle a new cycling program was used that included an additional two hour hold at the peak of the temperature cycle. These two temperature cycles are presented in Figures 4 and 5. Phase I lasted for 215 or 235 amount of cycles depending on the concrete mixture's testing start date and phase II was 310 cycles long.

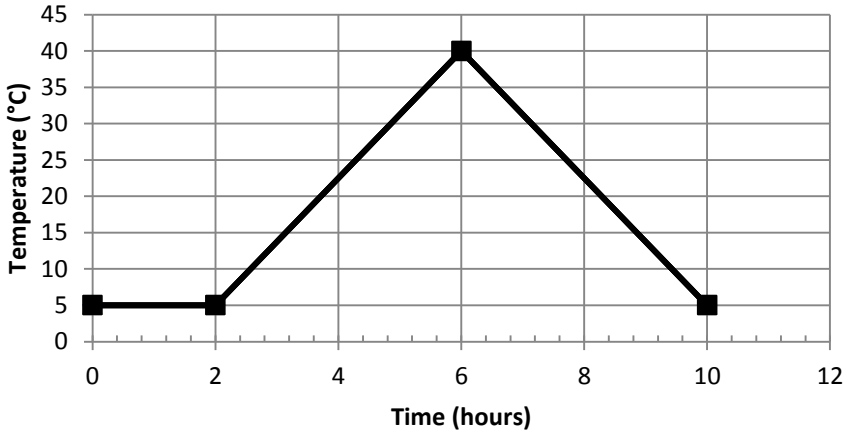

Figure 4: Phase I Environmental Chamber Cycle

(Note: °F = 1.8°C + 32)

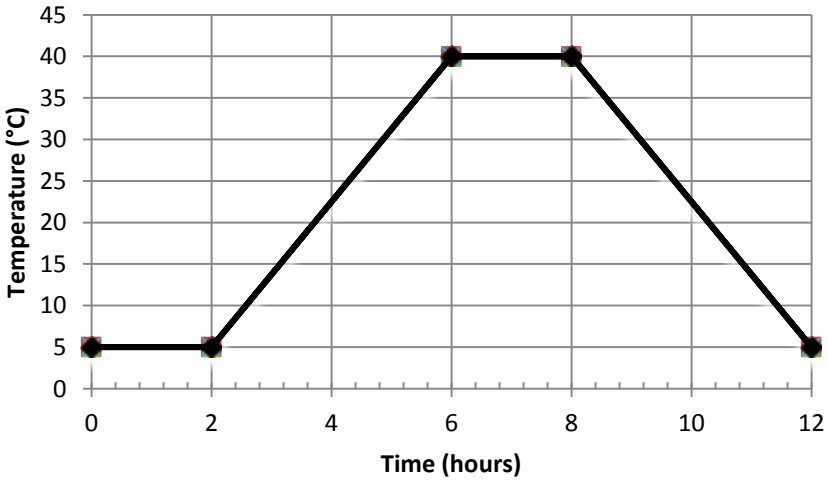

Figure 5: Phase II Environmental Chamber Cycle

(Note: °F = 1.8°C + 32)

The mass of the specimens was measured to obtain the mass gain or loss for each specimen in the testing regime. For measuring the specimens, all the containers (water and sodium sulfate) were removed from the environmental chamber at 68 to 77°F (20 to 25°C) on the temperature down cycle. Also, all the static testing containers were removed from the static storage area. The cycle upon removal for measurements is included in the total number of cycles to date, since the specimens have enough time to complete the sodium sulfate phase change. All samples in the deionized water were measured first to prevent cross contamination; however, the scale was cleaned with alcohol between the types of measurements. The static and cyclical specimens were measured in rounds where all the specimens from the given exposure condition are measured before the other environmental condition was measured. Then, groups of the sodium sulfate samples, from either the static or cyclical conditions, were removed from the containers and placed on paper towels to dry. In addition, both ends and the sides of the specimens were dried off with paper towels. Crystals, scaling cement paste, and loose aggregates were removed from the surface of the specimens. The samples generally contained crystals in the exterior pores. Samples were dried and measured in order of removal from solution starting with the first one removed. Each round of specimen measurements had generally 9 to 10 specimen containers and the specimens remained out of the solution for approximately 20 minutes. After measuring, but before the specimens were placed back into the solution, any sodium sulfate crystals in the solution were broken up by hand. All the specimens were returned to the containers in the opposite orientation from the previous measurement. In other words, the specimens were placed in the opposite orientation as the previous testing duration, either right-side up or upside down. Deionized water or 30% (by mass of solution) sodium sulfate per specimen group was added to the containers as needed to obtain a solution level over the specimens. All the

samples were randomized in sampling order and in placement in the given storage condition to ensure minimal bias in testing. Both in the static and the cyclical specimen containers the solution evaporates during storage, thus leaving the solution level in the containers slightly below the top of the specimens by the next measuring time. At various measurement periods, photographs were taken of the pairs of static and cyclical sodium sulfate specimens to document the deterioration of each mixture proportion throughout the test. These specimens per mixture proportion were compared to the same control cylinder segment for all the photographs. The Section B cylinder segment was always placed to the left and the Section C cylinder segment was always placed to the right of the control cylinder segment for the photographs.

2.2.2.2 XRD Procedure

In order to break and remove concrete for the X-ray diffraction (XRD) analysis, the specimens were placed in a plastic bag and mechanically broken with a hammer. Then, the collected samples were crushed with a mortar and pestle to pass through a #325 sieve (45 microns). Once the sample passed through the sieve, it was placed into vials and stored under vacuum in a desiccator until tested. The samples were first unsealed in the desiccator for approximately one week to ensure all the moisture was removed before the containers were sealed and left in the desiccator for storage.

A Siemens D500 diffractometer with a front loading sample holder was used to scan each sample from 5° to 65° 2θs. An internal standard was not placed within each sample, thus only a semi-quantitative analysis was used to determine the phases within the sample. The semi-quantitative analysis only allows the determination of relative amounts of crystalline phases present in the sample. A full quantitative analysis with an

internal standard would allow the weight percentages for the phases present in the sample to be calculated. Rietveld analysis through the use of Topas (Bruker) software was used to determine and provide general information on the phases within the sample. The phases of interest were portlandite, ettringite, gypsum, and thenardite. Rietveld analysis is a non-linear least-squares technique that refines the x-ray peaks in a scan to profile fittings for certain crystalline phases and provides figure of merits for the certainty of the phases determined in the sample.

2.2.2.3 Permeability Procedure

As part of this study, it was decided to evaluate the transport mechanisms for the various mixtures to determine if any trends existed between permeability (or actually electrical resistivity), capillary absorption, and deterioration.

Each mixture proportion had several cylinder segment cuts that remained in the moist-curing room while the laboratory testing was being performed. In order to determine the permeability of each mixture proportion, the Section B segments, which are the middle cut segment that contains two cut surfaces, were removed from the moist-cure room at approximately 409 days after casting for the permeability testing. These segments were not exposed to any sulfates or deionized water. Previous research by Riding et al. showed that ASTM C1202 or the rapid chloride permeability test (RCPT) can be modified to one reading taken after 5 minutes to calculate the concrete resistivity (Riding et al. 2008). This method was used to calculate the permeability of all the different concrete mixtures. In addition, select specimens were also run following ASTM C1202's 6 hour test to further validate the results. All of the specimens that had both permeability methods conducted on the concrete specimens resulted in the same chloride

ion permeability classification according to ASTM C1202. All of the specimens were rinsed off with tap water and returned to the moist-cure room once the RCPT was completed on all the concrete mixtures.

2.2.2.4 Absorption Procedure

In order to evaluate the capillary absorption of the physical sulfate attack testing specimens, two cylinder cuts were taken from the moist-cure room at approximately 502 days after casting to undergo ASTM C1585. Two of the top cut of the cylinder segments, Section A segments, were used in the absorption testing. These cut cylinder segments contained the finished surface of the cylinder. Section A segments were selected for testing, because the standard calls for at least the average of two specimens for reporting and the only segments with two specimens was Section A. In addition, the same cylinder segments that were used in the RCPT testing were analyzed in the absorption test.

2.3 Experimental Results and Discussion

After 130 cycles into the laboratory testing most of the cyclical 30% (by mass of solution) sodium sulfate containers had fine concrete powder in the bottom of the container. In addition, exposed surfaces showed enhanced degradation. Containers with Type V cement had more loose fines than containers with Type I cement. Also, higher w/cm ratios showed more fines in the solution than the containers with lower w/cm. Many of the 0.50 w/cm specimens had formed pores on the surface from fine aggregate pop outs. At three months into the testing, static specimens with Type I cement and Class C fly ash showed signs of chemical sulfate attack. Specimens with 20% Class C fly ash by mass replacement showed the most deterioration.

A 30% (by mass of solution) sodium sulfate solution is near the saturation limit causing the sodium sulfate to remain crystallized in the bottom third of the containers' solution when the specimens were removed for measurements. This mass of crystallization locks around the bottom and sides of the specimens which sometimes caused damage to the concrete matrix when the specimens were removed for measurements.

Table 9 shows the overall mass change results from the laboratory study and Table 10 provides the average values for the static and cyclical 30% (by mass of solution) sodium sulfate specimens. Figures 14 to 24 show the mass change of various groups of specimens' performance and how they progressed over the duration of the laboratory testing.

Table 9: Laboratory Results

Mix Description	Cycles	Total Mass Change			Static		Cyclical	
		Static 30% Na_2SO_4	Cyclical 30% Na_2SO_4	Cyclical H_2O	30% Na_2SO_4 (B)	30% Na_2SO_4 (C)	30% Na_2SO_4 (B)	30% Na_2SO_4 (C)
0.40 - I	712	-0.113%	-52.956%	0.390%	-0.284%	0.059%	-58.774%	-47.035%
0.40 - I - 20C	731	-3.412%	-17.298%	0.287%	-1.814%	-5.081%	-20.613%	-13.892%
0.40 - I - 40C	731	-0.583%	-9.648%	0.556%	-0.458%	-0.711%	-8.272%	-11.121%
0.40 - I - 20F	731	-0.060%	-7.965%	0.365%	-0.179%	0.060%	-7.271%	-8.673%
0.40 - I - 30F	731	-0.060%	-8.729%	0.363%	-0.099%	-0.018%	-7.871%	-9.577%
0.40 - I - 35S	731	-0.090%	-1.886%	0.304%	-0.294%	0.123%	-1.207%	-2.602%
0.40 - I - 50S	731	-0.096%	-3.473%	0.326%	-0.260%	0.067%	-3.674%	-3.267%
0.40 - V	710	0.028%	-18.558%	0.250%	-0.174%	0.223%	-23.958%	-12.918%
0.45 - I	712	-0.859%	-35.554%	0.087%	-1.057%	-0.644%	-39.502%	-31.496%
0.45 - I - 20C	712	-5.264%	-30.078%	0.036%	-2.993%	-7.654%	-32.551%	-27.537%
0.45 - I - 40C	712	-1.926%	-12.742%	0.291%	-0.889%	-3.014%	-11.769%	-13.712%
0.45 - I - 20F	712	-0.339%	-12.484%	0.273%	-0.330%	-0.347%	-12.110%	-12.847%
0.45 - I - 30F	712	-0.266%	-11.679%	0.196%	-0.473%	-0.060%	-8.057%	-15.398%
0.45 - I - 35S	712	-0.348%	-4.875%	0.224%	-0.564%	-0.135%	-4.602%	-5.153%
0.45 - I - 50S	712	-0.135%	-1.378%	0.297%	-0.261%	0.000%	-0.773%	-2.032%
0.45 - V	710	0.184%	-40.812%	0.056%	0.109%	0.261%	-38.138%	-43.784%
0.50 - I	710	0.327%	-67.242%	0.521%	0.223%	0.425%	-67.242%	-17.7 @ 374 cycles
0.50 - I - 20C	712	-19.370%	-42.280%	0.207%	-19.370%	-15.1% @ 376 cycles	-42.280%	-14.0 @ 376 cycles
0.50 - I - 40C	710	-2.144%	-17.492%	0.085%	-1.243%	-3.087%	-16.542%	-18.483%
0.50 - I - 20F	712	-1.343%	-24.005%	0.398%	-0.294%	-2.408%	-20.619%	-27.510%
0.50 - I - 30F	710	0.277%	-14.669%	0.322%	0.249%	0.309%	-12.742%	-16.523%
0.50 - I - 35S	712	-0.313%	-11.564%	0.213%	-0.561%	-0.054%	-12.892%	-10.237%
0.50 - I - 50S	710	-0.177%	-6.143%	0.212%	-0.278%	-0.071%	-6.824%	-5.439%
0.50 - V	710	0.319%	-47.568%	0.158%	0.281%	0.359%	-17.4 @ 374 cycles	-47.568%
0.50 - V - 40C	710	0.218%	-19.655%	0.222%	0.159%	0.279%	-22.376%	-16.844%
0.50 - V - 30F	710	-0.124%	-21.297%	0.353%	-0.300%	0.062%	-20.739%	-21.902%
0.50 - V - 50S	710	-0.077%	-7.524%	0.197%	-0.227%	0.090%	-6.417%	-0.406%

Table 10: Averaged Laboratory Results

			Total Mass Change			10% Mass Loss Failure Criterion	
Mix Description	f_c', psi (Mpa)	Cycles	Static 30% Na_2SO_4	Cyclical 30% Na_2SO_4	Cyclical H_2O	Cycles	Mass (%)
0.40 - I	7138 (49.2)	712	-0.11%	-52.96%	0.39%	412	-10.48%
0.40 - I - 20C	6757 (46.6)	731	-3.41%	-17.30%	0.29%	731	-17.30%
0.40 - I - 40C	7782 (53.7)	731	-0.58%	-9.65%	0.56%	-	-
0.40 - I - 20F	6093 (42.0)	731	-0.06%	-7.96%	0.36%	-	-
0.40 - I - 30F	7085 (48.9)	731	-0.06%	-8.73%	0.36%	-	-
0.40 - I - 35S	7408 (51.1)	731	-0.09%	-1.89%	0.30%	-	-
0.40 - I - 50S	6392 (44.1)	731	-0.10%	-3.47%	0.33%	-	-
0.40 - V	9087 (62.6)	710	0.03%	-18.56%	0.25%	710	-18.56%
0.45 - I	6832 (47.1)	712	-0.86%	-35.55%	0.09%	376	-10.08%
0.45 - I - 20C	6397 (44.1)	712	-5.26%	-30.08%	0.04%	444	-10.28%
0.45 - I - 40C	7373 (50.8)	712	-1.93%	-12.74%	0.29%	712	-12.74%
0.45 - I - 20F	7253 (50.0)	712	-0.34%	-12.48%	0.27%	712	-12.48%
0.45 - I - 30F	5903 (40.7)	712	-0.27%	-11.68%	0.20%	712	-11.68%
0.45 - I - 35S	7512 (51.8)	712	-0.35%	-4.88%	0.22%	-	-
0.45 - I - 50S	6519 (44.9)	712	-0.13%	-1.38%	0.30%	-	-
0.45 - V	8170 (56.3)	710	0.18%	-40.81%	0.06%	442	-10.41%
0.50 - I	5315 (36.6)	710	0.33%	-67.24%	0.52%	374	-14.39%
0.50 - I - 20C	6131 (42.3)	712	-19.37%	-42.28%	0.21%	376	-11.95%
0.50 - I - 40C	5393 (37.2)	710	-2.14%	-17.49%	0.09%	550	-10.11%
0.50 - I - 20F	5096 (35.1)	712	-1.34%	-24.01%	0.40%	552	-13.00%
0.50 - I - 30F	4402 (30.3)	710	0.28%	-14.67%	0.32%	710	-14.67%
0.50 - I - 35S	7230 (49.8)	712	-0.31%	-11.56%	0.21%	712	-11.56%
0.50 - I - 50S	6021 (41.5)	710	-0.18%	-6.14%	0.21%	-	-
0.50 - V	7324 (50.5)	710	0.32%	-47.57%	0.16%	374	-14.03%
0.50 - V - 40C	5814 (40.1)	710	0.22%	-19.65%	0.22%	710	-19.65%
0.50 - V - 30F	4464 (30.8)	710	-0.12%	-21.30%	0.35%	442	-11.15%
0.50 - V - 50S	6743 (46.5)	710	-0.08%	-7.52%	0.20%	-	-

Given the aggressive environmental conditions and duration of the test, most mixtures start deteriorating rapidly at some point due to the increasing concentrations of sodium sulfate in the specimens and the repeated crystallization cycles. To get a better grasp on the different mixtures, a failure criterion was created for further inspection of the data. A cutoff point was used in analysis to compare how many cycles it took each mixture proportion to reach a mass loss of at least 10%. This 10% mass loss failure criterion is also shown in Table 9. As the testing progressed, the time between measurements increased so it is important to also take note of the mass loss percentage that was past the 10% limit since several concrete mixtures overshot the criterion by a substantial margin. Figure 6 compares the straight cement mixture at all each w/cm used in the study. As the w/cm decreases, the Type of cement seems to have a bigger role, in that at a 0.40 w/cm the Type V straight cement mixtures took many more cycles to reach the criterion. Figures 7 and 8 are images of the 0.40 w/cm straight Type I and Type V cement mixtures that are depicted in Figure 6 at this over 10% mass loss criterion. These images show that the deterioration mechanism looks very similar between the two, even though a sulfate attack resisting cement was used in one of the concrete mixtures.

The next set of images, Figures 9 to 12, shows the 0.50 w/cm straight cement mixtures in the cyclical then static testing. These images clearly depict the aggressiveness and severity of physical sulfate attack (cyclical) as compared to chemical sulfate attack (static). As previously stated, due to the long duration of the test, the cyclical 30% (by mass of solution) sodium sulfate specimens we bound to experience some chemical sulfate attack but physical sulfate attack dominated the deterioration. In Figures 13 and 14, Type I and Type V cements are compared at the end of their cycle in 30% (by mass of solution) sodium sulfate testing with the incorporation of 50% slag by cementitious mass. These concrete mixtures suffered minimal distress as compared to the vast majority of the

other mixtures. In Figures 7, 8, and 11-14 an untested cylinder segment was placed in the middle of the two laboratory tested cylinder segments in order to show the degree of the distress undergone in testing from the original condition of the cylinder segments. In Figures 9 and 10, the cylinder segment on the right was also this untested, control cylinder segment used for comparison to the level of distress that the cylinders had undergone in testing.

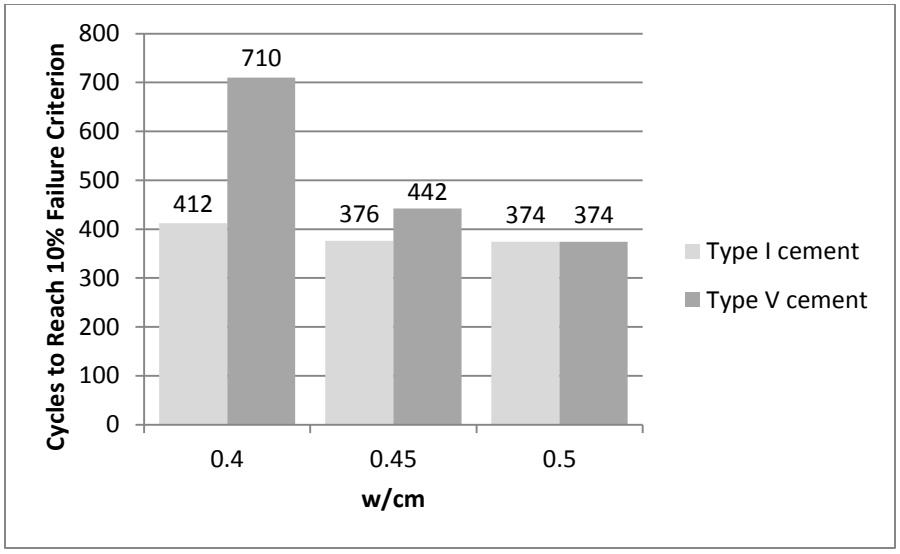

Figure 6: Type I versus Type V Straight Cement 10% Mass Loss Criterion

Figure 7: 0.40 – I Cyclical 30% (by mass of solution) Sodium Sulfate at 412 Cycles and 10.48% Mass Loss

Figure 8: 0.40 – V Cyclical 30% (by mass of solution) Sodium Sulfate at 710 Cycles and 18.56% Mass Loss

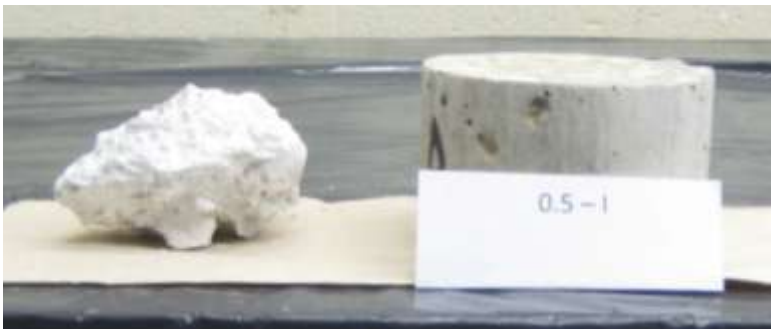

Figure 9: 0.50 – I Cyclical 30% (by mass of solution) Sodium Sulfate at end of test

Figure 10: 0.50 – V Cyclical 30% (by mass of solution) Sodium Sulfate at end of test

Figure 11: 0.50 – I Static 30% (by mass of solution) Sodium Sulfate at end of test

Figure 12: 0.50 – V Static 30% (by mass of solution) Sodium Sulfate at end of test

Figure 13: 0.50 – I – 50S Cyclical 30% (by mass of solution) Sodium Sulfate at end of test

Figure 14: 0.50 – V – 50S Cyclical 30% (by mass of solution) Sodium Sulfate at end of test

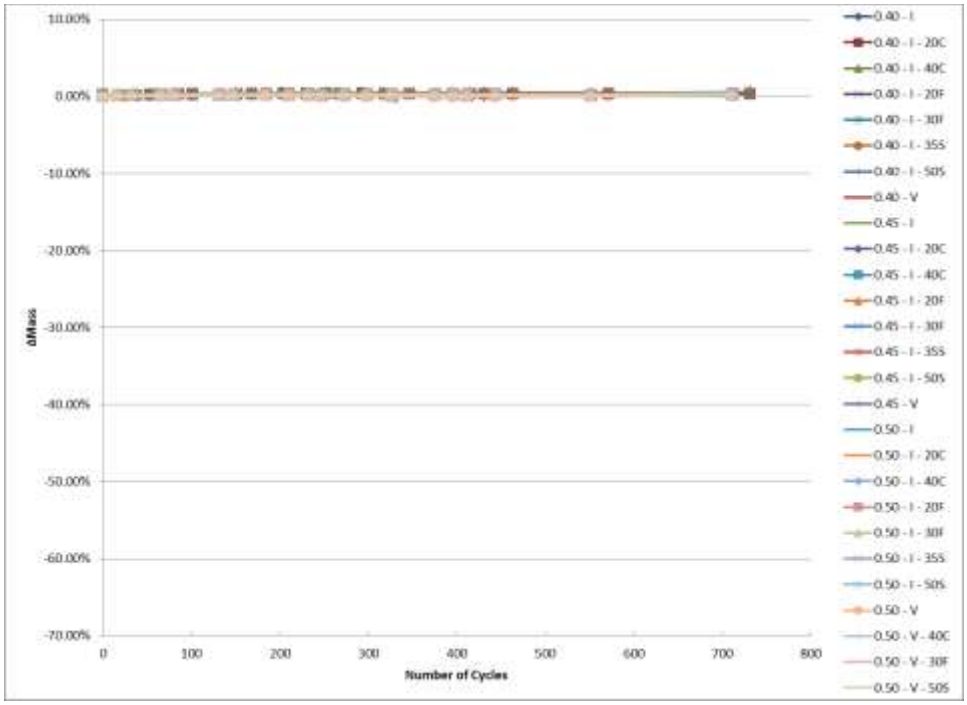

Figure 15: Cyclical Testing – All Deionized Water Controls

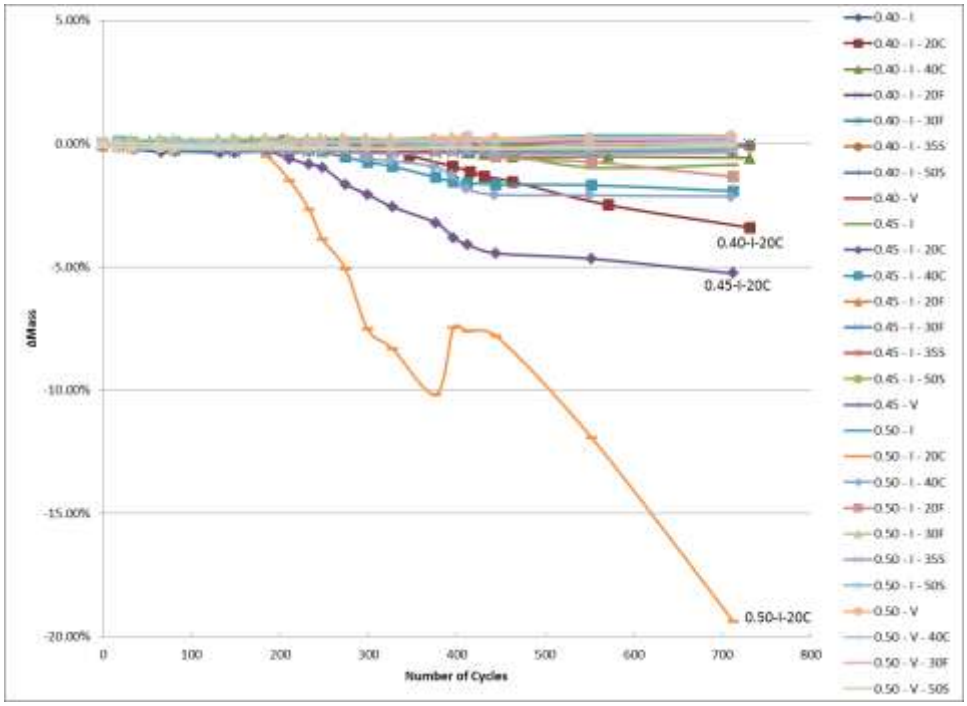

Figure 16: Static Testing – All Enlarged

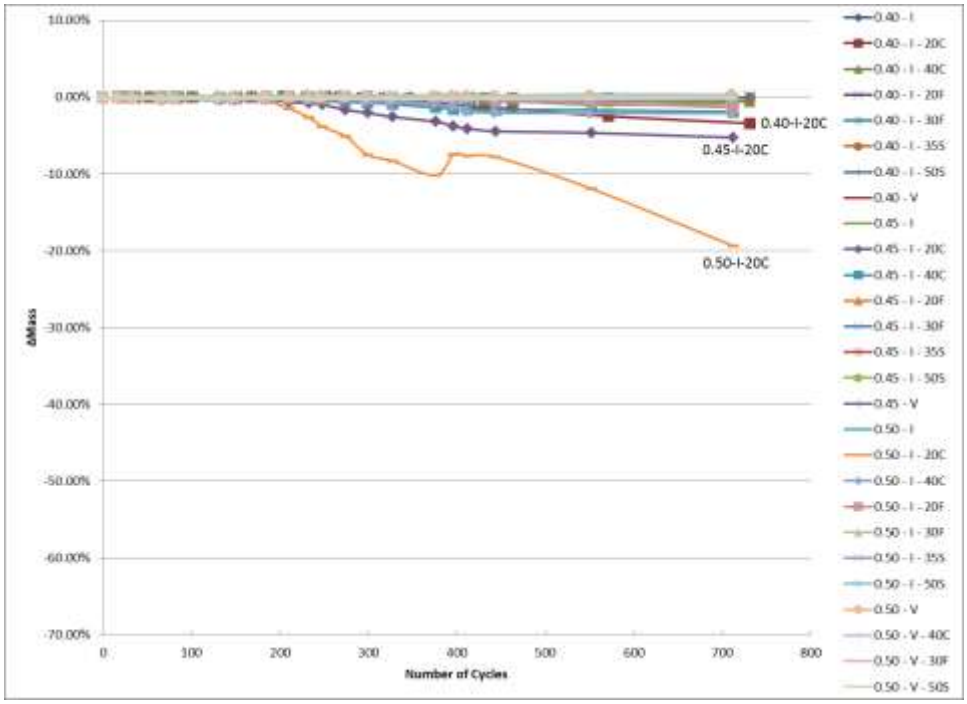

Figure 17: Static Testing - All

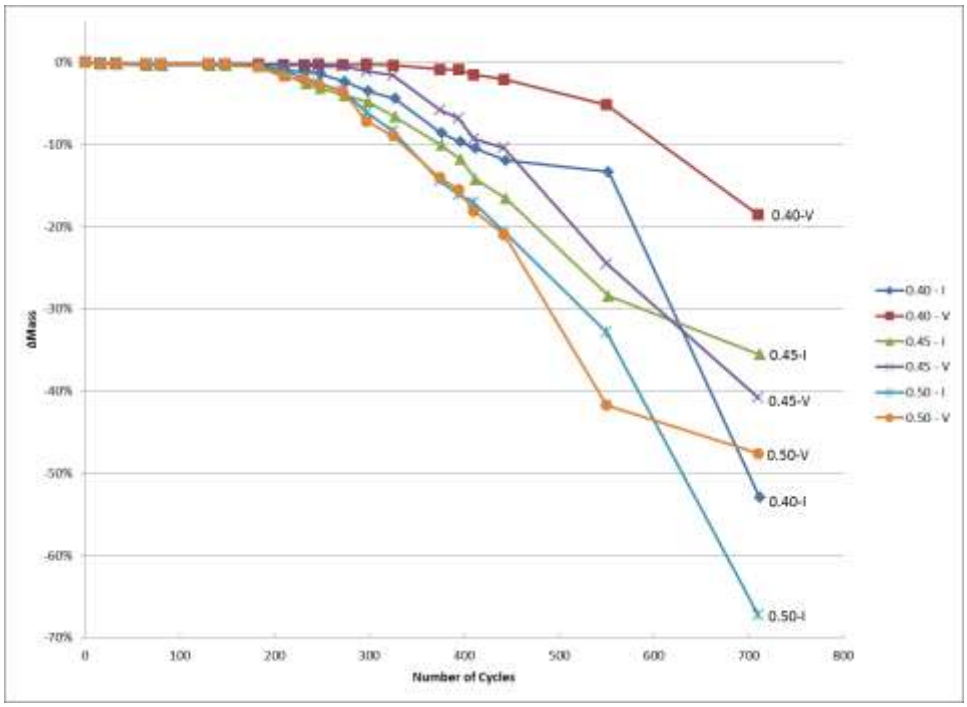

Figure 18: Cyclical Testing – w/cm Straight Cement

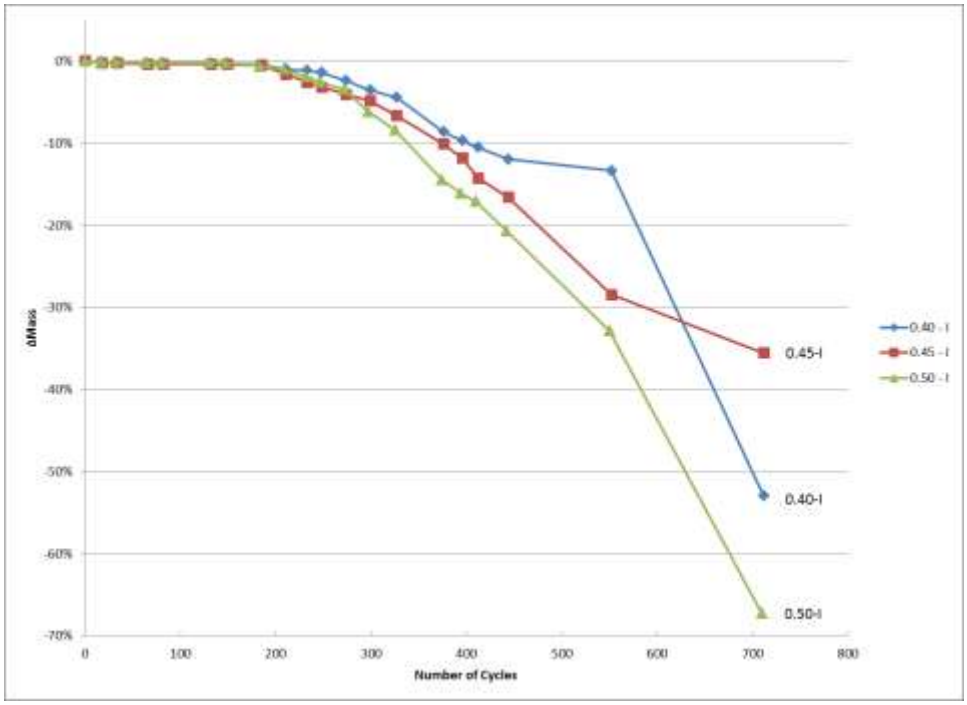

Figure 19: Cyclical Testing – w/cm Straight Type I Cement

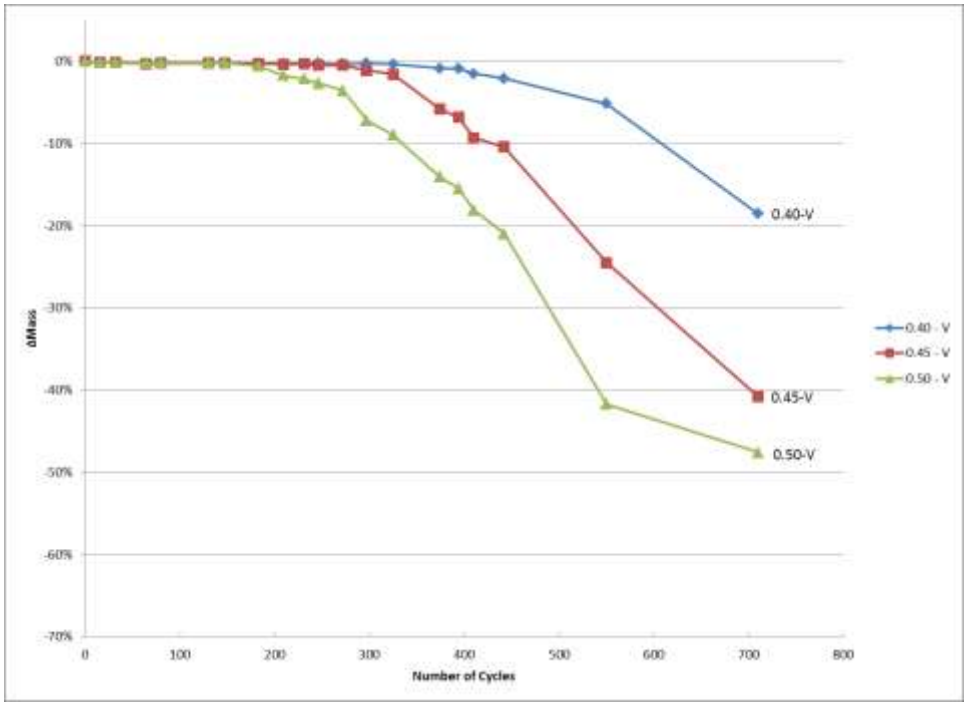

Figure 20: Cyclical Testing – w/cm Straight Type V Cement

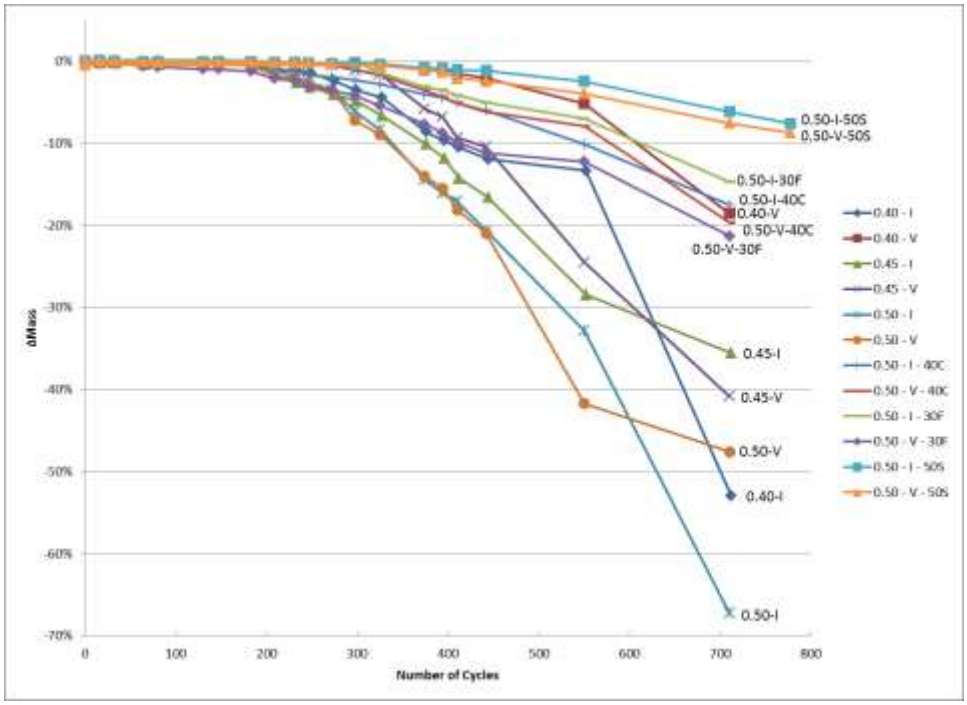

Figure 21: Cyclical Testing – Type I versus Type V Cement

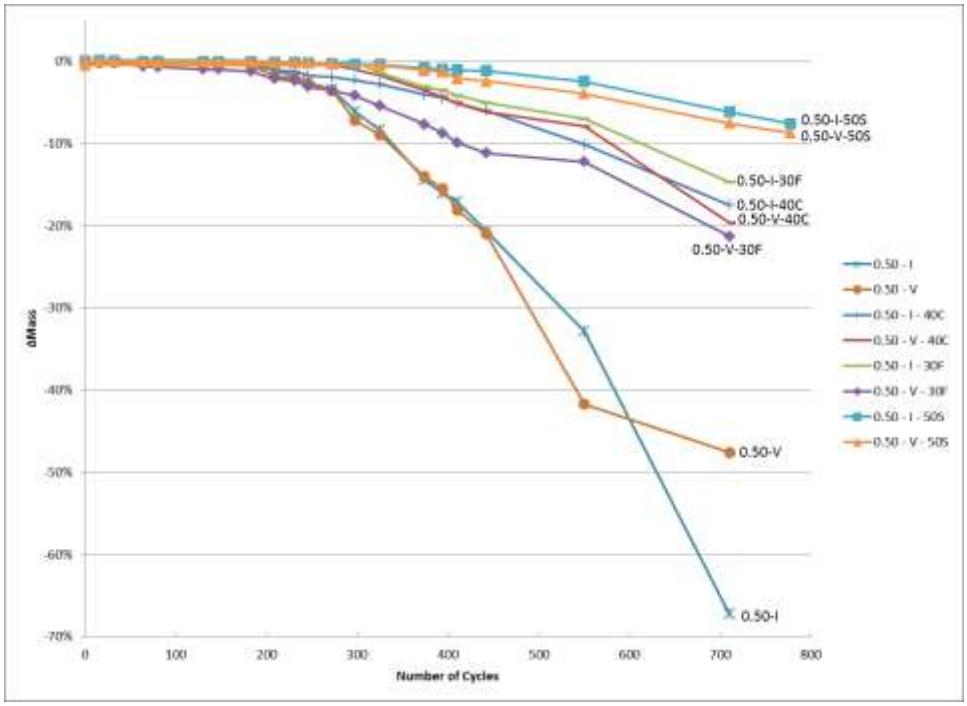

Figure 22: Cyclical Testing – Type I versus Type V Cement with 0.50 w/cm

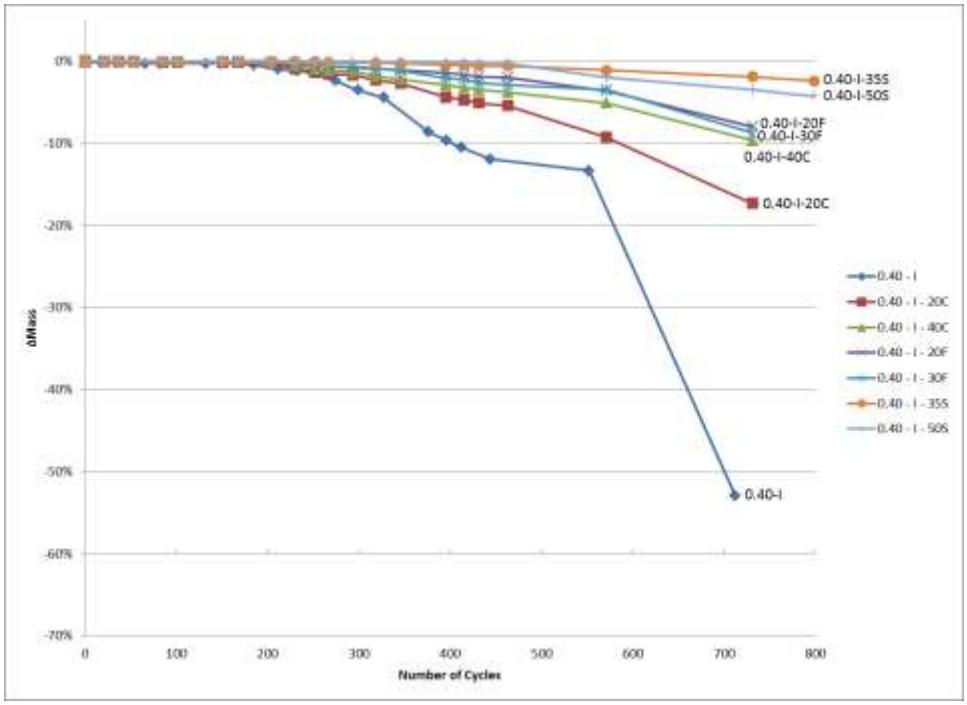

Figure 23: Cyclical Testing – 0.40 w/cm with SCMs

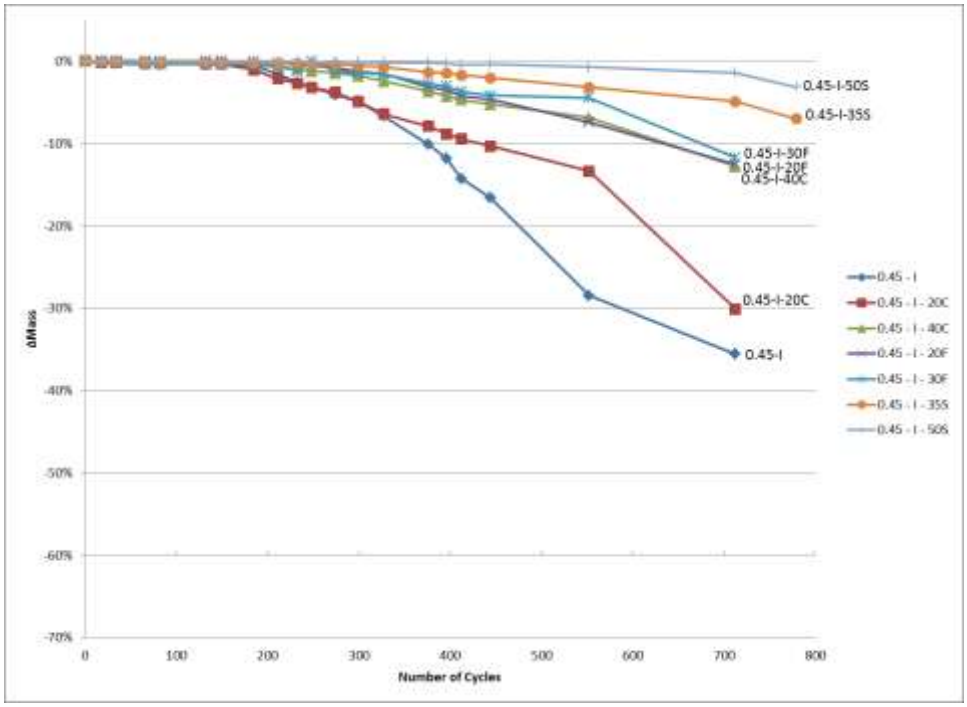

Figure 24: Cyclical Testing – – 0.45 w/cm with SCMs

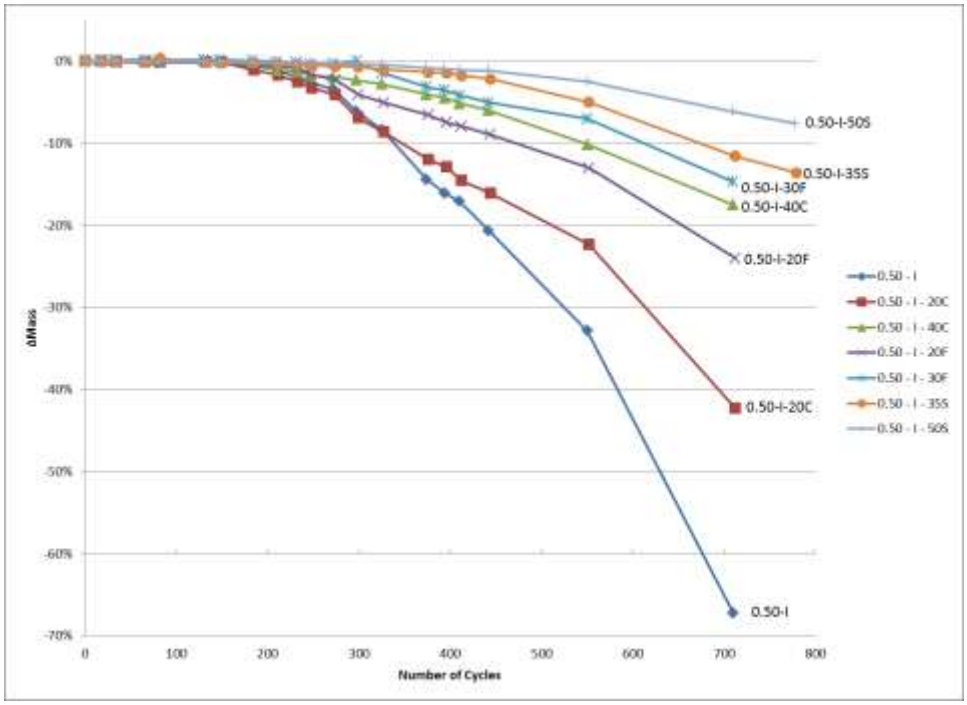

Figure 25: Cyclical Testing – – 0.50 w/cm with SCMs

2.3.1 Chemical Sulfate Attack

In Figures 16 and 17, only a few mixtures suffered from minimal chemical sulfate attack. As expected, the mixture with Type I cement and 20% Class C fly ash would deteriorate from chemical sulfate attack due to the reactive calcium aluminates within the Class C fly ash, which is agreement with previous work by Drimalas (2007) and Clement (2009). Also, the mixture with Type I cement and 40% Class C fly ash performed poorly. Since the specimens were in the solution for over one year, some chemical attack was going to occur.

2.3.2 Physical Sulfate Attack

As previously stated, Figures 9 and 11, as well as 10 and 12, Type I and Type V cements, respectively, that physical sulfate attack was the dominate distress mechanism of the concrete specimens exposed to a 30% (by mass of solution) sodium sulfate solution in cyclical environmental conditions. The following sections will compare various concrete mixtures to evaluate their resistance to physical sulfate attack.

2.3.2.1 w/cm

The w/cm is compared in Figures 18-20. Figure 18 contains all the straight cement mixtures with both the Type I and Type V cement. In this figure and Figure 19 and 20, which depict the Type I and Type V straight cement mixtures, respectively; one can see that increasing the w/cm for either type of cement caused more distress in the specimens. For both Type I and V cements, it can be seen that lowering the w/cm will increase the time until they fail the 0.1% failure criteria.

2.3.2.2 Cement Type

Type I and Type V cement mixtures are compared in Figures 21 and 22. Figure 21 depicts all the mixture proportion comparisons made between the two cement types, whereas Figure 22 has only the cement type comparisons at a 0.50 w/cm. In Figure 21, the Type V mixtures for 0.40 and 0.50 w/cm perform superior to the straight Type I concrete mixtures; however, at the 0.45 w/cm the straight Type I mixture performed slightly better. Comparing the straight cement mixtures with 0.40 and 0.50 w/cm, the Type V cement performs superior by about twice the margin in 0.40 w/cm than in the 0.50 w/cm. In addition, it is interesting to note that in all the SCM mixtures with 0.50

w/cm, the mixtures with Type I cement perform superior than that of the ones with Type V cement, as seen in Figure 22.

2.3.2.3 Supplementary Cementing Materials

Figures 23 to 25 compare the incorporation of SCMs into the concrete matrix versus the control with straight cement mixtures for the 0.40, 0.45, and 0.50 w/cm, respectively. In Figure 23, which has the 0.40 w/cm concrete mixtures, high dosage of SCM replacement performed superior in the Class C fly ash, but performed worse in the Class F fly ash and in the slag concrete mixtures. However, in both the 0.45 and 0.50 w/cm SCM figures the high dosage of SCM replacement performed superior in cyclical testing than the lower percentage SCM dosage. In Figure 24, the 0.45 w/cm graph, the Class F fly ash and slag high and low percentage replacements are fairly close to one another; however, in Figure 25, the 0.50 w/cm graph, the higher SCM dosage percentage performed better by a larger margin. It appears that as the pore structure is refined with lowering the w/cm, then the lower dosage of SCMs performs superior. However, when the w/cm is increased to 0.50, the higher dosage of SCMs performs superior. This relationship could be signifying that a lower w/cm is more susceptible to the absorption mechanism of physical sulfate attack, whereas at a higher w/cm, a higher dosage of SCMs is needed to refine the pore structure and thus reduce the permeability of the concrete matrix.

2.3.2.4 X-ray Diffraction

Samples for XRD were taken from select specimens after 325 or 327 cycles. Table 8 shows the specimens and their mass loss when the specimens were removed from

the testing regime and prepared for XRD analysis. For each cylinder cut that was removed for XRD analysis, a section was taken near the center (core), as well as an outer edge section of the cylinder cuts. The inside sample was taken from the interior core of the cylinder segments, whereas the outside XRD sample was taken from the exterior edge of the cylinder segment so that a comparison could be made between the inside and outside of the cylinder segments.

XRD analysis was also done on the concrete pieces that were in the bottom of the containers, but they would have been totally consumed by chemical sulfate attack so they were not depicted in Figures 27 through 30. The specimens should have some degree of chemical sulfate attack because they were in 30% (by mass of solution) sodium sulfate for approximately 269 days; however, based on the data presented in Section 2.3 it is clear that chemical sulfate attack is only minimal for most concrete mixtures when the mass loss of the static versus cyclical environment for each mixture proportion are compared. Due to the duration of the test, more chemical attack was observed than desired, but physical sulfate attack dominated the distress. As shown in Figure 28, the 0.50-V mixture did not show any signs of chemical attack since no ettringite for gypsum formations were found in the system. ; however, it had approximately the same mass loss as the 0.50-I sample in cyclical testing which did show some signs of chemical attack. Figure 27 shows that the 0.50-I specimen with the reduction of portlandite as ettringite and gypsum were formed. Also, the degree of attack increases from the inside to the outside of the specimen.

Figure 26: Location of XRD Sampling from Cylinder Segments

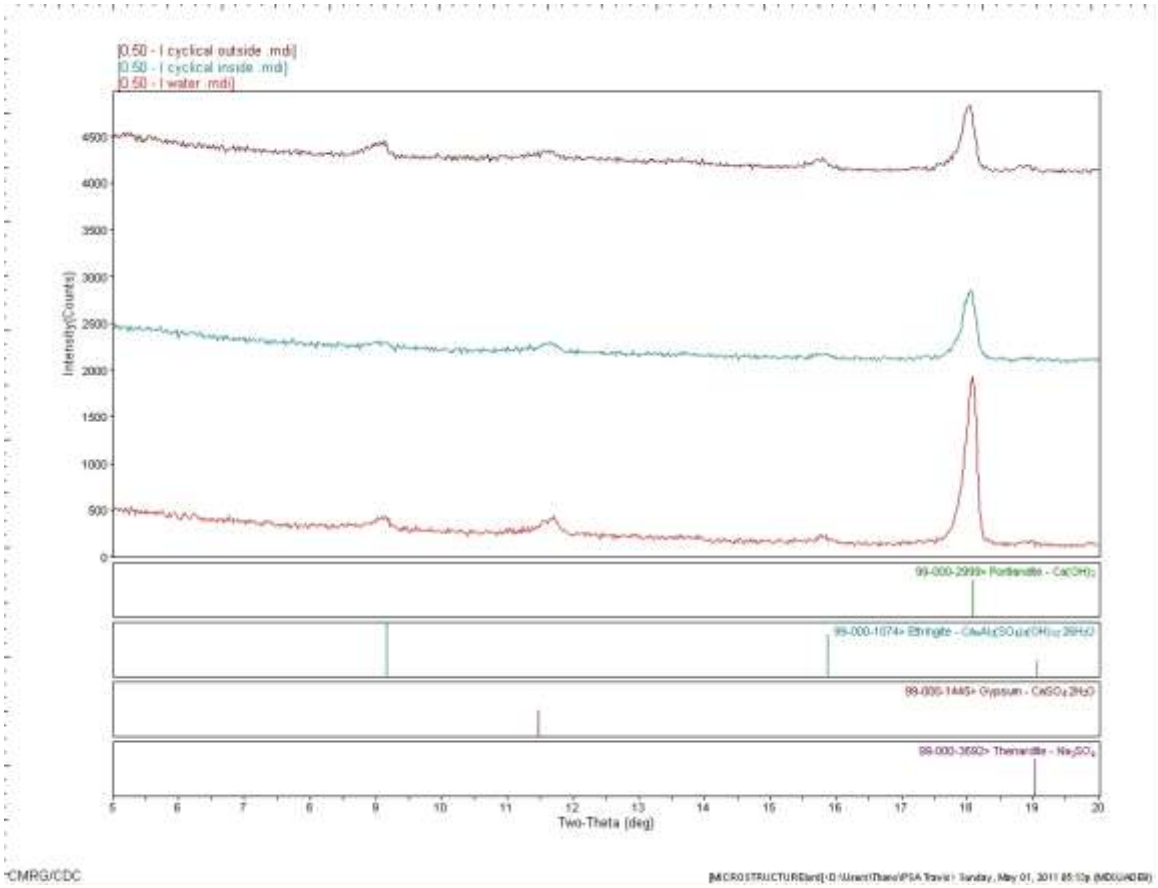

Figure 27: 0.50 – I Cyclical Testing XRD Results

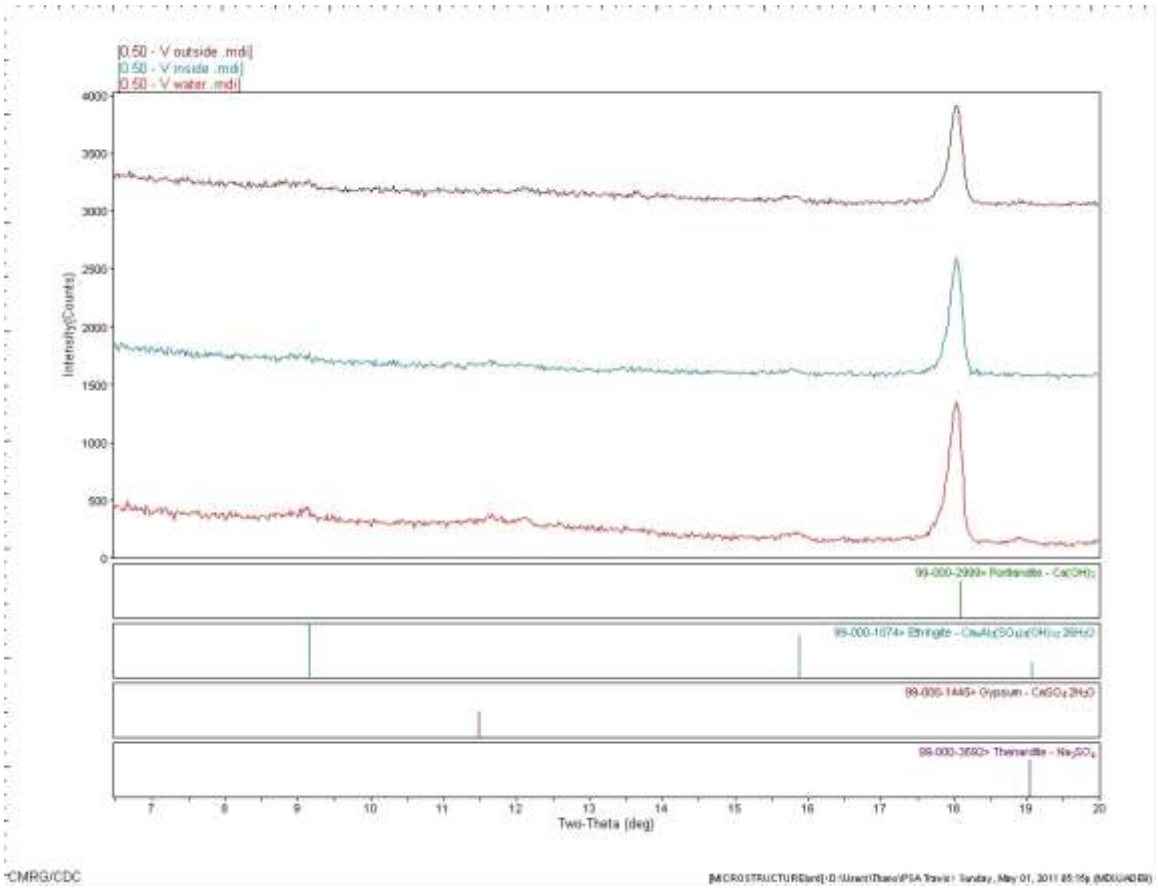

Figure 28: 0.50 – V Cyclical Testing XRD Results

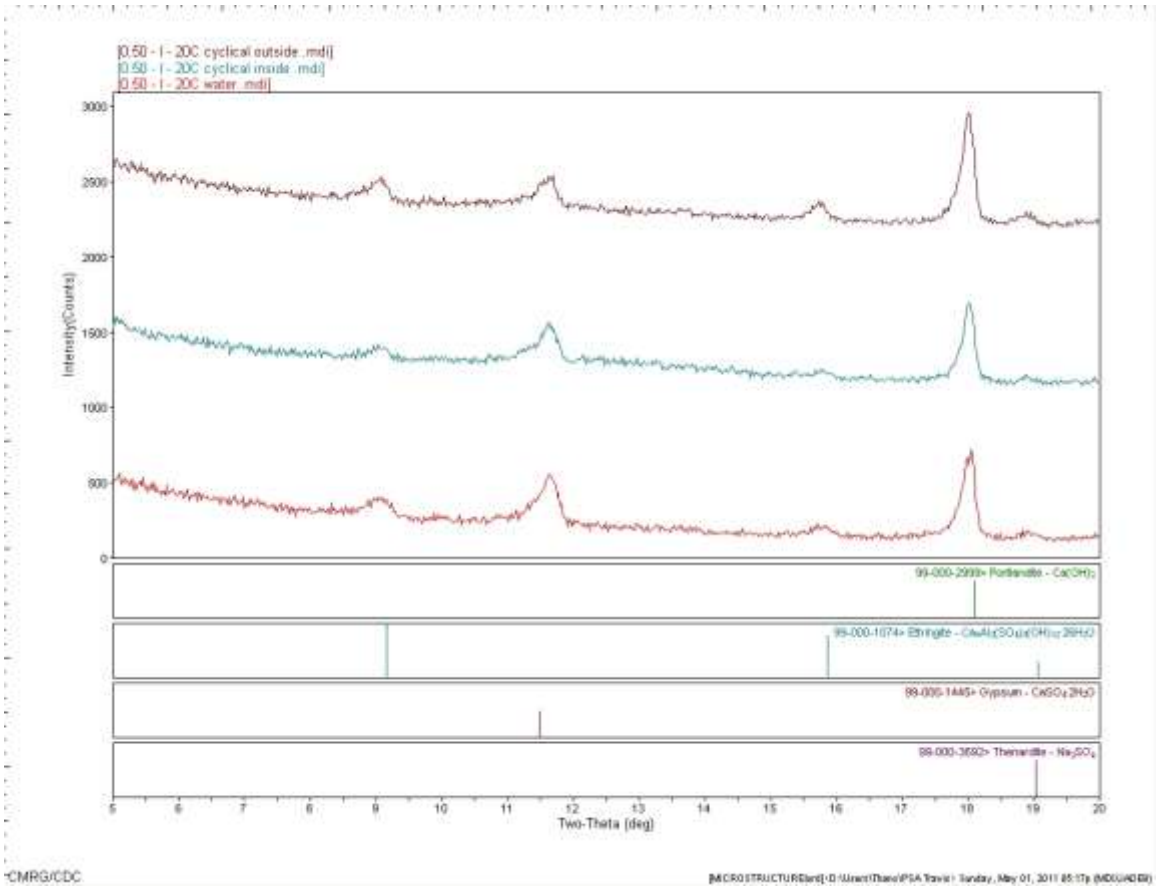

Figure 29: 0.50 – I – 20C Cyclical Testing XRD Results

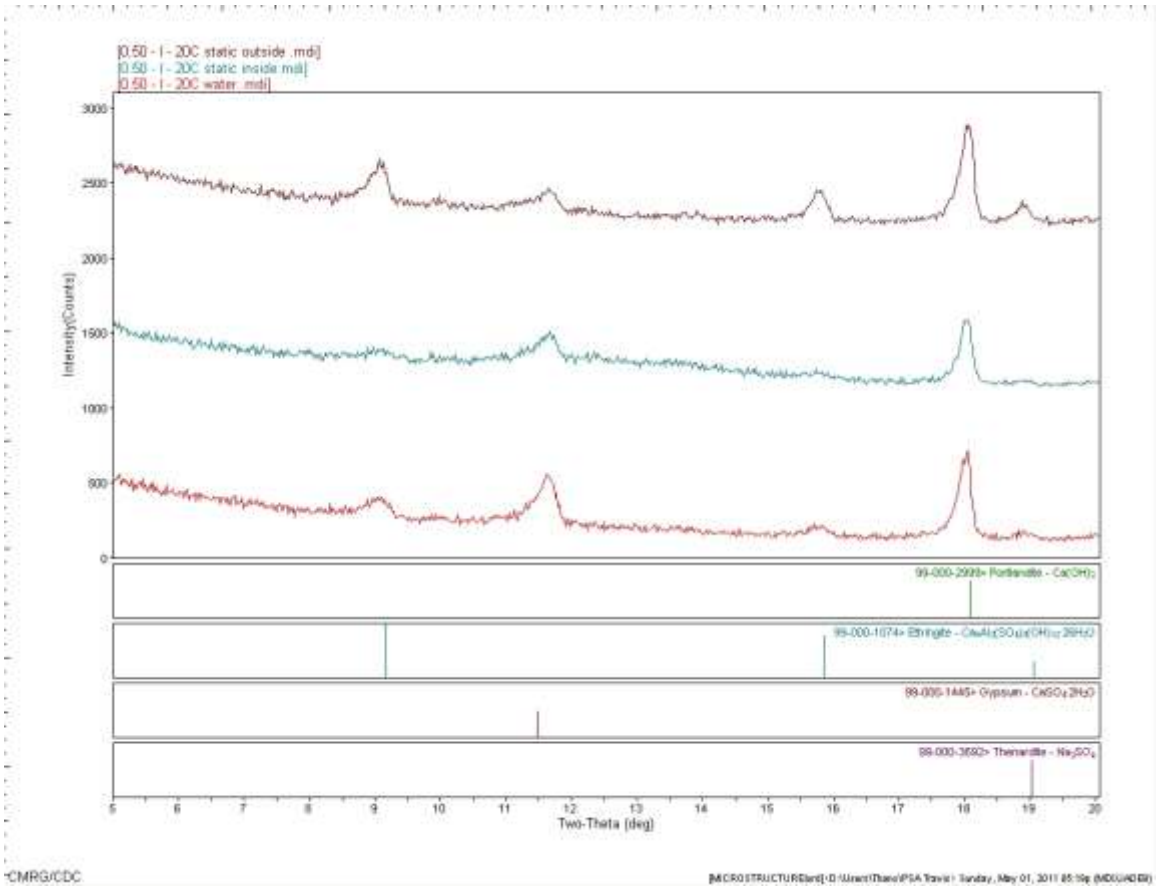

Figure 30: 0.50 – I – 20C Static Testing XRD Results

In the XRD analysis, it was found that even the concrete cylinder cuts that were only stored fully submerged in deionized water for the entire testing regime contained traces of ettringite and gypsum. This effect was seen in both the Type I and Type V cement specimens. It is not uncommon in the field for ettringite to be found in concrete samples; however gypsum generally should not be found in a specimen that is not affected by a concrete durability issue. Work is being done to analyze this issue, but the results will not be presented herein. In order to evaluate this presence of both ettringite and gypsum, cement paste was created using the same Type I cement with a w/cm of 0.33. The sample was allowed to air-cure for one day then it was broken into three

sections of approximately equal volume. One section was immediately placed in a desiccator to preserve the hydration products after the one day air-curing. The second piece was placed fully submerged in deionized water in a sealed plastic container, while the third was left on top of this container in ambient, atmospheric conditions. These two specimens were left in their conditions for 28 days before being placed in a desiccator. XRD analysis will be performed on the three concrete segments to see if ettringite and gypsum are present in any of them. Further conclusions will be drawn upon the completion of this XRD study.

2.3.3 Permeability

As part of this study, it was decided to evaluate the transport mechanisms for the various mixtures to determine if any trends existed between permeability (or actually electrical resistivity), capillary absorption, and deterioration. These permeability results from the 5-minute modified RCPT (Riding et al. 2008) and ASTM C1202 test are presented in Table 11.

Table 11: RCPT Results

Mix Description	5 Minute Charge Passed (coulombs)		6 Hour ASTM C1202 Charge Passed (coulombs)		Chloride Ion Penetrability Classification (based on 2.5 in. 5-minute results)
	2.5 in. Specimen Length	Predicted 2 in. Specimen Length	2.5 in. Specimen Length	Predicted 2 in. Specimen Length	
0.40 - I	2270	1960	1940	1680	Moderate
0.40 - I - 20C	320	260	-	-	Very Low
0.40 - I - 40C	790	660	-	-	Very Low
0.40 - I - 20F	90	80	-	-	Negligible
0.40 - I - 30F	30	30	460	390	Negligible
0.40 - I - 35S	50	40	-	-	Negligible
0.40 - I - 50S	40	30	760	630	Negligible
0.40 - V	2530	2080	-	-	Moderate
0.45 - I	2270	1940	2820	2410	Negligible
0.45 - I - 20C	1480	1230	1440	1200	Low
0.45 - I - 40C	850	720	-	-	Very Low
0.45 - I - 20F	830	690	770	640	Very Low
0.45 - I - 30F	40	30	-	-	Negligible
0.45 - I - 35S	1210	1030	1065	910	Very Low
0.45 - I - 50S	780	670	830	710	Low
0.45 - V	2620	2100	-	-	Moderate
0.50 - I	1970	1620	2380	1950	Moderate
0.50 - I - 20C	1630	1410	-	-	Low
0.50 - I - 40C	270	220	-	-	Very Low
0.50 - I - 20F	280	240	-	-	Very Low
0.50 - I - 30F	310	270	-	-	Very Low
0.50 - I - 35S	1290	1100	1250	1070	Low
0.50 - I - 50S	330	280	-	-	Very Low
0.50 - V	3240	2730	-	-	Moderate
0.50 - V - 40C	70	60	-	-	Negligible
0.50 - V - 30F	380	320	-	-	Very Low
0.50 - V - 50S	40	30	120	100	Negligible

2.3.4 Absorption

Another potential driving mechanism of physical sulfate attack is the sorption (sorptivity) of the concrete specimen. Sorptivity is a near surface effect where water uptake is governed by capillary suction of the concrete. Water saturated with deleterious salts' absorption into concrete could be the overlying driving force of physical sulfate attack. These absorption results are shown in Table 12 and 13. The only modification to the ASTM standard was that a weighing scale with a 0.1 gram precision was used instead of the 0.01 gram precision that the standard calls for and the specimens were slightly longer than required. According to ASTM C1585, the initial absorption is denoted as the slope of the line that is best fit to I (absorption) plotted against the square root of time using least-squares linear regression analysis from 1 minute to 6 hours. The secondary absorption is from 1 day to 7 days. Readings were taken out to 9 days, in order to get better correlation with some of the secondary absorption values when needed. For both absorption values, the data has to have a linear relationship, which means a correlation coefficient greater or equal to 0.98 and show systematic curvature. Some of the absorption values were slightly adjusted to show a slight increase in mass or the same mass as the previous measurement, because several measurements showed a loss in mass during testing which should not happen. Also, all specimens had a good absorption increase over time even though a scale with a precision to 0.1 grams instead of the ASTM specified 0.01 gram precision was used. All of the values were considered valid for our concerns, even though data sets failed the 0.98 correlation coefficient criteria. These "failed ASTM" data sets didn't show a sufficient enough mass increase between measurements so the data was considered to not be linear enough by the ASTM standards. Generally, when the same specimen mixture proportion has two fairly different absorption values the higher of the two has a better correlation coefficient.

Table 12: Absorption Results for Averaged Segment A's

Mix Label	Initial Rate of Absorption (mm/√s)	Correlation Coefficient (≥ 0.98)	Secondary Rate of Absorption (mm/√s)	Correlation Coefficient (≥ 0.98)
0.4 I	0.0004	0.9695	0.00025	0.987
0.4 V	0.0002	0.9115	0.0002	0.98
0.4 I 20C	0.00085	0.988	0.00025	0.9815
0.4 I 40C	0.0008	0.9765	0.0002	0.9765
0.4 I 20F	0.00065	0.974	0.0001	0.949
0.4 I 30F	0.00095	0.987	0.0002	0.986
0.4 I 35S	0.0012	0.9815	0.00025	0.985
0.4 I 50S	0.0011	0.9765	0.00015	0.9655
0.45 I	0.0004	0.9605	0.00025	0.9865
0.45 V	0.0008	0.977	0.00045	0.996
0.45 I 20C	0.00055	0.9765	0.0002	0.9895
0.45 I 40C	0.00095	0.9705	0.0003	0.9905
0.45 I 20F	0.001	0.9875	0.0002	0.9815
0.45 I 30F	0.001	0.984	0.00025	0.9825
0.45 I 35S	0.00105	0.971	0.0002	0.977
0.45 I 50S	0.0012	0.971	0.0002	0.993
0.5 I	0.00065	0.9845	0.0004	0.9905
0.5 V	0.0003	0.943	0.00045	0.994
0.5 I 20C	0.001	0.9905	0.00045	0.9935
0.5 I 40C	0.00105	0.9785	0.0003	0.978
0.5 I 20F	0.001	0.967	0.0003	0.995
0.5 I 30F	0.0016	0.9965	0.00055	0.9915
0.5 I 35S	0.0014	0.9695	0.0003	0.9785
0.5 I 50S	0.0019	0.9855	0.0004	0.9905
0.5 V 40C	0.00175	0.9795	0.0004	0.993
0.5 V 30F	0.00175	0.9855	0.0003	0.9705
0.5 V 50S	0.0017	0.981	0.0003	0.9815

Table 13: Absorption Results for Segment B (used in RCPT)

Mix Label	Initial Rate of Absorption (mm/√s)	Correlation Coefficient (> 0.98)	Secondary Rate of Absorption (mm/√s)	Correlation Coefficient (> 0.98)
0.4 I	0.0003	0.952	0.0002	0.976
0.4 V	0.0002	0.867	0.0001	0.964
0.4 I 20C	0.0008	0.981	0.0002	0.985
0.4 I 40C	0.0008	0.987	0.0002	0.971
0.4 I 20F	0.0007	0.976	0.0001	0.908
0.4 I 30F	0.0009	0.984	0.0002	0.986
0.4 I 35S	0.0012	0.974	0.0003	0.991
0.4 I 50S	0.0010	0.975	0.0002	0.973
0.45 I	0.0003	0.941	0.0002	0.989
0.45 V	0.0004	0.970	0.0004	0.994
0.45 I 20C	0.0003	0.974	0.0001	0.988
0.45 I 40C	0.0008	0.963	0.0003	0.986
0.45 I 20F	0.0011	0.984	0.0002	0.984
0.45 I 30F	0.0010	0.990	0.0003	0.988
0.45 I 35S	0.0009	0.970	0.0002	0.980
0.45 I 50S	0.0010	0.972	0.0002	0.994
0.5 I	0.0006	0.990	0.0003	0.988
0.5 V	0.0003	0.956	0.0003	0.998
0.5 I 20C	0.0010	0.990	0.0004	0.994
0.5 I 40C	0.0009	0.989	0.0003	0.977
0.5 I 20F	0.0009	0.957	0.0003	0.997
0.5 I 30F	0.0018	0.995	0.0007	0.993
0.5 I 35S	0.0015	0.955	0.0003	0.975
0.5 I 50S	0.0014	0.987	0.0004	0.991
0.5 V 40C	0.0016	0.978	0.0004	0.995
0.5 V 30F	0.0013	0.987	0.0003	0.976
0.5 V 50S	0.0016	0.977	0.0003	0.981

Generally, the straight cement mixtures had the lowest absorption rate and the Type V cements had lower absorption than the Type I cement specimens in two out of the three different water to cementitious ratios. Some trends that were evident in the absorption data are shown below:

- 0.40 < 0.45 < 0.50
- Class C Fly Ash < Class F Fly Ash
- Straight cement < Fly Ash < Slag

The mixtures containing slag had almost all the highest absorption values. Also, the five highest absorption values had a 0.50 w/cm and the highest SCM replacement with three of them containing Type V cement.

2.4 SUMMARY

This chapter presented and discussed the results of concrete cylinder segments exposed to 30% (by mass of solution) sodium sulfate in both physical and chemical sulfate attack conditions. The most significant findings from these measurements were:

- Physical sulfate attack was found to be more severe and aggressive than chemical sulfate attack, using the testing regimes described herein.
- In cyclical testing, the straight cement mixtures had the highest mass losses, while the concrete mixtures with slag had the least amount of mass loss and distress. Concrete mixtures with a Class F fly ash perform superior in chemical and physical sulfate attack than concrete mixtures with Class C fly ash.
- Overall, the lower w/cm mixtures performed superior in chemical and physical sulfate attack and SCMs improved the durability.

- Generally, the straight cement mixtures had higher permeability than the SCM blended mixtures. If permeability is the overlying mechanism governing the durability of concrete to physical sulfate attack, then the straight cement mixtures should show the most distress.
- General absorption trends observed from lowest to highest initial rate of absorption:
  - $0.40 < 0.45 < 0.50$ $^{w}/_{cm}$
  - high CaO fly ash < low CaO fly ash
  - straight cement < fly ash < slag

Overall, the data presented in this chapter showed that physical sulfate attack can be quite damaging. However, it should be noted that the specimens tested in this laboratory program were quite small and the testing regime was very aggressive. To better evaluate more realistic (larger) concrete elements in a more realistic environment, a comprehensive program was launched using the aforementioned outdoor exposure site, which is described in the next chapter. Comparisons are also made in the next chapter on the performance of the various mixtures in the lab vs. the field.

2.5 WORKS CITED

ACI 201.2R, "Guide to Durable Concrete." Manual of Concrete Practice, 2001.

ACI 318-08, "Building Code Requirements for Structural Concrete and Commentary" American Concrete Institute. Farmington Hills, MI, 2008.

ASTM C 33, "Standard Specification for Concrete Aggregates," ASTM International, West Conshohocken, PA, 2009.

ASTM C 138, "Standard Test Method for Density (Unit Weight), Yield, and Air Content (Gravimetric) of Concrete," ASTM International, West Conshohocken, PA, 2010.

ASTM C 143, “Standard Test Method for Slump of Hydraulic-Cement Concrete,” ASTM International, West Conshohocken, PA, 2010.

ASTM C 150, “Standard Specification for Portland Cement,” ASTM International, West Conshohocken, PA, 2009.

ASTM C 192, “Standard Practice for Making and Curing Concrete Test Specimens in the Laboratory,” ASTM International, West Conshohocken, PA, 2005.

ASTM C 618, “Standard Specification Coal Fly Ash and Raw or Calcined Natural Pozzolan for Use in Concrete,” ASTM International, West Conshohocken, PA, 2008.

ASTM C 778, “Standard Specification for Standard Sand,” ASTM International, West Conshohocken, PA, 2006.

ASTM C 1012, “Standard Test Method for Length Change of Hydraulic-Cement Mortars Exposed to a Sulfate Solution,” ASTM International, West Conshohocken, PA, 2004.

ASTM C 1202, “Standard Test Method for Electrical Indication of Concrete’s Ability to Resist Chloride Ion Penetration,” ASTM International, West Conshohocken, PA, 2009.

ASTM C 1240, “Standard Specification for Silica Fume Used in Cementitious Mixtures,” ASTM International, West Conshohocken, PA, 2011.

ASTM C 1585, “Standard Test Method for Measurement of Rate of Absorption of Water by Hydraulic-Measurement of Rate of Absorption of Water by Hydraulic-Cement Concretes,” ASTM International, West Conshohocken, PA, 2004.

Clement, J. C. *Laboratory and Field Evaluations of External Sulfate Attack, Phase II.* Austin, Texas: The University of Texas at Austin, 2009.

Drimalas, T. *Laboratory and Field Evaluations of External Sulfate Attack.* Austin, Texas: The University of Texas at Austin, 2007.

Folliard, K.J. and Sandberg, P., "Mechanisms of Concrete Deterioration by Sodium Sulfate Crystallization," *Proceedings, Third International ACI/CANMET Conference on Concrete Durability*, Nice, France, pp. 933-945, 1994.

Haynes, H., O’Neill, R., and Mehta, P.K., “Concrete Deterioration from Physical Attacks by Salts,” *Concrete International*, V.18, No. 1, pp. 63-68, January 1996.

Haynes, H., O'Neill, R., Neff, M., and Mehta, P. K, "Salt Weathering Distress on Concrete Exposed to Sodium Sulfate Environment," *ACI Materials Journal,* V. 105, No. 1, Jan.-Feb., pp. 35-43, 2008.

Haynes, H., O'Neill, R., Neff, M., and Mehta, P.K., "Salt Weathering of Concrete by Sodium Carbonate and Sodium Chloride," *ACI Materials Journal,* V. 107, No. 3, May-June, pp. 258-266, 2010.

Hime, W. G., Martinek, R. A., Backus, L. A., and Marusin, S. L. "Salt Hydration Distress." *Concrete International,* V. 23, pp. 43-50, 2001.

Nehdi, M., and Hayek, M., "Behavior of Blended Cement Mortars Exposed to Sulfate Solutions Cycling in Relative Humidity," *Cement and Concrete Research,* V. 35, pp. 731-742, 2005.

Riding, K. A., Poole, J. L., Schindler, A. K., Juenger, M. C., and Folliard, K. J. "Simplified Concrete Resistivity and Rapid Chloride Permeability Test Method." *ACI Materials Journal,* V. 105, No. 4, pp. 390-394, 2008.

Rodriguez-Navarro, C., Doehne, E., and Sebastian, E. "How Does Sodium Sulfate Cyrstallize? Implications for the Decay and Testing of Building Materials." *Cement and Concrete Research,* V. 30, pp. 1527-1534, 2000.

Scherer, G. W. "Stress from Crystallization of Salt." *Cement and Concrete Research,* V. 34, pp. 1611-1624, 2004.

Skalny, J., Marchand, J., and Odler, I. "*Sulfate Attack on Concrete."* London: Spon Press, 2002.

Stark, D., "Longtime Study of Concrete Durability in Sulfate Soils," *Research and Development Bulletin RD086,* Portland Cement Association, Stokie, Ill., p. 13, 1984.

Stark, D., "Durability of Concrete in Sulfate Rich Soils," *Research and Development Bulletin RD 097,* Portland Cement Association, Skokie, Ill., p. 14, 1989.

Stark, D. C. "*Performance of Concrete in Sulfate Environments," RD129.* Skokie, Illinois: Portland Cement Association, 2002.

Chapter 3: Evaluation of Concrete Specimens in a Sodium Sulfate Field Exposure Site

3.1 INTRODUCTION

Physical sulfate attack (or salt hydration distress) involves phase changes of salt solution as temperature and relative humidity changes. The distress mechanism is caused by crystallization pressures of supersaturated salts in the pores at or near the evaporation surface of concrete (Scherer 2004). Sodium sulfate is the most common culprit. This physical attacking mechanism used to be characterized as chemical sulfate attack; however, chemical reactions are not involved in this physical distress mechanism (Stark 2002). Physical sulfate attack can happen in poor quality, porous concrete and occurrences have been documented in the field and by laboratory research (Stark 1984, 1989, 2002; O'Neill 1992; Folliard and Sandberg 1994; Haynes et al. 1996, 2008, 2010; Nehdi and Hayek 2005).

Research is needed to evaluate aspects of physical sulfate attack that are not fully understood. Currently, there are no standard test methods for evaluating a concrete mixture's resistance to physical sulfate attack. A testing regime was designed to evaluate and analyze aspects of physical sulfate attack. In Chapter 2, the laboratory evaluation of physical sulfate attack was presented, which involved accelerated exposure testing in an environmental chamber. In addition, shortly after the laboratory testing was commenced, a parallel field exposure site was developed to evaluate the same concrete mixtures' performance in alternative wetting and drying cycles in sodium sulfate-rich soil. Concrete cylinders from 27 different concrete mixtures were placed in a 5% (33,000 ppm) sulfate concentration in the field exposure site. It was desired to develop a correlation between the laboratory and field performance of the different concrete mixture designs. This

chapter presents the second phase of the study, which evaluated the field performance of concrete cylinders of two different sizes partially submerged in 5% (33,000 ppm) sodium sulfate solution. In the field site, concrete cylinders were exposed to alternative wetting and drying conditions, along with, temperature fluctuations that would promote alternate cycles of conversion between anhydrous sodium sulfate (thenardite) and decahydrate sodium sulfate (mirabilite). A discussion of results from this study will also be presented.

As stated in the previous chapter, there was a concern that the 4 in x 8 in (100 mm x 200 mm) cylinders, which are typically used for concrete testing, are too small to give representative results of physical sulfate attack in the field. They are considered to be unrepresentative of field physical sulfate attack because the samples are more susceptible to distress due to a shorter distance necessary for the salt ions to penetrate the concrete specimen. To investigate this concern additional $11^1/_2$ in x $14^1/_2$ in (300 mm x 3 mm) tapered concrete cylinders were cast to correlate to the 4 in x 8 in (100 mm x 200 mm) cylinder samples. Of the 27 concrete mixtures, 14 were selected for casting the larger tapered cylinders for the size comparison. Due to the size of these samples, it may take much longer for deterioration to occur. To date all the samples show signs of physical sulfate attack at the evaporation front. Most of these specimens already have coarse aggregate exposure due to the salt scaling distress. Also, duplicate $11^1/_2$ in x $14^1/_2$ in (300 mm x 375 mm) tapered cylinder specimens were taken to a gypsum exposure site located in West Texas. The discussion of the West Texas gypsum exposure site is presented in Section 5.1.2 (Recommendations for Future Work) because no data to date will be presented from this field site.

This chapter presents a background on the design of the exposure site at the Concrete Durability Center (CDC) at the University of Texas at Austin. The field exposure site was loosely based on the PCA's outdoor exposure test facility in

Sacramento, California. To evaluate the different concrete mixtures, two visual numerical rating systems for the concrete cylinders' performance and wicking action were used, as well as, mass change values for the 4 in x 8 in (100 mm x 200 mm) cylinders. A literature review on sulfate attack was previously presented in Chapter 2. A discussion of results from this study will also be presented.

3.1.1 Research Significance

Further research is needed to fully understand the mechanisms underlying physical sulfate attack. The testing regime evaluated the resistance of various w/cm, portland cement concretes, and SCMs to the physical attack caused by sodium sulfate (Na_2SO_4). When all phases of testing are completed, the results should provide engineering guidance on how best to produce durable concrete in severe sulfate exposure conditions. This research presents the results of the field exposure site on physical sulfate attack. Overall, the goal of the study was to use mixture designs that would not suffer from chemical sulfate attack, in order to, further understand the mechanisms and most durable concrete mixtures for physical sulfate attack.

3.1.2 Literature Review: Physical Sulfate Attack Field Studies

A long-term field and laboratory test program at the PCA's sodium sulfate soils test facility in Sacramento, California has provided evidence of the physical deterioration process of salt crystallization by repeated wetting and drying cycles in sodium sulfate solution. The field exposure site subjected concrete specimens to alternative wetting and drying cycles in a 6.5% (65,000 ppm) sulfate concentration for up to 16 years (Stark 2002). Companion specimens were fully submerged in the same solution in a static

laboratory environment. Stark (2002) reported that only field specimens deteriorated and concluded that the w/cm and its subsequent permeability were the primary factors governing the durability of the specimens in the outdoor exposure conditions. Lowering the w/cm improved the performance of the specimens. In addition, Stark (2002) established that cement composition had little importance to the specimen's performance in the cyclical exposure. The field study used ASTM Type I, Type II, and Type V portland cements in the PCA testing regime.

Drimalas (2007) and Clement (2009) evaluated various concentrations of sodium sulfate, magnesium sulfate, and calcium sulfate in an exposure site developed at the CDC at the University of Texas at Austin. The research showed that sodium sulfate is the most aggressive of the salt solutions tested. Drimalas (2007) evaluated 30 concrete mixtures in S3 exposure of sodium sulfate in Phase I of an external sulfate attack study, which is the most severe class listed in Table 2 from ACI 318-08. Drimalas (2007) used a 0.40 and 0.70 w/cm. In Phase II of this study, Clement (2009) simulated ACI 318-08's S1 and S2 exposure classifications, which also incorporated a w/cm of 0.45 and 0.50 in addition to the previous w/cm used by Drimalas (2007). Both phases of the external sulfate attack study used concrete prisms with dimensions of 3 in x 3 in x 11.25 in (75 mm x 75 mm x 285 mm) exposed in an outdoor sulfate exposure site in Austin, TX. Expansion measurements and mass loss was recorded over the life of these studies and continues to date. Each mixture proportion contained two completely submerged and three vertically stored with 6 in (150 mm) of the prism submerged in the sulfate-bearing soil (Clement 2009). Clement also statically stored three more concrete prisms in a modified ASTM C1012 storage condition in the same concentration of sodium sulfate as the outdoor exposure. Drimalas (2007) and Clement's (2009) prior research concluded that:

- The rate of distress to the prisms increased with increasing w/cm.

- Concrete prisms in S3 conditions expanded more than concrete prisms exposed to S1 and S2 conditions.
- Concrete prisms experienced increased damage above the soil line due to physical sulfate attack rather than because of external sulfate attack below the soil line.
- The concrete prisms in sodium sulfate generally performed worse in the majority of the testing, including laboratory and field conditions.
- Sodium sulfate was the most aggressive of the solutions tested.

Concrete prisms constructed with Type V cement at a 0.40 w/cm in a ternary blend of Class C fly ash and silica fume or having used Class F fly ash performed superior.

3.2 EXPERIMENTAL METHODS

3.2.1 Materials

Two ASTM C 150 cements were used in this study, a Type I and a Type V cement. The coarse aggregate selected was an ASTM C33 No. 57 gradation dolomitic limestone from Georgetown, TX, USA and the fine aggregate selected was natural siliceous river sand from Austin, Texas, USA. The fine aggregate was procured from a sand and gravel pit located along the Colorado River, approximately 4.3 miles (7 km) to the east of Austin, Texas, USA. In order to create have only sulfate attack as the only deterioration non to low reactive ASR aggregates were chosen. The coarse aggregate is considered to be non-reactive, while the fine aggregate is a low reactive aggregate. The pertinent aggregate properties are shown in Table 14. Six concrete mixtures that included SCM blends were used in the mix matrix. The SCM blends included a Grade 120 slag (meeting ASTM C1240), a Class C fly ash, and a Class F fly ash (as per ASTM C618).

Table 15 contains the chemical composition (oxide analysis) of the two cements used, whereas Table 16 contains the chemical composition of the SCMs, which was taken from their mill sheets.

Table 14: Aggregate Properties

Aggregate	Bulk SG (OD)	Bulk SG (SSD)	Apparent SG	Absorption (%)	Mineralogy
C1	2.47	2.55	2.67	3.21	dolomitic limestone
F1	2.57	-	-	0.93	siliceous sand

Table 15: Cement Chemical Composition

Chemical Composition	Cement	
	Type I	Type V
SiO_2, %	19.87	20.55
Al_2O_3, %	5.53	4.19
Fe_2O_3, %	2.52	5.32
Sum of SiO_2, Al_2O_3, Fe_2O_3, %	27.92	30.06
CaO, %	63.21	63.36
MgO, %	1.19	0.83
SO_3, %	3.4	3.81
Na_2O, %	0.128	0.32
K_2O, %	0.97	-
Na_2O Eq., %	0.77	-
LOI, %	-	-
Free CaO, %	-	-
C_3S, %*	55.91	-
C_2S, %*	14.77	-
C_3A, %*	10.39	2.11
C_4AF, %*	7.66	-

Table 16: SCM's Chemical Composition

Chemical Composition	Fly Ashes		Other SCMs
	Class F	Class C	Slag
SiO_2, %	52.07	30.76	35.91
Al_2O_3, %	23.65	17.75	11.98
Fe_2O_3, %	4.55	5.98	0.94
Sum of SiO_2, Al_2O_3, Fe_2O_3, %	80.27	54.49	48.83
CaO, %	12.76	28.98	44.1
MgO, %	2.02	6.55	8.9
SO_3, %	0.78	3.64	1.63
Na_2O, %	0.31	2.15	-
K_2O, %	0.80	0.30	-
Na_2O Eq., %	0.84	2.35	0.58
LOI, %	0.95	0.44	-

The mixture matrix consists of 27 concrete mixtures with varying w/cm, cement types, and SCMs. Table 17 and 18 shows the mixture proportions used in this study. Since ACI 201.2R-08 (2008) recommends a w/cm of 0.40 to 0.50 for casting in an aggressive environment, three water to cementitious materials ratios were selected in that range for the mix matrix. The mixture proportions were calculated using a typical seven sack cement proportion. Each mixture was proportioned with 658 $^{lb}/_{yd^3}$ (390 $^{kg}/_{m3}$) of cementitious materials. ACI 201.2R-08 (2008) has guidelines for cement content replacement by mass with SCMs for sulfate-resisting enhancement. It is recommended that either a fly ash proportion between 25% and 35% by mass or a slag proportion between 40% and 70% by mass be used in the mixture proportions. Based on these criteria, three SCMs were selected to improve the durability of the concrete: Class F fly ash, Class C fly ash, and Grade 120 slag. Each type of SCM had a low and high percentage replacement by cementitious mass in the testing regime. The two Class F ash

mixtures were tested at a 20% and 30% replacement of the cement by mass with a specific gravity of 2.34; whereas the Class C fly ash mixtures were tested at 20% and 40% replacement of the cement by mass with a specific gravity of 2.62. The Grade 120 slag mixtures were tested at a 35% and 50% replacement of the cement by mass with a specific gravity of 2.87. These SCMs' percentage cement replacements by mass values are typical dosages in the field. A polycarboxylate-based high-range water reducer was added to mixtures as needed to obtain a two to four inch slump. Normal dosages for the admixture range from 3 to 10 $^{oz}/_{cwt}$ (195 to 650 $^{ml}/_{100kg}$).

Table 17: w/cm Mixture Proportions

Material	Weight, lb. (kg)		
w/c	0.40	0.45	0.50
Water	263.2 (119.4)	296.1 (134.3)	329 (149.2)
Cement	658 (298.5)	658 (298.5)	658 (298.5)
Coarse Aggregate	1790.2 (812.0)	1790.2 (812.0)	1790.2 (812.0)
Fine Aggregate	1098.38 (498.2)	1098.38 (498.2)	1098.38 (498.2)

Table 18: SCM Mixture Proportions

Ternary Blend Description	Cement, $^{lb}/_{yd^3}$ ($^{kg}/_{m^3}$)	SCMs, $^{lb}/_{yd^3}$ ($^{kg}/_{m^3}$)
20 % Welsh	526.4 (312)	131.6 (78.1)
40 % Welsh	394.8 (234)	263.2 (156)
20% Rockdale	526.4 (312)	131.6 (78.1)
30% Rockdale	460.6 (273)	197.4 (117)
35% Slag	427.7 (254)	230.3 (137)
50% Slag	329 (195)	329 (195)

3.2.1.1 Nomenclature

Given the robust mix matrix, a labeling system was designed to simplify presentation of the data. The labeling system has three components: w/cm, cement type, and percentage of SCM replacement by mass, if any. This labeling system is presented in Table 19. For example, 0.50 - V – 30F has a w/cm of 0.50 with Type V cement that has a 30% Class F fly ash replacement by mass, calculated as percentage by mass of the total cementitious material. The mixture proportion labels that are bolded in Table 19 signifies that the mixture proportion also had two $11^1/_2$ in x $14^1/_2$ in (300 mm x 375 mm) tapered cylinders cast.

Table 19: Label System for Mixture Proportions

		w/cm		
		0.40	0.45	0.50
Type I Cement	control	0.40 - I	0.45 - I	**0.50 - I**
	20% C fly ash	**0.40 - I – 20C**	0.45- I – 20C	0.50 - I – 20C
	40% C fly ash	**0.40 - I – 40C**	0.45 - I – 40C	**0.50 - I – 40C**
	20% F fly ash	**0.40 - I – 20F**	0.45 - I – 20F	0.50 - I – 20F
	30% F fly ash	**0.40 - I – 30F**	0.45 - I – 30F	**0.50 - I – 30F**
	35% slag	**0.40 - I - 35S**	0.45 - I - 35S	0.50 - I - 35S
	50% slag	**0.40 - I - 50S**	0.45 - I - 50S	**0.50 - I - 50S**
Type V Cement	control	0.40 - V	0.45 - V	**0.50 - V**
	20% C fly ash	-	-	-
	40% C fly ash	-	-	**0.50 - V – 40C**
	20% F fly ash	-	-	-
	30% F fly ash	-	-	**0.50 - V – 30F**
	35% slag	-	-	-
	50% slag	-	-	**0.50 - V - 50S**

3.2.2 Test Procedure

All the concrete test specimens were batched, mixed, and cast at the Concrete Durability Center of the University of Texas at Austin. A revised ASTM C192 was used for mixing the concrete. All of the materials for the concrete mixtures were placed in the mixing room at least 24 hours before mixing to ensure that all the materials reached equilibrium with the temperature of the room. The mixing room is kept at 73 ±3 °F (23 ±1.67 °C). First, the aggregates were blended in a steel drum concrete mixer, and then the first half of the mixing water was added and mixed for 30 seconds. Next, the cementitious materials were added and blended for 30 seconds before the second half of the mixing water was added. The second half of the mixing water was poured in the mixer over a 30 second time period, at the end of which is the starting time for the age of the concrete specimens. The cementitious material was mixed for a total of two minutes, including the 30 seconds of mixing water addition, after which the concrete mixture was allowed to rest for 3 minutes before it was mixed again for 2 minutes. When needed, superplasticizer was added to the fresh concrete mixture to obtain a two to four inch. Usually, any incorporation of SCMs required a minimum dosage of the superplasticizer. Then, the fresh concrete was poured into wheel barrels for casting specimens. The slump of the mixtures was measured following ASTM C143 and the corresponding unit weight was calculated using ASTM C138.

Next, five 4 in x 8 in (100 mm x 200 mm) cylinders were cast for each of the 27 concrete mixtures, along with, two $11^1/_2$ in x $14^1/_2$ in (300 mm x 375 mm) tapered cylinders for 14 of the concrete mixtures, including: 0.40-I-20C, 0.40-I-40C, 0.4-I-20F, 0.40-I-30F, 0.40-I-35S, 0.40-I-50S, 0.50-I, 0.50-I-40C, 0.50-I-30F, 0.50-I-50S, 0.5-V, 0.50-V-40C, 0.50-V-30F, and 0.50-V-50S. The 4 in x 8 in (100 mm x 200 mm) cylinder specimens were cast in two equal volume lifts with at least 25 steel roddings after each

lift for consolidation, according to ASTM C192. The concrete was placed in the plastic cylinder molds using a scoop and the cylinders were tapped with a steel rod 12 to 16 times before consolidation to remove any entrapped air. The second rodding went to a depth of at least a third into the previous lift layer. The concrete cylinders were tapped by the rubber mallet after both lifts and consolidations. Then, the two $11^1/_2$ in x $14^1/_2$ in (300 mm x 375 mm) tapered cylinders per mixture proportion were cast in plastic, five gallon pails with three lifts. After each lift a 1 in. (25 mm) diameter vibrator was placed down the center of the five gallon pails for a few seconds to consolidate the specimens and remove any entrapped air. The vibrator was turned on right after insertion into the concrete five gallon pails and pushed down axial through the depth of the layers for a few seconds to minimize over consolidation. The vibrator was also turned off before the tip was removed from the fresh concrete thus following common practice in the field. If the concrete in the wheel barrel was stagnant for more than approximately 10 minutes, it was re-mixed with scoops to ensure that segregation did not occur. After all the cylinders had been cast for the mix, the excess concrete was removed from the top of the cylinders with a wooden trowel and allowed to bleed during setting. Depending on the concrete mixtures, the concrete cylinders were allowed to set for 30 to 60 minutes before being finished first with a wooden trowel, and then with a magnesium float. Next, the freshly made 4 in x 8 in (100 mm x 200 mm) concrete cylinders were capped with plastic lids to minimize water loss into the atmosphere. Also, groups of concrete cylinders were covered with wet burlap to further ensure adequate curing. The five gallon pails also had plastic covering the wet burlap sacks to minimize moisture loss. Curing was executed on the mix matrix as specified in ASTM C192.

After casting, specimens were demolded at 24 ± 1 hour and placed in a moist-curing room at 73 ºF (23 ºC) and 100% relative humidity that meets ASTM C192

specifications for a curing environment. The cylinder specimens were demolded with air pressure, which resulted in minor surface defects at the base of some of the 4 in x 8 in (100 mm x 200 mm) specimens. Due to a shortage of plastic 4 in x 8 in (100 mm x 200 mm) cylinder molds for the robust amount of specimens that were cast; the cylinder molds were re-used for this project. In order to re-use these 4 in x 8 in (100 mm x 200 mm) plastic cylinder molds a hole was drilled in the bottom of the molds, so that air pressure could be used to pop off the molds from the concrete cylinders. Before casting the cylinders, painter's tape was placed in the bottom of the plastic cylinder molds to eliminate cement paste bleeding through the hole. The tape was placed on the exterior and interior of the cylinder molds. The cylinders were moist-cured for 28 days before testing began. Before the concrete cylinders were placed in the field exposure site, each specimen was weighed in a moist condition. This means that the concrete cylinders were removed from the moist-cure room and then weighted for the initial weight measurements. The concrete cylinders were placed in the exposure ponds and subjected to 5% (33,000 ppm) sodium sulfate solution at approximately 96 days after being casting.

3.2.2.1 Exposure Site Design

The excavation of large trenches was avoided for this project by using above-ground tanks. Figure 31 shows these two above-ground tanks that were added to the sulfate exposure field that was previously created by Drimalas (2007) and expanded by Clement (2009). The two above-ground tanks were different shapes and composed of different material. One was an oval, galvanized steel tank 9.5 ft x 2.75 ft (2.9 m x 0.84 m) with an arc radius of 1.25 ft (0.38 m) that is denoted as Tank A. The other tank is a circular hexagon, denoted Tank B, in nature with an approximate diameter of 5.2 ft (1.58

m) and composed of polypropylene plastic. A sandy loam used for residential foundations in Austin, Texas was used as the fill material in the tanks, filled to a depth of 16 in (400 mm). Clement (2009) tested the loam and confirmed that sulfates were not present. Next, one 4 in x 8 in (100 mm x 200 mm) concrete cylinder and one $11^1/_2$ in x $14^1/_2$ in (300 mm x 375 mm) tapered concrete cylinder per mixture proportion was placed embedded in the sandy loam. The $11^1/_2$ in x $14^1/_2$ in (300 mm x 375 mm) tapered concrete cylinder were embedded to a depth of 7 ±½ in. (178 ±13 mm) and the 4 in x 8 in (100 mm x 200 mm) concrete cylinder were embedded one-third of the specimen's length. Then, sodium sulfate solutions of 5% (33,000 ppm) concentration were then added to each of the two tanks. To add the sodium sulfate solution, it was first mixed in 55 gallon drums by mechanical agitation, then the solution was pumped into the tanks. Following Drimalas (2007) and Clement's (2009) prior research, the sulfate solutions were initially kept at a height 3 in (75 mm) above the soil. The vertical cylinders provided the following three areas of exposure: submerged (in sulfate solution below grade), soil/solution interface zone (wetting/drying zone), and non-contact zone (above solution but subject to wicking action) (Drimalas 2007). Figure 32 is a diagram of the different concrete mixtures and the different sized concrete cylinder's locations in the two above-ground tanks.

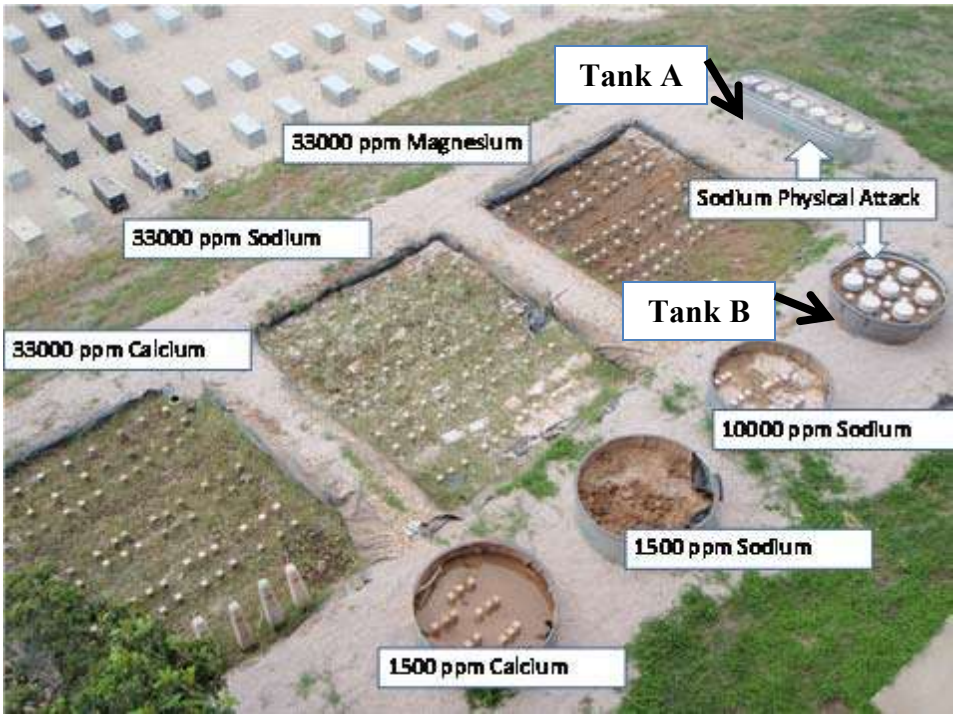

Figure 31: Sulfate Exposure Site in Austin, TX (Clement 2009)

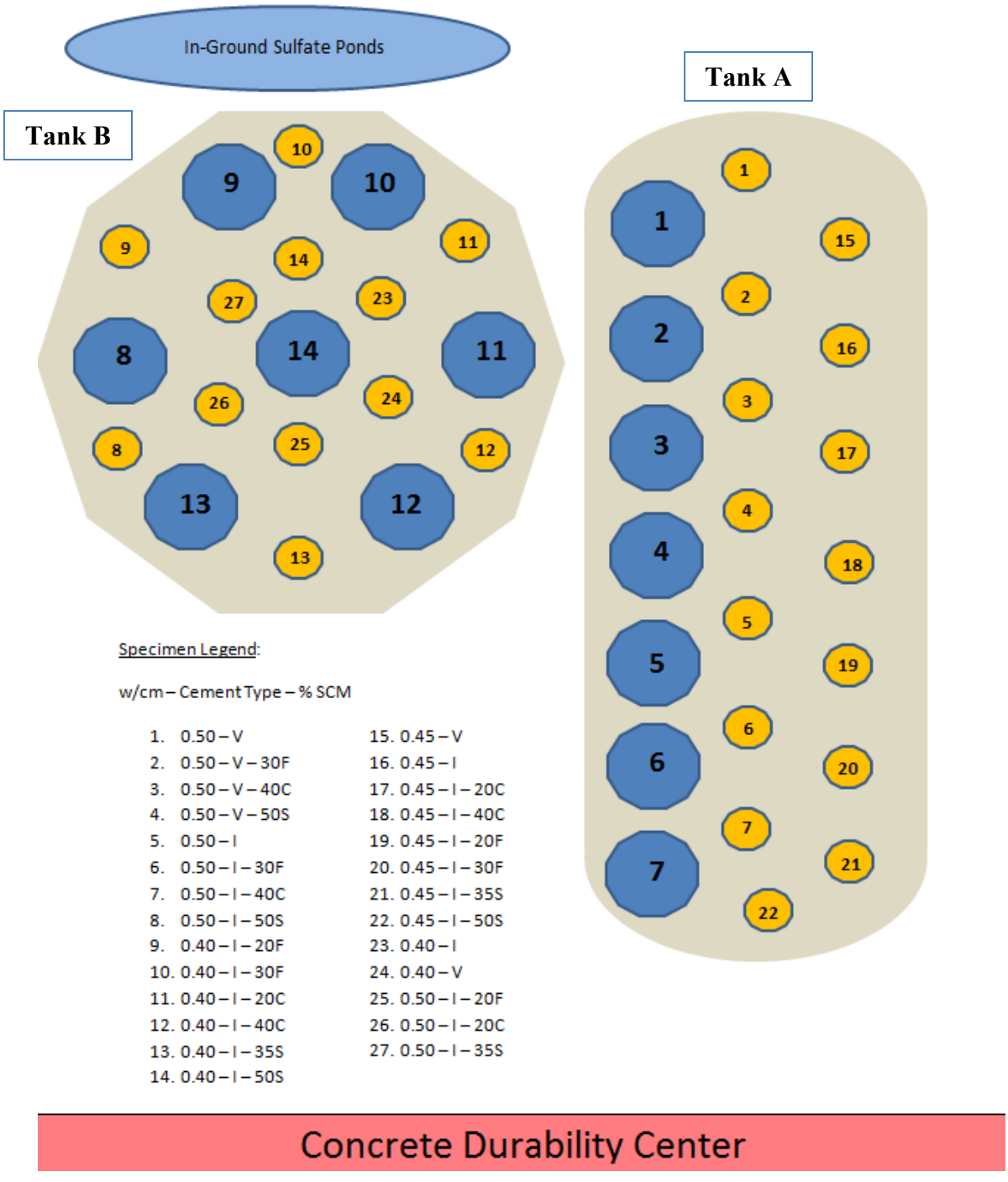

Figure 32: Sulfate Exposure Site Specimen Map in Austin, TX

The tanks were subsequently monitored and allowed to evaporate until the solutions reached the soil level and were then filled with water. As such, the concentrations of sulfates in the tanks are at a minimum when the water levels are at their highest (and initial) level and at a maximum when the water has evaporated to the point where the solution reaches the soil level or below (Drimalas 2007). The concentrations of the sodium sulfate solution also changed with time. Sodium sulfate has a high potential for wicking, therefore wicking salts could be blown out of the tanks by wind. The sulfate concentration levels in the tanks were checked several times over the course of the field testing. Based on the results, sodium sulfate was added to the tanks when needed to try to increase the concentration closer to a S3 sulfate exposure classification, as well as, maintain a balance between the two tanks in sulfate concentrations. Figure 31 shows the water-soluble sulfate concentrations in the soil of the tanks, according to ASTM C1580, after implementation of the 5% (33,000 ppm) sodium sulfate solution concentration at the start of the study. An 8:1 and 80:1 extraction ratio was used in the ASTM standard. For the first and second soil analysis sampling and testing, the soil samples were taken from the bottom layer of the tanks and a few inches below the top surface of the soil for both tanks, which were tested separately. The results showed that more sulfates were present in the upper layer of soil. Based on this result and the fact that this upper soil layer was where the concrete cylinders were exposed to sulfate ions, the later ASTM C1580 tests only tested samples from a few inches below the top surface of the soil. When taking any soil samples for each tank, soil samples were taken from several locations to get an averaged concentration of sulfates in the soil for the given tank. The first set of concentration results is not depicted in Table 20 because the results didn't qualify as valid under ASTM C1580 due to inexperience with the test method's dilution ratios and data validation criteria. After each soil test was run, ten to fifteen pounds of technical grade

sodium sulfate was added to each tank in an attempt to get it to a S3 sulfate exposure classification (Table 2).

Table 20: Water-Soluble Sulfate in Soil

	Sampling Dates							
	9/6/2010				10/21/2010		12/30/2010	
	Bottom Sample		Top Sample					
	Sulfate Concentrations							
Tank	% SO_4	$\frac{\text{mg } SO_4}{\text{kg soil}}$	% SO_4	$\frac{\text{mg } SO_4}{\text{kg soil}}$	% SO_4	$\frac{\text{mg } SO_4 \text{ kg}}{\text{soil}}$	% SO_4	$\frac{\text{mg } SO_4 \text{ kg}}{\text{soil}}$
Tank A - Oval	0.55	5500	0.85	8500	0.90	9000	1.06	10600
Tank B - Circle	0.49	4900	0.38	3800	1.08	10800	2.15	21500

In Table 20 for the majority of the testing duration, the tanks were below a S3 sulfate classification (2% SO_4 or 20,000 $\frac{\text{mg SO4}}{\text{kg soil}}$). The increased sulfate concentration in Tank B over Tank A in the last measurement is attributed to an improper ratio of sodium sulfate additions to the tanks. Tank B suffered solution loss due to a crack in the tank right at the soil line. The crack had gone un-noticed for several months before crack propagation and sulfate crystallization in the crack made it visible. All of the solution above the soil line leaked out of the tank before the crack was sealed. Also, several attempts had to be made to adequately seal the crack. Sulfate crystallization extruded from the crack and salt crystals were found all over the outer surface and exterior soil in the vicinity of the tank's crack. An improper amount of sodium sulfate was added to Tank B to account for this loss of sulfate solution, thus the concentration between the two tanks was imbalanced. Adjustments were made to make the exposure conditions comparable between the two tanks but will not be presented herein. In addition, more severe distress was seen in the specimens of Tank A, even after this sulfate imbalance occurred between the two tanks.

3.2.2.2 Visual Rating System

Two visual rating systems were created to quantify the visual distress from salt scaling and to quantify the propensity of sulfate wicking. It was only practical to measure the mass gain or loss in the 4 in x 8 in (100 mm x 200 mm) concrete cylinders due to the size and weight of the larger $11^1/_2$ in x $14^1/_2$ in (300 mm x 375 mm) tapered concrete cylinders. The first visual rating system was used to assign values to the degree of scaling distress that occurred from the sodium sulfate solution. The other visual rating system analyzed the degree of wicking action, as quantified by the sodium sulfate wicking's coverage area. The two different rating scales were assigned a visual numerical rating ranging from 0 to 5. Both visual rating systems assigned separate numerical values to the sides of the concrete cylinders and another to the top surface of the concrete cylinders. The visual rating condition of the surface distress was taken directly from ASTM C672-03 and is:

0) No scaling
1) Very slight scaling (3mm [1/8 in] depth max, no coarse aggregate visible)
2) Slight to moderate scaling
3) Moderate scaling (some coarse aggregate visible)
4) Moderate to severe scaling
5) Severe scaling (coarse aggregate visible over entire surface)

The visual rating system for the wicking action seen on the different concrete cylinders by the amount of surface area covered by the crystalized sodium sulfate is:

0) 0%
1) <25%
2) ≥25%
3) ≥50%

4) ≥75%

5) ≈100%

The bottom surfaces and lower portions of the vertical faces were embedded in the soil and not inspected for either visual rating system. Examples of each numerical ranking value of the cylinders' surfaces are presented in Figures 33 to 38 for the scaling distress and Figures 39 to 44 for the wicking action. The specimens that depict the visual ratings on distress is for the $11^{1}/_{2}$ in x $14^{1}/_{2}$ in (300 mm x 375 mm) tapered concrete cylinders, while the 4 in x 8 in (100 mm x 200 mm) concrete cylinders depict the visual ratings on sulfate wicking coverage area because these type of specimens show the whole spectrum of values.

Figure 33: Visual Distress Rating of 0

Figure 34: Visual Distress Rating of 1

Figure 35: Visual Distress Rating of 2

Figure 36: Visual Distress Rating of 3

Figure 37: Visual Distress Rating of 4

Figure 38: Visual Distress Rating of 5

Figure 39: Wicking Area Rating of 0 (0%)

Figure 40: Wicking Area Rating of 1 (<25%)

Figure 41: Wicking Area Rating of 2 (≥25%)

Figure 42: Wicking Area Rating of 3 (≥50%)

Figure 43: Wicking Area Rating of 4 (≥75%)

Figure 44: Wicking Area Rating of 5 (≈100%)

3.2.2.3 Mass Change of 4 in x 8 in (100 mm x 200 mm) Concrete Cylinders

Mass change was recorded several times to date for each of the 4 in x 8 in (100 mm x 200 mm) concrete cylinders. One day prior to the measurement, the concrete cylinders were removed from the exposure site, cleaned of adhered soil and sulfates, wrapped with moist towels, and placed in a temperature and humidity controlled environment at 73 ºF (23 ºC) and a RH < 50% to ensure that thermal or moisture effects would not substantially impact the weights measured. After recording the mass change of all the specimens, photographs were taken to document the visual distress over time of the field trial.

3.2.2.4 Permeability Procedure

As part of this study, it was decided to evaluate the transport mechanisms for the various mixtures to determine if any trends existed between permeability (or actually electrical resistivity), capillary absorption, and deterioration.

Each mixture proportion had several cylinder segment cuts that remained in the moist-curing room while the laboratory testing was being performed. In order to determine the permeability of each mixture proportion, the Section B segments, which are the middle cut segment that contains two cut surfaces, were removed from the moist-cure room at approximately 409 days after casting for the permeability testing. These segments were not exposed to any sulfates or deionized water. Previous research by Riding et al. showed that ASTM C1202 or the rapid chloride permeability test (RCPT) can be modified to one reading taken after 5 minutes to calculate the concrete resistivity (Riding et al. 2008). This method was used to calculate the permeability of all the different concrete mixtures. In addition, select specimens were also run following ASTM

C1202's 6 hour test to further validate the results. All of the specimens that had both permeability methods conducted on the concrete specimens resulted in the same chloride ion permeability classification according to ASTM C1202. All of the specimens were rinsed off with tap water and returned to the moist-cure room once the RCPT was completed on all the concrete mixtures.

3.2.2.5 Absorption Procedure

In order to evaluate the capillary absorption of the physical sulfate attack testing specimens, two cylinder cuts were taken from the moist-cure room at approximately 502 days after casting to undergo ASTM C1585. Two of the top cut of the cylinder segments, Section A segments, were used in the absorption testing. These cut cylinder segments contained the finished surface of the cylinder. Section A segments were selected for testing, because the standard calls for at least the average of two specimens for reporting and the only segments with two specimens was Section A. In addition, the same cylinder segments that were used in the RCPT testing were analyzed in the absorption test.

3.3 EXPERIMENTAL RESULTS AND DISCUSSION

3.3.1 Physical Sulfate Attack

The results for the visual rating system are presented in Tables 21 for the 4 in x 8 in (100 mm x 200 mm) concrete cylinders and Table 22 for the $11^1/_2$ in x $14^1/_2$ in (300 mm x 375 mm) tapered concrete cylinders. The visual ratings of the cylinders' surface distress is after 2 years of field exposure to approximately 5% (33,000 ppm) of sodium sulfate solution. Water was sprayed onto the cylinders to remove the salt crystallization

from the cylinders prior to the visual surface distress recording. Also, the ratings for the wicking action were started at the 2 year mark of exposure, after all the crystallized salt particles were removed from the cylinders for inspection. The values for the rating of the wicking action were recorded over several days to get some insight to the rates of wicking from the different concrete mixtures. Day 0 is the 2 year mark of exposure, when all the cylinders were cleaned of any salt crystallization with water. Then, the visual rating of the wicking was recorded over a several day period. The measurements were taken within 2 hours of the same time that the measurements were taken on Day 0. No rain or other kinds of precipitation occurred during this wicking action analysis.

Due to the size of the 4 in x 8 in (100 mm x 200 mm) concrete cylinders, most of the specimens are suffering from moderate to severe damage. Now referencing Table 22, the $11^1/_2$ in x $14^1/_2$ in (300 mm x 375 mm) tapered concrete cylinders that have lower surface distress values show signs of paste cracking all across the evaporation front, similar to shrinkage cracks. Even though the visual distress is minimal, it can be safe to assume that the sulfate concentrations at the evaporation front are increasing to the point that scaling of the cement paste will occur in the near future.

Table 21: 4 in x 8 in (100 mm x 200 mm) Concrete Cylinders' Wicking Action

Mix Description	Day 0				Day 1		Day 3		Day 5	
	Visual Rating of Surface Distress (0-5)		Visual Rating of Wicking Action (0-5)		Visual Rating of Wicking Action (0-5)		Visual Rating of Wicking Action (0-5)		Visual Rating of Wicking Action (0-5)	
	Side Surface	Top Surface	Side Surface	Top Surface	Side Surface	Top Surface	Side Surface	Top Surface	Side Surface	Top Surface
0.40 - I	2	3	0	0	2	1	3	1	4	2
0.40 - I - 20C	3	3	0	0	3	0	4	1	4	3
0.40 - I - 40C	4	3	0	0	3	1	3	0	5	3
0.40 - I - 20F	2	4	0	0	2	1	4	1	4	3
0.40 - I - 30F	3	3	0	0	3	1	4	1	5	4
0.40 - I - 35S	3	3	0	0	4	1	4	1	5	4
0.40 - I - 50S	3	3	0	0	4	1	4	2	5	3
0.40 - V	1	2	0	0	1	0	2	1	3	0
0.45 - I	3	2	0	0	1	1	2	0	2	0
0.45 - I - 20C	4	3	0	0	3	1	3	0	4	1
0.45 - I - 40C	4	3	0	0	1	1	2	0	3	1
0.45 - I - 20F	4	2	0	0	1	1	2	0	3	1
0.45 - I - 30F	4	3	0	0	1	1	2	0	4	1
0.45 - I - 35S	3	3	0	0	1	1	2	0	3	0
0.45 - I - 50S	4	3	0	0	1	0	2	0	3	1
0.45 - V	2	3	0	0	1	0	2	0	3	0
0.50 - I	3	3	0	0	1	0	1	0	3	0
0.50 - I - 20C	4	3	0	0	4	1	4	2	5	4
0.50 - I - 40C	4	3	0	0	3	1	3	0	4	1
0.50 - I - 20F	4	2	0	0	4	1	4	1	5	4
0.50 - I - 30F	4	3	0	0	3	1	2	1	4	3
0.50 - I - 35S	3	5	0	0	4	2	4	1	5	4
0.50 - I - 50S	4	4	0	0	3	4	5	4	5	4
0.50 - V	3	4	0	0	1	0	2	0	4	1
0.50 - V - 40C	4	5	0	0	4	0	3	0	5	4
0.50 - V - 30F	5	4	0	0	4	1	4	1	5	2
0.50 - V - 50S	4	4	0	0	3	1	3	0	4	1

Table 22: $11^1/_2$ in x $14^1/_2$ in (300 mm x 375 mm) Concrete Cylinders' Surface Distress

Mix Description	Day 0				Day 1		Day 3		Day 5	
	Visual Rating of Surface Distress (0-5)		Visual Rating of Wicking Action (0-5)		Visual Rating of Wicking Action (0-5)		Visual Rating of Wicking Action (0-5)		Visual Rating of Wicking Action (0-5)	
	Side Surface	Top Surface	Side Surface	Top Surface	Side Surface	Top Surface	Side Surface	Top Surface	Side Surface	Top Surface
0.40 - I - 20C	1	2	0	0	1	0	2	0	2	1
0.40 - I - 40C	2	1	0	0	1	0	1	0	3	1
0.40 - I - 20F	3	3	0	0	1	0	2	0	2	1
0.40 - I - 30F	4	4	0	0	1	1	2	0	3	1
0.40 - I - 35S	3	2	0	0	1	0	2	0	2	1
0.40 - I - 50S	2	3	0	0	1	0	2	0	2	1
0.50 - I	3	1	0	0	1	0	2	0	2	1
0.50 - I - 40C	3	2	0	0	1	0	1	0	2	1
0.50 - I - 30F	3	2	0	0	2	0	2	0	2	1
0.50 - I - 50S	4	2	0	0	1	0	2	0	3	1
0.50 - V	3	1	0	0	1	0	2	0	2	0
0.50 - V - 40C	4	2	0	0	2	1	2	0	2	1
0.50 - V - 30F	5	4	0	0	3	1	3	0	4	1
0.50 - V - 50S	3	3	0	0	1	0	2	0	2	1

The mass change of the 4 in x 8 in (100 mm x 200 mm) concrete cylinders is presented in Table 23. Some of the specimens showed mass gain in some of the measurements; however, the visual distress of the cylinders depicts that there should have been a mass loss recorded. This could be the result of increased sulfate concentrations within the concrete at the evaporation front. Figures 45 to 48 depict this occurrence, which were taken at the last mass measurement for the specimens. All the damage and mass losses of the 4 in x 8 in (100 mm x 200 mm) concrete cylinders occurred at the evaporation front. Excavation around many of the $11^1/_2$ in x $14^1/_2$ in (292 mm x 368 mm) tapered concrete cylinders' bases also proved that damage was only occurring at the

evaporation front of the specimens. The location of damage to these 4 in x 8 in (100 mm x 200 mm) concrete cylinders supports Drimalas (2007) and Clement's (2009) prior research that sodium sulfate is more aggressive in the physical mechanism than from chemical sulfate attack.

Table 23: 4 in x 8 in (100 mm x 200 mm) Concrete Cylinders' Mass Change

Approximate Age of Specimens (days):	96	589		817	
Mix Label	Initial Weight (g)	Weight (g)	Mass Change	Weight (g)	Mass Change
0.4 I	3905.3	3857.6	-1.22%	3865.1	**-1.03%**
0.4 I 20C	3958.0	3933.0	-0.63%	3931.2	-0.68%
0.4 I 40C	3853.6	3832.4	-0.55%	3809.6	-1.14%
0.4 I 20F	3878.1	3847.3	-0.79%	3847.6	**-0.79%**
0.4 I 30F	3882.4	3864.6	-0.46%	3852.4	-0.77%
0.4 I 35S	3925.6	3913.2	-0.32%	3908.2	-0.44%
0.4 I 50S	3907.4	3887.7	-0.50%	3876.3	-0.80%
0.4 V	3941.0	3891.9	-1.25%	3896.1	**-1.14%**
0.45 I	3914.8	3869.8	-1.15%	3869.7	**-1.15%**
0.45 I 20C	3902.3	3862.5	-1.02%	3830.3	-1.85%
0.45 I 40C	3978.6	3952.7	-0.65%	3908.5	-1.76%
0.45 I 20F	3898.2	3877.6	-0.53%	3860.4	-0.97%
0.45 I 30F	3904.8	3883.6	-0.54%	3853.6	-1.31%
0.45 I 35S	3926.7	3903.4	-0.59%	3898.5	-0.72%
0.45 I 50S	3909.1	3893.3	-0.40%	3873.8	-0.90%
0.45 V	3965.9	3914.6	-1.29%	3913.9	-1.31%
0.5 I	3875.1	3831.4	-1.13%	3829.8	-1.17%
0.5 I 20C	3872.8	3838.8	-0.88%	3781.0	-2.37%
0.5 I 40C	3883.1	3854.1	-0.75%	3812.1	-1.83%
0.5 I 20F	3809.0	3784.4	-0.65%	3755.7	-1.40%
0.5 I 30F	3813.5	3792.6	-0.55%	3733.3	-2.10%
0.5 I 35S	3846.1	3820.3	-0.67%	3796.8	-1.28%
0.5 I 50S	3841.6	3816.8	-0.65%	3771.3	-1.83%
0.5 V	3916.8	3862.2	-1.39%	3855.8	-1.56%
0.5 V 40C	3878.2	3858.0	-0.52%	3784.9	-2.41%
0.5 V 30F	3807.2	3779.2	-0.74%	3647.3	-4.20%
0.5 V 50S	3850.9	3829.5	-0.56%	3727.6	-3.20%

Figure 45: 0.40 – I's 4 in x 8 in (100 mm x 200 mm) Outdoor Exposure

Figure 47: 0.40 - V 4 in x 8 in (100 mm x 200 mm) Outdoor Exposure

Figure 46: 0.40 – I – 20F 4 in x 8 in (100 mm x 200 mm) Outdoor Exposure

Figure 48: 0.45 - I 4 in x 8 in (100 mm x 200 mm) Outdoor Exposure

3.3.1.1 w/cm

For the 4 in x 8 in (100 mm x 200 mm) concrete cylinders there was visually more damage in the two higher w/cm mixtures, which could be due to the slight reduction in permeability from the lower w/cm, as seen in Table 21. Also, the mixtures with tapered cylinders at lower w/cm show less visual distress than the high w/cm. In Table 23, it shows that decreasing the w/cm improved the durability of the mixture proportion since less mass loss occurred as the w/cm was decreased.

3.3.1.2 Cement Type

The three concrete mixtures that had the most mass loss to date contained the Type V cement, as seen in Table 23. Once again, Type V cement appears to be a chemical solution to a physical distress mechanism. Also, in each set of w/cm, the Type V straight cement had more mass loss than the Type I cement for the same w/cm.

3.3.1.3 Supplementary Cementing Materials

In Table 21, it can be seen that in each w/cm grouping of concrete mixtures, the straight cement mixtures have lower visual distress values than the concrete mixtures with SCMs. Adding SCMs to a mixture proportion reduces the permeability of the specimen, but these concrete mixtures show more signs of visual distress; therefore, increased absorption could be adversely affecting their performance. Generally, the higher SCM percentages have more visual wicking action than the lower percentage replacements. Also, many of the 0.50 w/cm $11^{1}/_{2}$ in x $14^{1}/_{2}$ in (300 mm x 375 mm) tapered concrete cylinders in Table 22 with SCMs show more visual distress than the 0.50 w/cm with straight Type I or Type V cement. In addition, it appears from the data

that the higher SCM replacements have a higher propensity for sulfate wicking, which could be due to higher sorptivity of these concrete mixtures.

In Table 23, the majority of SCM mixture pairs for any given w/cm show that increasing the percentage replacement by mass of the SCM degraded the concrete mixtures durability to physical sulfate attack. This could signify that the increased absorption and not the reduced permeability of the concrete matrix affects the performance of the mixture proportion to the physical distress mechanism. It is important to note that the three concrete mixtures with the highest mass loss were 0.50 w/cm with Type V cement and contained the higher SCM replacement percentage. Also, the high SCM percentages' reduced permeability should have improved the durability of these specimens to physical sulfate attack. Further conclusions were drawn from this occurrence when the data was also compared to the laboratory results later in Section 3.3.4 (Field and Laboratory Comparison).

3.3.2 Permeability

At the conclusion to the laboratory study only a few of the concrete cylinders in the outdoor exposure were showing signs of surface distress; therefore, no insight could be given from the correlation of the field and laboratory exposure conditions. To supplement this data to allow for future correlations when deterioration becomes more pronounced, the mixtures were evaluated to determine their electrical resistivity (as surrogate for permeability/diffusion assessment) and surface absorption.

As part of this study, it was decided to evaluate the transport mechanisms for the various mixtures to determine if any trends existed between permeability (or actually electrical resistivity), capillary absorption, and deterioration. These permeability results

from the 5-minute modified RCPT (Riding et al. 2008) and ASTM C1202 test are presented in Table 24.

Table 24: RCPT Results

Mix Description	5 Minute Charge Passed (coulombs)		6 Hour ASTM C1202 Charge Passed (coulombs)		Chloride Ion Penetrability Classification (based on 2.5 in. 5-minute results)
	2.5 in. Specimen Length	Predicted 2 in. Specimen Length	2.5 in. Specimen Length	Predicted 2 in. Specimen Length	
0.40 - I	2270	1960	1940	1680	Moderate
0.40 - I - 20C	320	260	-	-	Very Low
0.40 - I - 40C	790	660	-	-	Very Low
0.40 - I - 20F	90	80	-	-	Negligible
0.40 - I - 30F	30	30	460	390	Negligible
0.40 - I - 35S	50	40	-	-	Negligible
0.40 - I - 50S	40	30	760	630	Negligible
0.40 - V	2530	2080	-	-	Moderate
0.45 - I	2270	1940	2820	2410	Negligible
0.45 - I - 20C	1480	1230	1440	1200	Low
0.45 - I - 40C	850	720	-	-	Very Low
0.45 - I - 20F	830	690	770	640	Very Low
0.45 - I - 30F	40	30	-	-	Negligible
0.45 - I - 35S	1210	1030	1065	910	Very Low
0.45 - I - 50S	780	670	830	710	Low
0.45 - V	2620	2100	-	-	Moderate
0.50 - I	1970	1620	2380	1950	Moderate
0.50 - I - 20C	1630	1410	-	-	Low
0.50 - I - 40C	270	220	-	-	Very Low
0.50 - I - 20F	280	240	-	-	Very Low
0.50 - I - 30F	310	270	-	-	Very Low
0.50 - I - 35S	1290	1100	1250	1070	Low
0.50 - I - 50S	330	280	-	-	Very Low
0.50 - V	3240	2730	-	-	Moderate
0.50 - V - 40C	70	60	-	-	Negligible
0.50 - V - 30F	380	320	-	-	Very Low
0.50 - V - 50S	40	30	120	100	Negligible

3.3.3 Absorption

Another potential driving mechanism of physical sulfate attack is the sorption (sorptivity) of the concrete specimen. Sorptivity is a near surface effect where water uptake is governed by capillary suction of the concrete. Water saturated with deleterious salts' absorption into concrete could be the overlying driving force of physical sulfate attack. These absorption results are shown in Table 25 and 26. The only modification to the ASTM standard was that a weighing scale with a 0.1 gram precision was used instead of the 0.01 gram precision that the standard calls for and the specimens were slightly longer than required. According to ASTM C1585, the initial absorption is denoted as the slope of the line that is best fit to I (absorption) plotted against the square root of time using least-squares linear regression analysis from 1 minute to 6 hours. The secondary absorption is from 1 day to 7 days. Readings were taken out to 9 days, in order to get better correlation with some of the secondary absorption values when needed. For both absorption values, the data has to have a linear relationship, which means a correlation coefficient greater or equal to 0.98 and show systematic curvature. Some of the absorption values were slightly adjusted to show a slight increase in mass or the same mass as the previous measurement, because several measurements showed a loss in mass during testing which should not happen. Also, all specimens had a good absorption increase over time even though a scale with a precision to 0.1 grams instead of the ASTM specified 0.01 gram precision was used. All of the values were considered valid for our concerns, even though data sets failed the 0.98 correlation coefficient criteria. These "failed ASTM" data sets didn't show a sufficient enough mass increase between measurements so the data was considered to not be linear enough by the ASTM standards. Generally, when the same specimen mixture proportion has two fairly different absorption values the higher of the two has a better correlation coefficient

Table 25: Absorption Results for Averaged Segment A's

Mix Label	Initial Rate of Absorption (mm/√s)	Correlation Coefficient (≥ 0.98)	Secondary Rate of Absorption (mm/√s)	Correlation Coefficient (≥ 0.98)
0.4 I	0.0004	0.9695	0.00025	0.987
0.4 V	0.0002	0.9115	0.0002	0.98
0.4 I 20C	0.00085	0.988	0.00025	0.9815
0.4 I 40C	0.0008	0.9765	0.0002	0.9765
0.4 I 20F	0.00065	0.974	0.0001	0.949
0.4 I 30F	0.00095	0.987	0.0002	0.986
0.4 I 35S	0.0012	0.9815	0.00025	0.985
0.4 I 50S	0.0011	0.9765	0.00015	0.9655
0.45 I	0.0004	0.9605	0.00025	0.9865
0.45 V	0.0008	0.977	0.00045	0.996
0.45 I 20C	0.00055	0.9765	0.0002	0.9895
0.45 I 40C	0.00095	0.9705	0.0003	0.9905
0.45 I 20F	0.001	0.9875	0.0002	0.9815
0.45 I 30F	0.001	0.984	0.00025	0.9825
0.45 I 35S	0.00105	0.971	0.0002	0.977
0.45 I 50S	0.0012	0.971	0.0002	0.993
0.5 I	0.00065	0.9845	0.0004	0.9905
0.5 V	0.0003	0.943	0.00045	0.994
0.5 I 20C	0.001	0.9905	0.00045	0.9935
0.5 I 40C	0.00105	0.9785	0.0003	0.978
0.5 I 20F	0.001	0.967	0.0003	0.995
0.5 I 30F	0.0016	0.9965	0.00055	0.9915
0.5 I 35S	0.0014	0.9695	0.0003	0.9785
0.5 I 50S	0.0019	0.9855	0.0004	0.9905
0.5 V 40C	0.00175	0.9795	0.0004	0.993
0.5 V 30F	0.00175	0.9855	0.0003	0.9705
0.5 V 50S	0.0017	0.981	0.0003	0.9815

Table 26: Absorption Results for Segment B (used in RCPT)

Mix Label	Initial Rate of Absorption (mm/√s)	Correlation Coefficient (> 0.98)	Secondary Rate of Absorption (mm/√s)	Correlation Coefficient (> 0.98)
0.4 I	0.0003	0.952	0.0002	0.976
0.4 V	0.0002	0.867	0.0001	0.964
0.4 I 20C	0.0008	0.981	0.0002	0.985
0.4 I 40C	0.0008	0.987	0.0002	0.971
0.4 I 20F	0.0007	0.976	0.0001	0.908
0.4 I 30F	0.0009	0.984	0.0002	0.986
0.4 I 35S	0.0012	0.974	0.0003	0.991
0.4 I 50S	0.0010	0.975	0.0002	0.973
0.45 I	0.0003	0.941	0.0002	0.989
0.45 V	0.0004	0.970	0.0004	0.994
0.45 I 20C	0.0003	0.974	0.0001	0.988
0.45 I 40C	0.0008	0.963	0.0003	0.986
0.45 I 20F	0.0011	0.984	0.0002	0.984
0.45 I 30F	0.0010	0.990	0.0003	0.988
0.45 I 35S	0.0009	0.970	0.0002	0.980
0.45 I 50S	0.0010	0.972	0.0002	0.994
0.5 I	0.0006	0.990	0.0003	0.988
0.5 V	0.0003	0.956	0.0003	0.998
0.5 I 20C	0.0010	0.990	0.0004	0.994
0.5 I 40C	0.0009	0.989	0.0003	0.977
0.5 I 20F	0.0009	0.957	0.0003	0.997
0.5 I 30F	0.0018	0.995	0.0007	0.993
0.5 I 35S	0.0015	0.955	0.0003	0.975
0.5 I 50S	0.0014	0.987	0.0004	0.991
0.5 V 40C	0.0016	0.978	0.0004	0.995
0.5 V 30F	0.0013	0.987	0.0003	0.976
0.5 V 50S	0.0016	0.977	0.0003	0.981

Generally, the straight cement mixtures had the lowest absorption rate with Type V cements had lower absorption than the Type I cement specimens in two out of the three different water to cementitious ratios. Some trends that were evident in the absorption data are shown below:

- 0.40 < 0.45 < 0.50
- Class C Fly Ash < Class F Fly Ash
- Straight cement < Fly Ash < Slag

The mixtures containing slag had almost all the highest absorption values. Also, the five highest absorption values had a 0.50 w/cm and the highest SCM replacement with three of them containing Type V cement.

3.3.4 Field and Laboratory Comparison

Based on all the previous laboratory data presented in Chapter 2 and the outdoor exposure data presented in this chapter several observations on physical sulfate attack could be made. The data was ranked according to the outdoor and laboratory performance separately to try to draw some trends between the two different testing conditions. In Table 27 the different concrete mixtures are ranked according to the performance of the 4 in x 8 in (100 mm x 200 mm) concrete cylinders in outdoor exposure evaluated from least to most mass loss to date. Then, in Table 28 the different concrete mixtures are ranked according to the performance of the 4 in x 8 in (100 mm x 200 mm) concrete cylinder segments in the cyclical laboratory exposure evaluated from least to most mass loss at the end of the test.

Overall, based on the outdoor data it seems that the incorporation of higher SCM dosages and Class C fly ash can be detrimental to a concrete specimen's durability to

physical sulfate attack. Also, lowering the w/cm improves the concrete's durability. Most of the specimen's in Table 27 that had higher mass loss recorded for the outdoor exposure had higher absorption values as compared to the other specimens. Also, many of the mixtures with higher permeability performed moderately in the outdoor testing. It is important to note that most of the concrete mixtures with less mass loss in the field testing had a 0.40 w/cm. In Table 28, shows that the permeability mechanism had more effect on the laboratory testing results because most of the specimen's with the higher permeability values for the testing matrix suffered the highest mass loss at the end of the study. The slag concrete mixtures had superior performance in the laboratory study but were scattered throughout the field data's ranking of performance.

Table 27: Data Comparison Ranked According to Outdoor 4 in x 8 in (100 mm x 200 mm) Concrete Cylinders' Performance

Mix Label	Outdoor Exposure 4x8in (100x200mm) Mass Gain/Loss	Visual Rating for Side Surface Distress (0-5)		Initial Rate of Absorption (mm/√s)	RCPT Charge Passed (coulombs)	f_c', psi (Mpa)	Lab Cyclical 30% Na_2SO_4		10% Mass Loss Failure Criterion	
		4x8 in (100x200 mm)	11.5x14.5 in (290x370 mm)				Mass Gain/Loss	Number of cycles	Mass Gain/Loss	Number of cycles
0.4 I 35S	-0.44%	3	3	0.0012	50	7408 (51.1)	-1.9%	731	-	-
0.4 I 20C	-0.68%	3	1	0.0009	320	6757 (46.6)	-17.3%	731	-17.30%	731
0.45 I 35S	-0.72%	3	-	0.0011	1210	7512 (51.8)	-4.9%	712	-	-
0.4 I 30F	-0.77%	3	4	0.0010	30	7085 (48.9)	-8.7%	731	-	-
0.4 I 20F	-0.79%	2	3	0.0007	90	6093 (42.0)	-8.0%	731	-	-
0.4 I 50S	-0.80%	3	2	0.0011	40	6392 (44.1)	-3.5%	731	-	-
0.45 I 50S	-0.90%	4	-	0.0012	780	6519 (44.9)	-1.4%	712	-	-
0.45 I 20F	-0.97%	4	-	0.0010	830	7253 (50.0)	-12.5%	712	-12.48%	712
0.4 I	-1.03%	2	-	0.0004	2270	7138 (49.2)	-53.0%	712	-10.48%	412
0.4 V	-1.14%	1	-	0.0002	2530	9087 (62.6)	-18.6%	710	-18.56%	710
0.4 I 40C	-1.14%	4	2	0.0008	790	7782 (53.7)	-9.6%	731	-	-
0.45 I	-1.15%	3	-	0.0004	2270	6832 (47.1)	-35.6%	712	-10.08%	376
0.5 I	-1.17%	3	3	0.0007	1970	5315 (36.6)	-67.2%	710	-14.39%	374
0.5 I 35S	-1.28%	3	-	0.0014	1290	7230 (49.8)	-11.6%	712	-11.56%	712
0.45 V	-1.31%	2	-	0.0008	2620	8170 (56.3)	-40.8%	710	-10.41%	442
0.45 I 30F	-1.31%	4	-	0.0010	40	5903 (40.7)	-11.7%	712	-11.68%	712
0.5 I 20F	-1.40%	4	-	0.0010	280	5096 (35.1)	-24.0%	712	-13.00%	712
0.5 V	-1.56%	3	3	0.0003	3240	7324 (50.5)	-47.6%	710	-14.03%	710
0.45 I 40C	-1.76%	4	-	0.0010	850	7373 (50.8)	-12.7%	712	-12.74%	712
0.5 I 40C	-1.83%	4	3	0.0011	270	5393 (37.2)	-17.5%	710	-10.11%	710
0.5 I 50S	-1.83%	3	4	0.0019	330	6021 (41.5)	-6.1%	710	-	-
0.45 I 20C	-1.85%	4	-	0.0006	1480	6397 (44.1)	-30.1%	712	-10.28%	444
0.5 I 30F	-2.10%	4	3	0.0016	310	4402 (30.3)	-14.7%	710	-14.67%	710
0.5 I 20C	-2.37%	4	-	0.0010	1630	6131 (42.3)	-42.3%	712	-11.95%	376
0.5 V 40C	-2.41%	4	4	0.0018	70	5814 (40.1)	-19.7%	710	-19.65%	710
0.5 V 50S	-3.20%	4	3	0.0017	40	6743 (46.5)	-7.5%	710	-	-
0.5 V 30F	-4.20%	5	5	0.0018	380	4464 (30.8)	-21.3%	710	-11.15%	442

Table 28: Data Comparison Ranked According to Cyclical Laboratory 4 in x 8 in (100 mm x 200 mm) Concrete Cylinders' Performance

Mix Label	Lab Cyclical 30% Na_2SO_4		10% Mass Loss Failure Criterion		Initial Rate of Absorption (mm/√s)	RCPT Charge Passed (coulombs)	f_c', psi (Mpa)	Outdoor Exposure 4x8in (100x200mm) Mass Gain/Loss	Visual Rating for Side Surface Distress (0-5)	
	Mass Gain/Loss	Number of cycles	Mass Gain/Loss	Number of cycles					4x8 in (100x200 mm)	11.5x14.5 in (290x370 mm)
0.45 I 50S	-1.4%	712	-	-	0.0012	780	6519 (44.9)	-0.90%	4	-
0.4 I 35S	-1.9%	731	-	-	0.0012	50	7408 (51.1)	-0.44%	3	3
0.4 I 50S	-3.5%	731	-	-	0.0011	40	6392 (44.1)	-0.80%	3	2
0.45 I 35S	-4.9%	712	-	-	0.0011	1210	7512 (51.8)	-0.72%	3	-
0.5 I 50S	-6.1%	710	-	-	0.0019	330	6021 (41.5)	-1.83%	4	4
0.5 V 50S	-7.5%	710	-	-	0.0017	40	6743 (46.5)	-3.20%	4	3
0.4 I 20F	-8.0%	731	-	-	0.0007	90	6093 (42.0)	-0.79%	2	3
0.4 I 30F	-8.7%	731	-	-	0.0010	30	7085 (48.9)	-0.77%	3	4
0.4 I 40C	-9.6%	731	-	-	0.0008	790	7782 (53.7)	-1.14%	4	2
0.5 I 35S	-11.6%	712	-11.56%	712	0.0014	1290	7230 (49.8)	-1.28%	3	3
0.45 I 30F	-11.7%	712	-11.68%	712	0.0010	40	5903 (40.7)	-1.31%	4	-
0.45 I 20F	-12.5%	712	-12.48%	712	0.0010	830	7253 (50.0)	-0.97%	4	-
0.45 I 40C	-12.7%	712	-12.74%	712	0.0010	850	7373 (50.8)	-1.76%	4	-
0.5 I 30F	-14.7%	710	-14.67%	710	0.0016	310	4402 (30.3)	-2.10%	4	3
0.4 I 20C	-17.3%	731	-17.30%	731	0.0009	320	6757 (46.6)	-0.68%	2	1
0.5 I 40C	-17.5%	710	-10.11%	550	0.0011	270	5393 (37.2)	-1.83%	4	3
0.4 V	-18.6%	710	-18.56%	710	0.0002	2530	9087 (62.6)	-1.14%	1	-
0.5 V 40C	-19.7%	710	-19.65%	710	0.0018	70	5814 (40.1)	-2.41%	4	4
0.5 V 30F	-21.3%	710	-11.15%	442	0.0018	380	4464 (30.8)	-4.20%	5	5
0.5 I 20F	-24.0%	712	-13.00%	552	0.0010	280	5096 (35.1)	-1.40%	4	-
0.45 I 20C	-30.1%	712	-10.28%	444	0.0006	1480	6397 (44.1)	-1.85%	4	-
0.45 I	-35.6%	712	-10.08%	376	0.0004	2270	6832 (47.1)	-1.15%	3	-
0.45 V	-40.8%	710	-10.41%	442	0.0008	2620	8170 (56.3)	-1.31%	2	-
0.5 I 20C	-42.3%	712	-11.95%	376	0.0010	1630	6131 (42.3)	-2.37%	4	-
0.5 V	-47.6%	710	-14.03%	374	0.0003	3240	7324 (50.5)	-1.56%	3	3
0.4 I	-53.0%	712	-10.48%	412	0.0004	2270	7138 (49.2)	-1.03%	2	-
0.5 I	-67.2%	710	-14.39%	374	0.0007	1970	5315 (36.6)	-1.17%	3	3

3.4 SUMMARY

This chapter presented and discussed the results of concrete cylinders exposed to approximately 5% (33,000 ppm) sodium sulfate in an outdoor sulfate exposure site in Austin, TX. The cylinders cast for the study were evaluated with a visual, numerical ranking system for both the concrete's scaling distress and wicking action. The smaller, 4 in x 8 in (100 mm x 200 mm) concrete cylinders were also measured for mass change. Comparisons to the laboratory results from Chapter 2 were reported.

The resistance to the physical sodium sulfate attack mechanism is most likely due to the reduced absorption in the concrete matrix. The lack of additional CaO into the concrete mixtures from a Class C fly ash also appears to improve the durability. The cement type does not play an important role in exposure to physical sulfate distress, although all the Type I cements for a given w/cm are superior to ones with Type V cement. Overall, reducing the w/cm seems to provide the most improved durability to physical sodium sulfate attack. The majority of the concrete mixtures with higher permeability performed moderately in the outdoor testing, however many of these specimens had the least durability in the laboratory testing previously presented in Chapter 2. No correlation to the slag's improved performance in the laboratory testing could be drawn by their outdoor performances because these mixtures fell sporadically in the outdoor ranked results. In conclusion, mixtures that correspond to suggestive preventative measures from ACI 318-08 performed poorly to the aggressive mechanisms of physical sodium sulfate attack. More research on the mechanisms behind this deterioration is needed in the near future to provide adequate guidelines for practitioners.

3.5 WORKS CITED

ACI 201.2R, "Guide to Durable Concrete." Manual of Concrete Practice, 2001.

ACI 318-08, “Building Code Requirements for Structural Concrete and Commentary” American Concrete Institute. Farmington Hills, MI, 2008.

ASTM C 33, “Standard Specification for Concrete Aggregates,” ASTM International, West Conshohocken, PA, 2009.

ASTM C 138, “Standard Test Method for Density (Unit Weight), Yield, and Air Content (Gravimetric) of Concrete,” ASTM International, West Conshohocken, PA, 2010.

ASTM C 143, “Standard Test Method for Slump of Hydraulic-Cement Concrete,” ASTM International, West Conshohocken, PA, 2010.

ASTM C 150, “Standard Specification for Portland Cement,” ASTM International, West Conshohocken, PA, 2009.

ASTM C 192, “Standard Practice for Making and Curing Concrete Test Specimens in the Laboratory,” ASTM International, West Conshohocken, PA, 2005.

ASTM C 618, “Standard Specification Coal Fly Ash and Raw or Calcined Natural Pozzolan for Use in Concrete,” ASTM International, West Conshohocken, PA, 2008.

ASTM C 672, “Standard Test Method for Scaling Resistance of Concrete Surface Exposed to Deicing Chemicals,” ASTM International, West Conshohocken, PA, 2004.

ASTM C 778, “Standard Specification for Standard Sand,” ASTM International, West Conshohocken, PA, 2006.

ASTM C 1012, “Standard Test Method for Length Change of Hydraulic-Cement Mortars Exposed to a Sulfate Solution,” ASTM International, West Conshohocken, PA, 2004.

ASTM C 1202, “Standard Test Method for Electrical Indication of Concrete’s Ability to Resist Chloride Ion Penetration,” ASTM International, West Conshohocken, PA, 2009.

ASTM C 1240, “Standard Specification for Silica Fume Used in Cementitious Mixtures,” ASTM International, West Conshohocken, PA, 2011.

ASTM C 1580, “Standard Test Method for Water-Soluble Sulfate in Soil,” ASTM International, West Conshohocken, PA. 2005.

ASTM C 1585, “Standard Test Method for Measurement of Rate of Absorption of Water by Hydraulic-Measurement of Rate of Absorption of Water by Hydraulic-Cement Concretes,” ASTM International, West Conshohocken, PA, 2004.

Clement, J. C. *Laboratory and Field Evaluations of External Sulfate Attack, Phase II.* Austin, Texas: The University of Texas at Austin, 2009.

Drimalas, T. *Laboratory and Field Evaluations of External Sulfate Attack.* Austin, Texas: The University of Texas at Austin, 2007.

Folliard, K.J. and Sandberg, P., "Mechanisms of Concrete Deterioration by Sodium Sulfate Crystallization," *Proceedings, Third International ACI/CANMET Conference on Concrete Durability*, Nice, France, pp. 933-945, 1994.

Haynes, H., O’Neill, R., and Mehta, P.K., “Concrete Deterioration from Physical Attacks by Salts,” *Concrete International*, V.18, No. 1, pp. 63-68, January 1996.

Haynes, H., O’Neill, R., Neff, M., and Mehta, P. K, “Salt Weathering Distress on Concrete Exposed to Sodium Sulfate Environment,” *ACI Materials Journal*, V. 105, No. 1, Jan.-Feb., pp. 35-43, 2008.

Haynes, H., O’Neill, R., Neff, M., and Mehta, P.K., “Salt Weathering of Concrete by Sodium Carbonate and Sodium Chloride,” *ACI Materials Journal*, V. 107, No. 3, May-June, pp. 258-266, 2010.

Nehdi, M., and Hayek, M., “Behavior of Blended Cement Mortars Exposed to Sulfate Solutions Cycling in Relative Humidity,” *Cement and Concrete Research*, V. 35, pp. 731-742, 2005.

Scherer, G. W. “Stress from Crystallization of Salt.” *Cement and Concrete Research*, V. 34, pp. 1611-1624, 2004.

Stark, D., “Longtime Study of Concrete Durability in Sulfate Soils,” *Research and Development Bulletin RD086*, Portland Cement Association, Stokie, Ill., p. 13, 1984.

Stark, D., "Durability of Concrete in Sulfate Rich Soils," *Research and Development Bulletin RD 097*, Portland Cement Association, Skokie, Ill., p. 14, 1989.

Stark, D. C. "*Performance of Concrete in Sulfate Environments," RD129.* Skokie, Illinois: Portland Cement Association, 2002.

Chapter 4: Investigation on Adapting ASTM C1293 Test for Low-alkali Concrete

4.1 INTRODUCTION

Previous research has shown that that the American Society for Testing and Materials (ASTM) C1293 (Concrete Prism Test) standard test method has a deficiency associated with evaluating aggregates and concrete mixtures for the susceptibility of the alkali-silica reaction (ASR) when testing job mixtures. The main concern is testing a mixture with lower alkali loadings as leaching from prisms can lower the internal alkali content below a specific mixture's alkali threshold. In these cases, aggregates may pass the concrete prism test, but fail in the field. Currently, the best method for evaluating an aggregates susceptibility to ASR is casting large exposure blocks, which is not practical due to the duration of exposure needed to validate a mixture proportion can be substantial. In order to improve the ability of the concrete prism test to evaluate low-alkali mixtures, various modifications to the prism test were made and reported herein, each with the goal of minimizing the potential for leaching while still providing sufficient moisture to drive ASR-induced expansion.

4.1.1 Research Significance

Folliard et al. (2006) and others have shown that low-alkali concrete mixtures tested using ASTM C 1293 storage conditions may pass show little or no expansion during the course of the laboratory test, whereas concrete blocks cast from the same mixture will expand and crack. This is generally not an issue for higher-alkali mixtures, such as the standard ASTM C 1293 concrete mixtures, where the alkali content is raised to 1.25 percent. In this case, the specimens will still be prone to leaching of alkalis but

the high-alkali content still provides enough alkalinity to generate expansion. The goal of this research project is to attempt to modify the testing regime such that low-alkali mixtures that fail in outdoor exposure sites will also fail in accelerated laboratory testing.

4.1.2 Literature Review: Alkali-Silica Reaction

Alkali-silica reaction (ASR) was first discovered in the late 1930s by Thomas Stanton of California State Division of Highways. Stanton published the first paper on ASR in 1940, which described the nature of the reaction and showed that the reaction could be prevented by using low-alkali cements. Stanton (1940) found that using cement that had an alkali content below 0.60% Na_2O_e or the incorporation of pumicite, a pozzolan, to the cementitious material content could deter the ASR. Incorporating a pozzolan reduces the amount of cement content needed for a mixture proportion, thus reducing the total alkali content of the concrete mixture. The requirements for ASR are:

- Reactive silica aggregate
- Sufficient alkalis
- Sufficient moisture

ASR is common across the country and is often found in bridge structures, pavements, and Jersey barriers. ASR opens up concrete (cracks), which allows other forms of attack to occur. Generally, ASR does not cause structural failure but opens up the concrete matrix to other forms of concrete deterioration.

4.1.2.1 Preventing Alkali-Silica Reaction

To prevent ASR there is usually a focus on optimizing the hydration reactions to minimize the amount of alkalis, which lowers the pH to prevent ASR. More alkalis in

concrete results in a higher pH of the pore solution, which also increases the amount of dissolved silica thus propagating the ASR. When the reaction runs out of reactive silica or available alkalis, it ceases.

The alkali content in the cement is represented by the alkali equivalent (Na_2O_e), which incorporates the sodium and potassium alkalis into one value. The Na_2O_e is calculated as a percentage with the equation: $\%Na_2O + 0.658 \times \%K_2O$. However, it is more important to know the total concrete alkali content to evaluate a concrete mixture's susceptibility to ASR. The equation to calculate the concrete alkali content is:

$$\text{concrete alkali content} = \text{cement content } [{}^{lb}/_{yd^3}\ ({}^{kg}/_{m^3})] + \%\ Na_2O_e \times \frac{1}{100}$$

This is also referred to as the alkali loading of the concrete. Currently, there is not a way to incorporate the addition of alkalis from aggregates and SCMs; therefore the concrete alkali content is based on straight cement mixtures. The threshold alkali content varies with the type of reactive aggregate. Above this alkali threshold value deleterious expansion occurs. In 2008 the Texas Department of Transportation (TxDOT) reduced the concrete alkali loading limit from 4.0 ${}^{lb}/_{yd^3}$ (2.37 ${}^{kg}/_{m^3}$) to 3.5 ${}^{lb}/_{yd^3}$ (2.08 ${}^{kg}/_{m^3}$) due to ASR observations in concrete with alkali loadings below 4.0 ${}^{lb}/_{yd^3}$ (2.37 ${}^{kg}/_{m^3}$).

The easiest method to prevent ASR is to not use a reactive aggregate, however this cannot always be economical and the non-reactive aggregate sources are being depleted across the country. Some areas may not even have a non-reactive aggregate source. In addition, aggregates may be incorrectly identified as non-reactive and aggregate reactivity may vary from a given source. The most common way to prevent ASR in a reactive aggregate is to use low-alkali cement, limit the alkali content in the concrete, use of suitable chemical admixtures, and/or incorporate a pozzolan by replacing a portion of the cementitious material. When a pozzolan is used in the concrete mixtures, a cement dilution effect occurs, thus reducing the concrete alkali loading which results in

a reduced pH of the pore solution. The SCMs dilute the alkalis in solution by reducing the amount of portland cement for the concrete mixture. Also, the incorporation of SCMs produces more calcium silicate hydrates from the pozzolonic reaction, which bind more alkalis and thus reduces the pH of the pore solution. In addition, lithium salts can be used to create a non-expansive gel. Lithium creates a protective layer around the reactive aggregate to slow down the silica dissolution and prevent the alkalis from penetrating the reactive aggregate.

Decreasing the amount of moisture exposure to concrete reduces the probability of ASR. This can be done through the design of a structure to improve drainage away from concrete or by topical treatments to dry out the concrete. Silanes create a semi-permeable membrane that allows water vapor out but not into the concrete substructure, thus removing the water source necessary for ASR. Wehrle (2010) found that a silane's effectiveness is dependent on the size of the reactive concrete element and silanes were found to significantly reduce expansion for reactive depths of less than 5 in (127 mm), which can be significant for protecting reinforcing steel.

There are several standard test methods from the ASTM for evaluating an aggregates susceptibility to ASR. These test methods have developed over the decades, but they still often result in falsely diagnosing a reactive aggregate as non-reactive after the required one or two year testing duration, depending on the materials used in the mixture. More recently agencies have adopted ASTM C1293, known as the concrete prism test, as the standard for evaluating a concrete mixtures susceptibility to ASR, but as stated, this method is not suitable for evaluating low-alkali mixtures.

4.1.2.2 Test Methods and Specifications

The accelerated mortar bar test (AMBT) ASTM C1260 is a fast and aggressive test method for evaluating an aggregates susceptibility to for alkali-silica reactivity. For the test, mortar bars are soaked in 1N NaOH solution, which has a pH of 14, at 176°F (80°C) for 14 days. After 24 hours of moist cure, the mortar bars are placed into water at 176°F (80°C) for 24 hours. Then, initial measurements are taken before immersion into the NaOH solution at 176°F (80°C). An aggregate is classified as non-reactive if expansion does not exceed 0.10% after 14 days of immersion in 1N NaOH. Thomas et al. (2006) presented a comparison of test results from the CPT and AMBT for 184 combinations of materials, in which a given concrete mixture either passed or failed both test methods only 54% of the time. The AMBT method for evaluating aggregate reactivity is considered to be overly severe and Thomas et al. (2006) recommended that the test should only be used to accept and not reject aggregates. In 1997, Thomas et al. recommended that if an aggregate failed the AMBT, then the CPT method should be used to confirm the results before any actions are taken for classifying the aggregate.

The CPT method was adopted by ASTM in 1995 and is known as ASTM C1293. In the CPT, 3 in x 3 in x 11.25 in (75 mm x 75 mm x 285 mm) concrete prisms are cast and allowed to cure for 24 hours before initial measurements are taken. The length of the specimens is recorded over either one or two years depending on if the test is determining the aggregate reactivity or preventative measures. This test method uses an expansion limit of 0.04% at one year or the same limit at two years for preventative measures. The concrete prisms are vertically stored above standing water in five-gallon bucket containers at 100°F (38°C). This environment provides a humid environment for the concrete prisms, in which water condensates on the specimens and drains to the standing water at the bottom of the containers. This repeating cycle leaches out alkalis from the

concrete prisms. Water is needed for ASR to occur, but now it is prevalently known that alkalis leach out from the specimens thus reducing the severity of the observed ASR expansion. In the standard test method, the alkalis are boosted to 1.25%. This need for boosting the alkali content prevents the test method from accurately determining the alkali threshold level for an aggregate. Also, the need for boosting a concrete mixture makes this method not practical for evaluating a specific mixture proportion from a job.

Several studies have evaluated an accelerated CPT with shorter testing durations by increasing the exposure temperature to 140°F (60°C). Studies have proposed either a 3 or 6 month duration with varying expansion limits to correlate to the CPT. Currently some of the studies lack in repeatability and there has been insufficient investigation into this accelerated test for evaluating preventative measures (Thomas et al. 2006). Fournier et al. (2004) found that the accelerated temperature increases the rate of alkali leaching and reduces the pore solution pH. Ideker et al. (2010) found a significant reduction in expansion in the accelerated concrete prism test compared to the CPT. Also, Ideker et al. (2010) concluded that the selection of the non-reactive fine aggregate for either concrete prism test methods plays a crucial role in the expansion observed.

Low alkali loadings can be impossible to test due to alkali leaching in standard test methods, so large exposure blocks are needed to minimize this leaching effect. However, large exposure blocks present many problems with ASR testing due to their size, amount of materials needed, necessary outdoor exposure locations for a given environment, and long duration needed to see significant expansion. This does not make exposure blocks practical for testing job mixtures.

4.2 EXPERIMENTAL METHODS

4.2.1 Materials

4.2.1.1 Aggregates

There were two fine aggregates used in the testing, one of which is classified as a highly reactive aggregate from El Paso, TX. The other aggregate is a lightweight fine aggregate (LWFA), expanded shale, that was used to provide an internal water source for the reaction. The coarse aggregate selected was an ASTM C33 No. 57 gradation dolomitic limestone from Georgetown, TX. This coarse aggregate is considered to be non-reactive. The coarse aggregate was graded and blended to meet the specification of ASTM C1293, which calls for a 33% by mass for each sieve size of the coarse aggregate fraction retained on the ½ in (12.5 mm), ⅜ in (9.5 mm), and No. 4 (4.75 mm) sieves. The aggregates are presented with their mineralogy in Table 29.

Table 29: Aggregate Properties

Aggregate	Bulk SG (OD)	Bulk SG (SSD)	Apparent SG	Absorption (%)	Mineralogy
C1	2.50	2.55	2.67	2.77	dolomitic limestone
F1	2.59	2.61	2.64	0.69	mixed quartz/chert/feldspar sand
F2	1.73	1.85	1.96	6.77	expanded shale

4.2.1.2 Saturated Lightweight Aggregate as Internal Water Source

The use of saturated lightweight aggregate (SLWA), known as internal curing, could be used to provide an internal water source for ASR. However, the *w/cm* specified

in ASTM C1293 (0.42 to 0.45 by mass) could be too high to drive the water out of the SLWA because no self-desiccation is occurring in the cement paste. Henkensiefken et al. (2009a) showed that the degree of hydration increases with the addition of a SLWA resulting in a denser microstructure of the concrete. In the 140°F (60°C) testing environment there is a possibility of self-desiccation of the concrete specimens, thus release of the water from the SLWA should occur. This could cause more ASR gel in these samples. During cement hydration, the pore sizes of the concrete decrease in size. Henkensifken et al. (2009b) found that as the pores decrease in size, the capillary pressure in the pores increases, thus pulling more water out of the SLWA. However, they also found that the internal relative humidity may not be enough to pull the water out of the SLWA (Henkensifken et al. 2009b). Given the storage environment for this testing regime, it is unclear whether using internal curing for an ASR water source will be beneficial or not in this study.

4.2.1.3 Cements

To evaluate the effects of the specimen size and water source modifications, up to four different cement alkali contents were selected for the study. Two cements were used to create the different cement alkali contents. An ASTM Type I cement and a Type I/II low alkali cement was used in this study (as per ASTM C150). The chemical composition (oxide analysis) of the two cements is shown in Table 30. Each mixture proportion used 708 $^{lb}/_{yd^3}$ (420 $^{kg}/_{m^3}$) of cement.

Table 30: Cement Chemical Composition

Chemical Composition	Cement	
	Type I	Type I/II LA
SiO_2, %	19.87	20.51
Al_2O_3, %	5.53	4.55
Fe_2O_3, %	2.52	3.58
Sum of SiO_2, Al_2O_3, Fe_2O_3, %	27.92	28.64
CaO, %	63.21	63.58
MgO, %	1.19	0.74
SO_3, %	3.4	2.95
Na_2O, %	0.128	0.039
K_2O, %	0.97	0.69
Na_2O Eq., %	0.78	0.49
LOI, %	-	-
Free CaO, %	-	-
C_3S, %*	55.91	-
C_2S, %*	14.77	-
C_3A, %*	10.39	-
C_4AF, %*	7.66	-

The mixture matrix consisted of four different alkali contents. The cement alkali contents as arbitrated by the sodium oxide equivalent (Na_2O_e) and the corresponding concrete alkali loadings are shown in Table 31. To achieve the 4.50 $^{lb}/_{yd^3}$ (2.67 $^{kg}/_{m^3}$) alkali loading in the concrete, a 50% to 50% by cementitious mass blend of the two different cements was used. Also, the 8.85 $^{lb}/_{yd^3}$ (5.25 $^{kg}/_{m^3}$) alkali loading in the concrete involved boosting the Type I cement mixture proportion with sodium hydroxide, which is the alkali loading needed in ASTM C1293. All of the alkali loading values for the concrete were calculated with the 708 $^{lb}/_{yd^3}$ (420 $^{kg}/_{m^3}$) of cementitious materials used in the mixture proportions.

Table 31: Alkali Contents

Cement Alkalis, Na_2O_e (%)	Concrete Alkali Loading , $^{lb}/_{yd^3}$ ($^{kg}/_{m^3}$)
0.49	3.47 (2.06)
0.635	4.50 (2.67)
0.78	5.52 (3.27)
1.25	8.85 (5.25)

4.2.2 Test Procedure

Five different types of specimen types were selected for modifying the ASTM C1293 standard. The different specimen types for the testing regime included:

- 3 in x 3 in x 11.25 in (75 mm x 75 mm x 285 mm) prisms
- 4 in x 4 in x 11.25 in (100 mm x 100 mm x 285 mm) prisms
- 6 in x 6 in x 11.25 in (150 mm x 150 mm x 285 mm) prisms
- 6 in x 12 in (150 mm x 300 mm) cylinders
- 4 in x 8 in (100 mm x 200 mm) cylinders

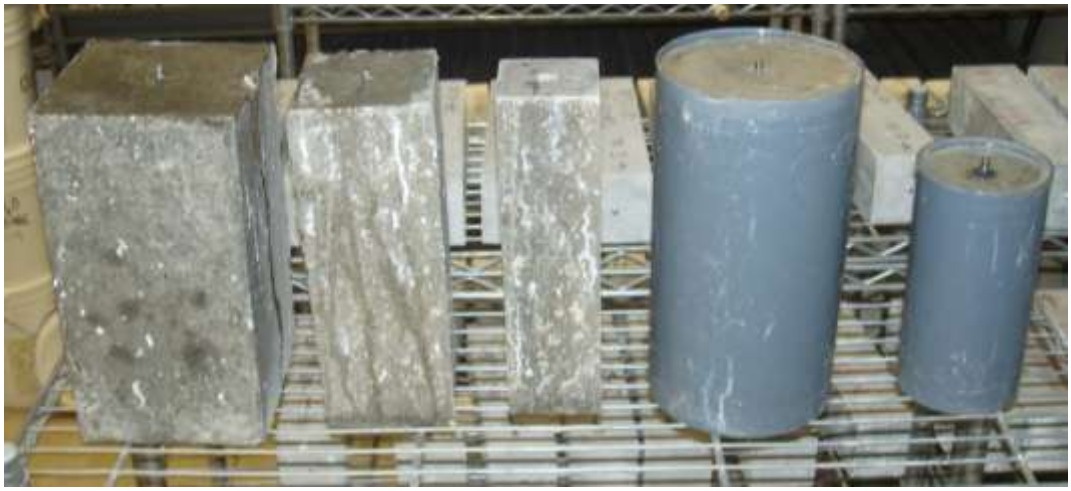

Figure 49: ASTM Modification Specimen Types

These specimens are shown in Figure 49, which were taken after testing had begun on the specimens, thus the specimens show alkali leaching streaks. ASTM C1293 requires the use of 3 in x 3 in x 11.25 in (75 mm x 75 mm x 285 mm) prismatic concrete specimens. The three prism specimen types will be used to analyze the size effect of alkali leaching with the same test setup as the standard. This size comparison using the concrete prisms had specimens for all four of the concrete alkali loadings in Table 32. The cylinder comparison used a closed (sealed) system with (2 mm) of standing to provide a water source for ASR. The cylinder specimens included only the 3.47 $^{lb}/_{yd^3}$ (2.06 $^{kg}/_{m^3}$), 5.52 $^{lb}/_{yd^3}$ (3.27 $^{kg}/_{m^3}$), and 8.85 $^{lb}/_{yd^3}$ (5.25 $^{kg}/_{m^3}$) concrete alkali loadings. These specimens were left inside their plastic molds and sealed between measurements to prevent alkali leaching from the humid storage environment. In addition, all the cylinder concrete mixtures were repeated with the addition of a SLWA to evaluate the effects of an internal water source. All the specimens were pinned to monitor the length change in them. The different mold types for a given cement alkali content is shown in Table 32.

Table 32: Alkali Contents for Specimen Type

Specimen Type	Cement Alkalis, Na_2O_e (%)			
	0.49	0.635	0.78	1.25
prisms	x	x	x	x
cylinders	x		x	x
cylinders with SLWA	x		x	x

A 0.42 w/cm was used in all the mixtures; however the saturated light weight aggregate (SLWA) was not included in this calculation. Each mixture was proportioned with 708 $^{lb}/_{yd^3}$ (420 $^{kg}/_{m^3}$) of cementitious materials. The SLWA, replaced 200 $^{lb}/_{yd^3}$ (119 $^{kg}/_{m^3}$) of the coarse aggregate because the fine aggregate is the reactive aggregate being

tested and it was desired to have the same percentage of the reactive aggregate in the concrete mixtures.

All of the materials were placed in the mixing room at least 24 hours before mixing to ensure that all the materials reached equilibrium with the temperature of the room. The mixing room is kept at 73 ±3 °F (23 ±1.67 °C). The LWFA was saturated for 24 hours prior to being added to the select concrete mixture. To saturate the LWFA, it was fully submerged in tap water, then placed and allowed to soak for 24 hours in the mixing room. In order to get the SLWA to approximately a uniform saturated surface dry condition, the SLWA was placed on a Number 200 (75 μm) sieve and allowed to dry in the sunlight. It was periodically mixed inside the sieve to get a uniform condition in the aggregate. This process of drying the SLWA took no more than one hour.

All the concrete prism molds were metal molds, but the two larger size prisms had wooden end blocks inside the metal mold to reduce the length of the specimen to 11.25 in (285 mm) to allow for comparator measurements. These wooden end blocks had the pins partially embedded in them, thus embedding the pins in the concrete prism during casting. For the cylinder molds, wooden boards were used to partially embed the metal pins. Then, a hole the size of these pins was drilled in the bottom of the plastic cylinder molds so that the bottom pin of the mold could be embedded during casting. Also, the 6 in x 12 in (150 mm x 300 mm) cylinders were cut down to 11.5 ± ⅛ in. (290 ± 3 mm) so that length measurements in the comparator could be made. The top pin of the cylinder specimens was embedded by modifying the cylinder lids to have the pins positioned just below the lid, so that the specimens could be capped with the lids for curing.

All the concrete test specimens were batched, mixed, and cast at the Concrete Durability Center of the University of Texas at Austin. A revised ASTM C192 was used for mixing the concrete. First, the aggregates were blended in a steel drum concrete

mixer, and then the first half of the mixing water was added and mixed for 30 seconds. Next, the cementitious materials were added and blended for 30 seconds before the second half of the mixing water was added. The second half of the mixing water was poured in the mixer over a 30 second time period, at the end of which is the starting time for the age of the concrete specimens. The cementitious material was mixed for a total of two minutes, including the 30 seconds of mixing water addition. After which, the concrete mixture was allowed to rest for 3 minutes before it was mixed again for 2 minutes. When the SLWA was used in the mixture proportioning, the workability of the mixture was significantly reduced. To obtain a workable mix for these concrete mixtures with the SLWA, a minimum dosage of a polycarboxylate-based high-range water reducer was added to the first bucket of mixing water. The minimum dosage for the high-range water reducer is 3 $^{oz}/_{cwt}$ (195 $^{ml}/_{100kg}$). For the boosted concrete mixtures, which were the 8.85 $^{lb}/_{yd^3}$ (5.25 $^{kg}/_{m^3}$) concrete alkali loading, sodium hydroxide (NaOH) was added to the first bucket of mixing water. Then, the fresh concrete was poured into wheel barrels for casting specimens. The slump of the concrete mixtures was obtained following ASTM C143 and the corresponding unit weight was calculated using ASTM C138.

Next, all the specimens, except the 6 in x 12 in (150 mm x 300 mm) cylinders, were cast in two equal volume lifts with at least 25 steel roddings after each lift for consolidation, according to ASTM C192. The 6 in x 12 in (150 mm x 300 mm) cylinders were cast in three equal lift volumes according to the ASTM. The concrete was placed in the plastic cylinder molds and steel prism molds using a metal scoop. The specimens were tapped with a rubber mallet 12 to 16 times before consolidation to remove any entrapped air. Each additional lifts' rodding went to a depth of at least a third into the previous lift layer. The concrete specimens were tapped by the rubber mallet after both lifts and consolidations. If the concrete in the wheel barrel was stagnant for more than

approximately 10 minutes, it was re-mixed with scoops to ensure that segregation did not occur. After all the specimens had been cast for the mix, the excess concrete was removed from the top of the specimens with a wooden trowel and allowed to bleed during setting. Depending on the concrete mixtures, the concrete prism specimens were allowed to set for 30 to 60 minutes before being finished first with a wooden trowel, and then with a magnesium float. The plastic cylinder molds were only filled to a depth of ⅜ ± ⅛ in. below the top of the cylinders to allow for standing water inside the sealed cylinders. The concrete cylinder specimens were allowed to bleed for 45 ± 15 minutes before the metal pins were inserted in the center of the topside of the cylinders, thus the cylinders were not finished. Next, the freshly made concrete cylinders were capped with plastic lids to minimize water loss into the atmosphere. Also, groups of concrete prisms were covered with wet burlap to ensure adequate curing.

For the concrete prism specimens, the initial comparator length reading was made after the specimens were removed from the mold at an age of 23.5 ± 0.5 hours. When possible the specimens were spun in the comparator counter-clockwise to ensure a valid length reading for the specimen. The 6 in x 6 in x 11.25 in (150 mm x 150 mm x 285 mm) prisms and the 6 in x 12 in (150 mm x 300 mm) cylinders were not able to spin on the comparator stand due to the arched arm of the stand's frame. An arrow was drawn on all the specimens to represent the measuring face and orientation of the specimens for the length measurements. The weights of the 3 in x 3 in x 11.25 in (75 mm x 75 mm x 285 mm) and the 4 in x 4 in x 11.25 in (100 mm x 100 mm x 285 mm) prisms were recorded at every measurement interval. Then the specimens were placed inside a 5 gal (19 L) polyethylene bucket with airtight lids. Inside this bucket, the specimens were placed on top of a perforated rack in the bottom of the storage container. The containers were filled with deionized water to a depth of 0.8 ± 0.2 in. (20 ± 5mm) above the bottom and this

level was maintained at every measurement for the test. A felt wick was placed around the inside wall of each container. The sealed cylinders were also placed in the same storage environment as the prism specimens. Due to the dimensions of the modified specimens, some had to be placed in separate storage buckets. There were three 3 in x 3 in x 11.25 in (75 mm x 75 mm x 285 mm) prisms in each bucket per mixture per mixture proportion; two 4 in x 4 in x 11.25 in (100 mm x 100 mm x 285 mm) prisms in one bucket per mixture proportion; two 6 in x 6 in x 11.25 in (150 mm x 150 mm x 285 mm) prisms with each separated into one bucket per mixture proportion; two 6 in x 12 in (150 mm x 300 mm) cylinders with each separated into one bucket per mixture proportion; three 4 in x 8 in (100 mm x 200 mm) cylinders in one bucket per mixture proportion. Measurements for all five types of specimens were taken at: initial, 7 day, 14 day, 28 day, 56 day, 3 month, 4 month, 5 month, 6 month, 9 month, and 1 year. Two different storage environments were selected for the testing regime, which is shown in Table 33. Only the low alkali content used a 140°F (60°C) oven storage environment, since this is the concrete mixture that is desired to fail the ASTM C1293 expansion limit. The increased temperature of this environment should increase the reaction rate of ASR, but the specimens could also dry out and/or more leaching could occur to prevent ASR.

Table 33: Storage Environments for Alkali Contents

Cement Alkalis, Na_2O_e (%)	Storage Condition	
	100°F (38°C)	140°F (60°C)
0.49	X	X
0.635	X	
0.78	X	
1.25	X	

Since there were issues associated with embedding the pins securely in the cylinder specimens, it was necessary to epoxy the pins with PC-7 epoxy when the prism molds were demolded at 23.5 ± 0.5 hours after casting. In addition, the bottom, exposed side of the molds needed epoxy around the pins to ensure that the cylinder was sealed from the atmosphere. Since high-grade epoxy was used due to the elevated temperatures in the testing regime, more time was needed for the epoxy to cure before the initial length measurements could be obtained. The cylinders were transferred to a moist-cure room at 73 ºF (23 ºC) and 100% relative humidity that meets ASTM C192 specifications for a moist-curing environment for 24 hours to allow the epoxy to gain full strength before the initial measurements were taken. In the moist-cure room, the cylinders were placed upside down due to the embedded pins, however a plastic sheet was placed on top of the mold to ensure that ponding did not occur, in order, to allow the epoxy to properly set. The initial measurements were taken at 48 ± 1 hour after casting the cylinder specimens. The length and weight was recorded for the 4 in x 8 in (100 mm x 200 mm) cylinders. For measuring the initial length of the 6 in x 12 in (150 mm x 300 mm) cylinders it was necessary to do some extra modifications since the cylinders were pinned, needed to fit in the large comparator, and the plastic molds had to be longer than the concrete specimen inside, in order, to contain the standing water. Due to interference with the arm of the comparator stand, a small area on the top surface of the cylinder was chiseled away so that the 6 in x 12 in (150 mm x 300 mm) cylinders' length could be recorded, as depicted in Figure 50. After these measurements were taken, 0.08 in (2 mm) of standing tap water was added to the interior cavity section of top part of the cast cylinders; this interior cylinder reservoir is depicted in Figure 51. Aluminum tape was encased around the perimeter of the cylinders, thus creating a seal over the lid and outer cylinder mold. The two different sized cylinders in the testing regime with an aluminum tape seal are

depicted in Figure 52. Then, the cylinder specimens were placed in the same storage conditions, except for the felt, as the concrete prism, which meets the ASTM C1293 criterion.

Figure 50: 6 in x 12 in (150 mm x 300 mm) Cylinder Modification to Fit Comparator

Figure 51: Cylinder Water Reservoir

Figure 52: Sealed Cylinders

To measure the subsequent length changes of the specimens with a comparator, the specimens were removed from the 100°F (38°C) or 140°F (60°C) oven storage environments and placed in a 73°F (23°C) with 50% relative humidity for a period of 16 ± 4 hours before reading. A leachate sample was collected from each prism bucket for all the measurements after the initial measurement. The prism specimens were inverted as compared with the previous storage period at every measurement to ensure uniformity in exposure. The minimum of the comparator reading, when the reference bar was removed after zeroing, was kept note of during measurements, in order, to ensure that the length measurement is accurate and not just the minimum reading. Since most of the mold types were irregular to measure and adjustments had to be made in the height of the comparator stand between some measurements. The specimen, top comparator boot, and bottom comparator boot were always placed in the same orientation to limit bias between measurements. Since the cylinder specimen measurements were in some cases complicated and difficult to perform, care was taken in the measurements and they were often re-checked for accuracy. Also, it was necessary to push down on the top boot of the

comparator for the larger specimens to ensure that it was a true reading, due to some slight angularity in the pin embedment for the top side of the cylinders.

For measuring the concrete cylinder specimens, the aluminum tape is first removed, and then the lid is taken off. Any remaining residue of the silicone seal or aluminum tape is removed from the plastic cylinder mold and lid. It was important to remove all the silicone remaining on the inner part of the cylinder lid, so that a new seal would be sufficient for maintaining a sealed system. Also, the water that condensed on the interior cylinder lids was drained to the reservoir on the top side of the cylinder mold. Then, the lid was completely dried off with cloth to help ensure a good silicon re-seal after the measurements. In addition, the upper part of the cylinder mold was dried off after measurements to help the silicone and aluminum tape seal. If any standing water still remained on the top reservoir of a cylinder then it was drained into a PVC end cap for the length and weight measurement when applicable, then poured back into the cylinder reservoir after the measurements. For the measurements prior to the 3 month mark, 0.08 in (2 mm) of standing water was only added if the cylinder's reservoir was practically completely dry. At the 3 month measurements mark, standing 0.08 in (2 mm) of standing water was always added to the cylinder's reservoir after the measurements had taken place. To add 0.08 in (2 mm) of standing water the volume needed per cylinder size was calculated, then converted to grams of water using 0.001 $\frac{g}{mm^3}$ as the density of water. The RTV silicone was initiated at the 3 month measurement mark for all the original concrete mixtures. The gap between the lid and plastic cylinder mold top was sealed with the aluminum tape. Additional tape was added to sections of the seal that appeared to not have sufficient bonding or coverage. After the tape was applied, it was pressed all the way around with hand pressure to help strengthen the seal. The sealed cylinders were previously shown in Figure 52.

During the testing process it was realized that the aluminum tape seal around the plastic lids wasn't sufficient for keeping the standing water inside the cylinder molds from leaching out to the inner 5 gallon bucket humidity environment. To solve this issue, clear RTV silicone was placed around the inner rim of the cylinder lids. Then, the lids were pressed on top of the cylinder molds to create the seal. Also, the cylinder lids were slightly torqued approximately ⅛ in. (3 mm) turn counter clockwise to ensure a fluid silicone seal. The bead of silicone used to seal the lids was ⅜ ± ⅛ in (3 ± 10 mm).

4.3 Experimental Results and Discussion

In testing the different storage conditions, water typically gets trapped between the outer rim of cylinders, the lid, and the aluminum tape seal. Sometimes when tape is removed from the cylinders, dry white residue plumes into the atmosphere. This white "dust" could be leached alkalis. Alkalis might still be being removed from the system. Originally it was observed that the white powder mostly comes from the areas on top of the tape where water condensation was visible underneath the tape. This deformity of the tape could also be from interaction with the humidity in the bucket environment with the tape. The affected zone of the tape has discoloration, scaling, and originally appeared to be over zones where water is stagnant underneath the tape. On the contrary, in the last round of all the concrete mixture measurements, most instances of white powder had no condensation underneath the aluminum tape, therefore these occurrences could possibly just be an interaction with the deionized water in the 5 gal. bucket containers. Powder has been collected during measurements, however not enough has been collected to run an

XRD analysis. The powder can also be analyzed with a flame photometer for alkalis present, but the flame photometer has been inoperable.

To date the flame photometer that is needed to measure the alkali content in the leachate samples from each measurement is not functional. A new flame photometer was purchased but issues related to the sodium alkali readings didn't allow any analysis of the leachate samples from all the prism measurements. The alkali leaching and size effect could not be analyzed and discussed herein, thus it presents difficulty in drawing some conclusions for this testing regime. In addition, the ASTM standard requires expansion measurements at the year mark for the test to govern the concrete mixtures potential of the highly reactive aggregate to expand deleteriously due to alkali-silica reactivity. The specimens in the testing regime have either reached 5 or 9 months of measurements depending on the concrete mixture.

On the other hand, the pH of the leachate samples was recorded to help give insight to the alkali levels of the standing water in the 1293 test buckets. At every measurement, the standing water in the 5 gal (19 L) bucket was re-filled when necessary with deionized water to maintain the 0.8 ± 0.2 in. (20 ± 5mm) water level. The leachate samples were taken before any water was added to the bucket, so that the leachate samples were not diluted. This dilution effect for subsequent measurements does not allow much insight on alkali leaching from the pH data, which is presented in Table 34. Also, carbonation of the leachate samples can affect the pH of the sample. As expected, the pH increases with time and with increases in the specimen size due to the leaching alkalis. Any significant drop in pH from a previous measurement should signify that deionized water was added at the previous measurement time.

Table 34: Concrete Prism's Leachate pH

Cement Alkalis, Na_2O_e (%)	Storage Temperature, °F (°C)	Specimen Dimensions, in. (mm)	Sample Age (weeks)								
			1	2	4	8	12	16	20	24	36
0.49 Na_2O_e	100°F (38°C)	3x3x11.25 (76x76x285)	7.00	8.39	11.98	12.04	8.88	7.98	12.03	9.95	0.00
		4x4x11.25 (101x101x285)	8.94	11.55	11.86	11.89	11.56	12.07	9.40	12.01	0.00
		6x6x11.25 (152x152x285) - A	11.23	11.69	11.85	11.93	11.73	11.64	12.02	12.17	0.00
		6x6x11.25 (152x152x285) - B	12.08	12.09	12.02	11.80	11.34	11.60	12.06	11.99	0.00
0.49 Na_2O_e	140°F (60°C)	3x3x11.25 (76x76x285)	11.79	11.80	11.68	11.40	10.74	10.91	10.78	11.41	0.00
		4x4x11.25 (101x101x285)	11.88	11.83	11.54	7.13	11.16	11.14	10.90	11.63	0.00
		6x6x11.25 (152x152x285) - A	11.98	12.14	11.93	10.90	8.00	7.06	11.69	11.59	0.00
		6x6x11.25 (152x152x285) - B	12.00	7.41	11.75	7.78	10.42	11.51	11.84	11.84	0.00
0.635 Na_2O_e	100°F (38°C)	3x3x11.25 (76x76x285)	11.41	11.95	12.14	12.21	0.00	0.00	0.00	-	-
		4x4x11.25 (101x101x285)	12.01	12.29	12.33	12.27	0.00	0.00	0.00	-	-
		6x6x11.25 (152x152x285) - A	11.36	11.93	12.16	12.28	0.00	0.00	0.00	-	-
		6x6x11.25 (152x152x285) - B	11.76	12.19	12.31	12.18	0.00	0.00	0.00	-	-
0.78 Na_2O_e	100°F (38°C)	3x3x11.25 (76x76x285)	10.90	11.77	12.08	12.30	12.33	11.16	11.59	11.58	0.00
		4x4x11.25 (101x101x285)	11.83	12.06	12.29	12.13	11.04	12.23	10.54	10.25	0.00
		6x6x11.25 (152x152x285) - A	11.37	11.97	12.19	12.16	12.21	12.32	12.33	12.28	0.00
		6x6x11.25 (152x152x285) - B	11.73	12.16	12.27	12.18	12.17	12.29	12.25	12.12	0.00
1.25 Na_2O_e	100°F (38°C)	3x3x11.25 (76x76x285)	11.96	12.39	12.51	12.37	12.42	12.48	12.41	12.37	0.00
		4x4x11.25 (101x101x285)	11.96	12.32	12.48	12.48	12.48	12.51	12.44	12.32	0.00
		6x6x11.25 (152x152x285) - A	12.17	12.45	12.43	12.47	12.55	12.54	12.48	12.33	0.00
		6x6x11.25 (152x152x285) - B	12.12	12.45	12.31	12.48	12.47	12.45	12.39	12.25	0.00

A relative humidity (RH) study was conducted to analyze the effect of the alkali concentration in the leachate water (standing water) of the five gallon buckets, as per the ASTM C1293 container requirement, on the RH inside the bucket. The same RH probe and reader was used for the entire test. To do this comparison on RH, 1293 buckets were taken out of the 100°F (38°C) or 140°F (60°C) oven and the concrete 3 in x 3 in x 11.25 in (75 mm x 75 mm x 285 mm) standard-sized prism specimens were removed from the buckets. A RH probe was epoxied to the top of one of the 1293 bucket lids for use in all the measurements. This lid was completely sealed to ensure a closed system when the lid was securely placed on top of a 1293 bucket. For each 1293 bucket that was evaluated, the buckets were first placed in the 73°F (23°C) to gain equilibrium in that environment with the RH probe lid securely fastened on top of the bucket. Then, after 24 hours the reader was plugged into the RH probe and was set to record for 48 hours every 10 minutes. Next, the bucket was immediately placed in either the 100°F (38°C) oven or 122°F (50°C) oven for approximately 24 hours. The 122°F (50°C) oven was used instead of a 140°F (60°C) for the relative humidity analysis because of the limited temperature range of the humidity probe. After that the bucket was put back in the 73°F (23°C) room, where the ASTM C1293 measurements are taken. This process was completed for both oven environments with a clean (free of alkali leaching), 0.49 Na_2O_e, and 1.25 Na_2O_e bucket. The "Clean Bucket" had fresh deionized water with a clean felt and a clean stand in it. The 1293 buckets for the 0.49 Na_2O_e and 1.25 Na_2O_e concrete mixtures from the 100°F (38°C) and 122°F (50°C) storage environments were after the 6 month measurement, so that sufficient alkalis had leached into the standing water of the buckets. These alkali concentrations change the relative humidity inside the bucket. The temperature also effects what the relative humidity will be inside the bucket with a given salt concentration. The buckets were stored in the same location in both the 73°F (23°C)

room and the two ovens to limit bias between measurement types. Figure 53 displays the results for the 100°F (38°C) oven environment and Figure 54 depicts the 122°F (50°C) oven environment.

In the two different environmental temperature changes, as depicted in Figure 53 and 54, the RH becomes more erratically unbalanced and follows sinusoidal behavior as the alkali content increases. This behavior is only minor for the 122°F (50°C) storage environment. Also, as the containers are transferred from the higher temperatures to the 73°F (23°C) environment the immediate drop in RH is far more drastic with the increased alkali concentration that are in the bucket's standing water. This immediate drop in RH, which signifies the 1293 bucket being placed in the specimen measurement environment, increases with the 122°F (50°C) oven transfer.

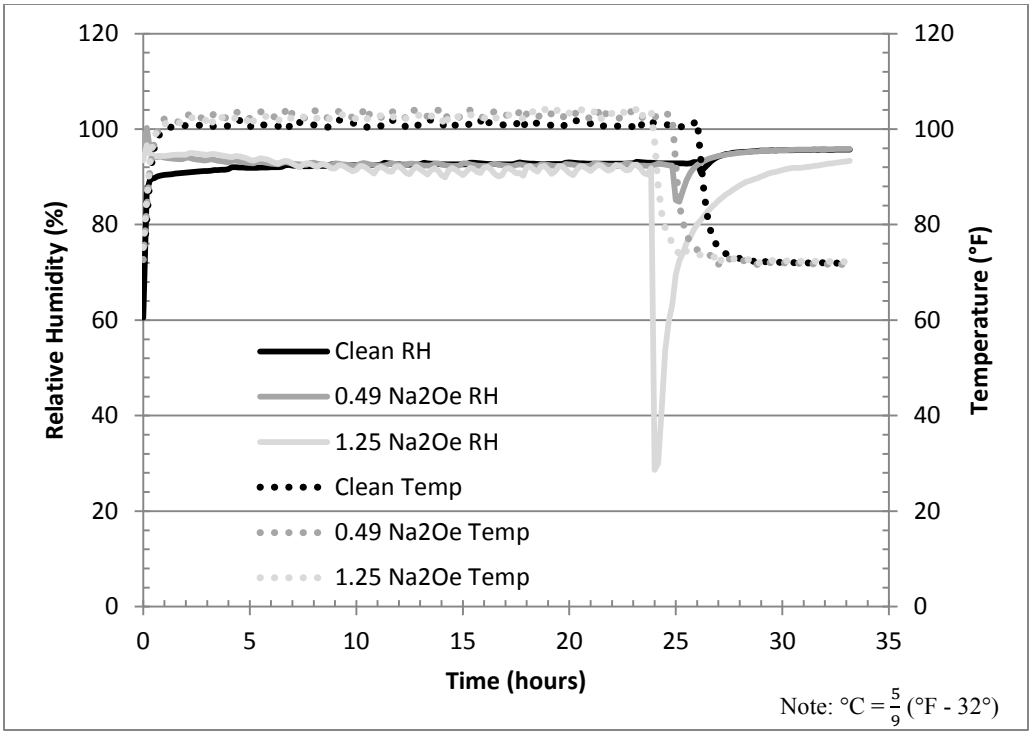

Figure 53: 100°F (38°C) to 73°F (23°C) Humidity Change in ASTM C1293 Buckets

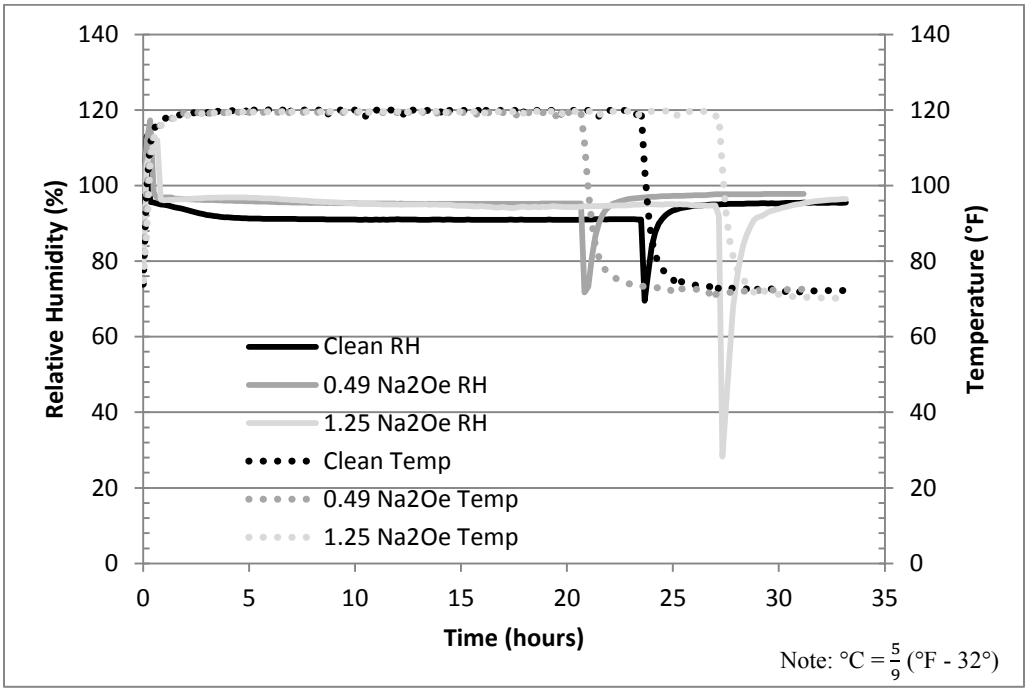

Figure 54: 122°F (50°C) to 73°F (23°C) Humidity Change in ASTM C1293 Buckets

4.3.1 Concrete Prism Specimens

To date, the 0.49%, 0.78%, and 1.25% Na_2O_e concrete prism specimens have been in storage for 9 months and the newer 0.635% Na_2O_e concrete mixtures have been in testing 5 months. All of the boosted, 1.25% Na_2O_e concrete prisms have failed the ASTM C1293 0.04% expansion limit criterion. Also, the 0.78% Na_2O_e, 6 in x 6 in x 11.25 in (150 mm x 150 mm x 285 mm) concrete prism failed the 0.04% expansion criterion approximately 4 months after the 1.25% Na_2O_e specimens did. In Figures 55 through 57, it is noticeable that as the specimen size increases, the expansion results of the 0.78% Na_2O_e concrete prisms gets closer to the 1.25% Na_2O_e specimens. This could show that when sufficient alkalis are originally present in the cement, the leaching problem decreases with increasing the specimen size. Currently, the low-alkali concrete mixtures (0.49 Na_2O_e) have minimal expansion activity in all of the concrete prism types.

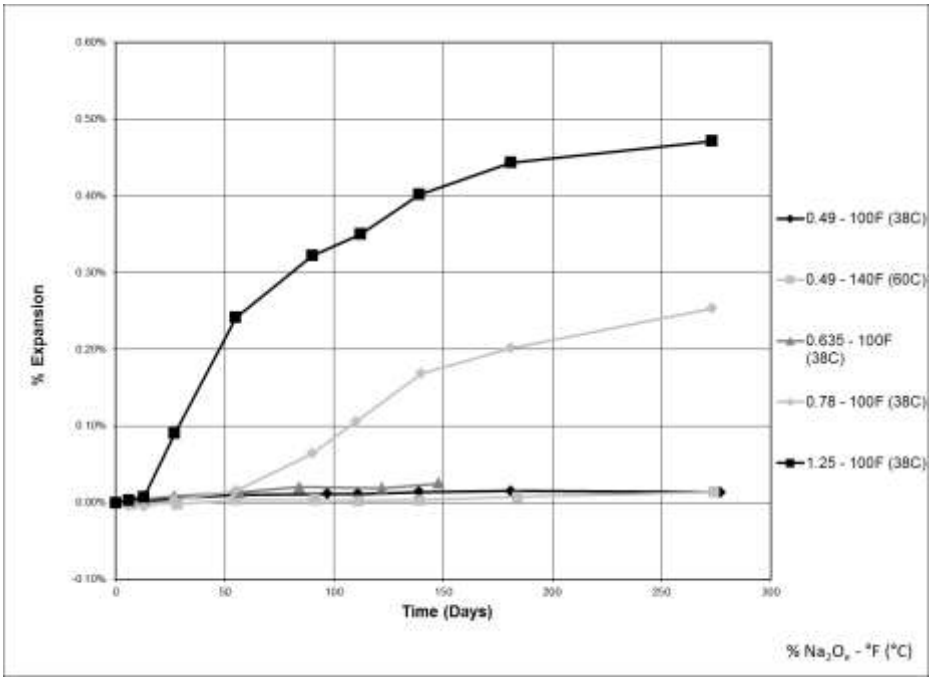

Figure 55: 3 in x 3 in x 11.25 in (75 mm x 75 mm x 285 mm) Prisms with Different Cement Alkalinities

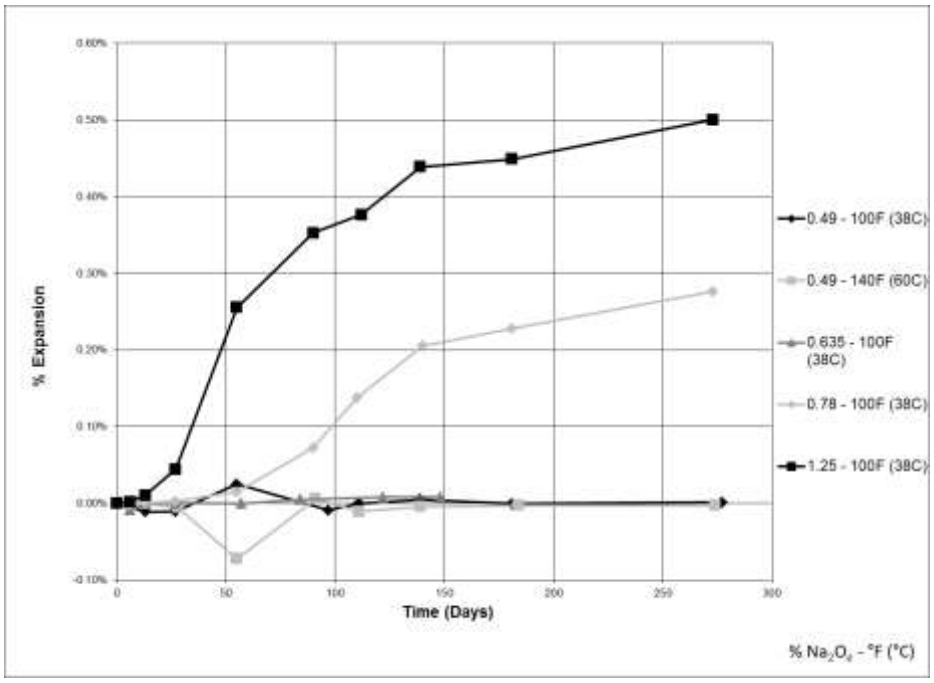

Figure 56: 4 in x 4 in x 11.25 in (100 mm x 100 mm x 285 mm) Prisms with Different Cement Alkalinities

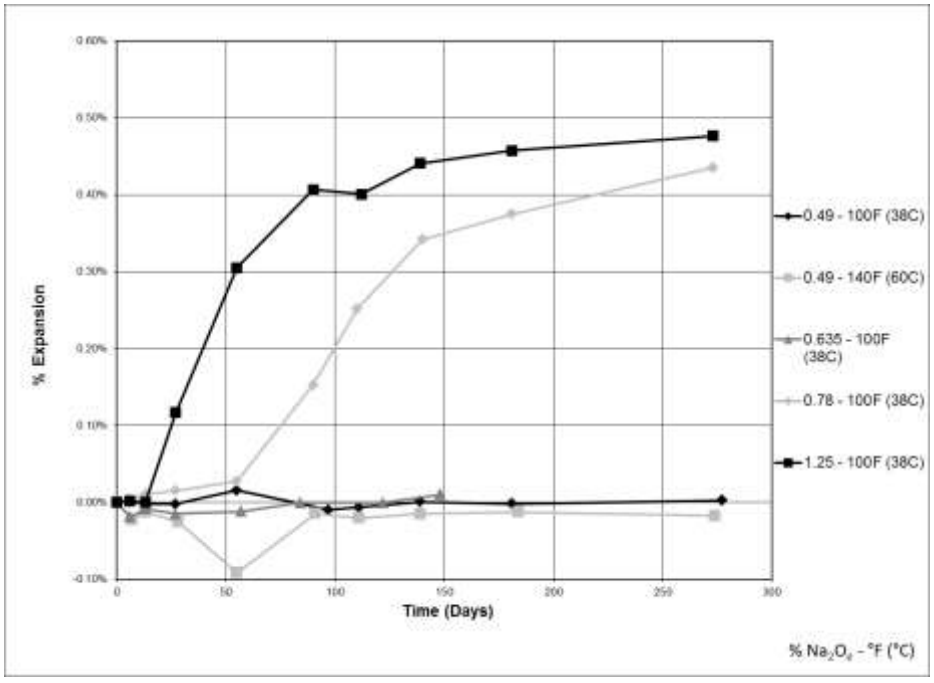

Figure 57: 6 in x 6 in x 11.25 in (150 mm x 150 mm x 285 mm) Prisms with Different Cement Alkalinities

4.3.2 Concrete Cylinder Specimens

To date, the original 0.49, 0.78, and 1.25 Na_2O_e concrete specimens have been measured through 9 months, as shown in Figures 58 and 59 for the 4 in x 8 in (100 mm x 200 mm) and the 6 in x 12 in (150 mm x 300 mm) cylinders, respectively. The repeated low-alkali (0.49 Na_2O_e) concrete cylinders with the silicone seal being initialized at the start of the testing have undergone 5 months of measurements to date. Also, standing water was added after each measurement period for these newer specimens. The original concrete mixtures began the silicone sealing and water addition at every measurement at the 3 month measurement mark. These repeated, low-alkali concrete mixtures are shown in Figures 60 and 61 for the 4 in x 8 in (100 mm x 200 mm) and the 6 in x 12 in (150 mm x 300 mm) cylinders, respectively. The only logical explanation for the erratic behavior of the 6 in x 12 in (150 mm x 300 mm) concrete cylinders in Figure 59 is that these specimens were especially difficult to measure the length change in the comparator. Over time, the measurements of these larger cylinders became more developed with experience as seen by the expansion in them becoming more systematic between measurements. The repeated, low-alkali concrete mixtures show slightly more expansion in the latest measurements as compared to the original concrete mixtures at the same measurement period. Also, these repeated cylinder mixtures do not exhibit the same erratic behavior as their predecessors, but in fact show slight systematic expansion in the 6 in x 12 in (150 mm x 300 mm) cylinders. In the 4 in x 8 in (100 mm x 200 mm) concrete cylinders the addition of the SLWA reduced the observed expansion, although the same trends were observed between the straight concrete mixtures and the corresponding mixtures with the SLWA. However, the SLWA caused more expansion in the 6 in x 12 in (150 mm x 300 mm) concrete cylinders at the two higher alkali levels. The SLWA in the 6 in x 12 in

(150 mm x 300 mm) low-alkali concrete cylinders caused contraction in the specimens to date.

The purpose of this project is to get a low-alkali concrete mixture to fail the 0.04% expansion limit of ASTM C1293, preferably within one year. To date, the concrete cylinders had better performance for the low-alkali concrete specimen types than the concrete prisms did. These results for the low-alkali concrete prisms are shown in Table 35. It is clear that several of the 4 in x 8 in (100 mm x 200 mm) concrete cylinder mixtures that were stored at 140°F (60°C) are close to the expansion limit and the newer concrete mixtures appear to be approaching this expansion limit at a faster rate. This is most likely due to the improved cylinder sealing that created a better closed system inside the cylinder molds. Alkali leaching is significant in the first month; therefore this improved cylinder sealing method could be preventative enough to result in failed low-alkali concrete mixtures according to the ASTM C1293 0.04% expansion limit. Breaches in the cylinders sealed were noticed throughout the testing. The aluminum tape seal was sometimes found to have a section that was not adhered to the plastic cylinder mold and white streaking was observed at some of these locations. It would be very interesting to use rigid molds to see if limiting the expansion to one axis would improve the results. The plastic cylinder molds that were used to contain the concrete cylinders are fairly pliable.

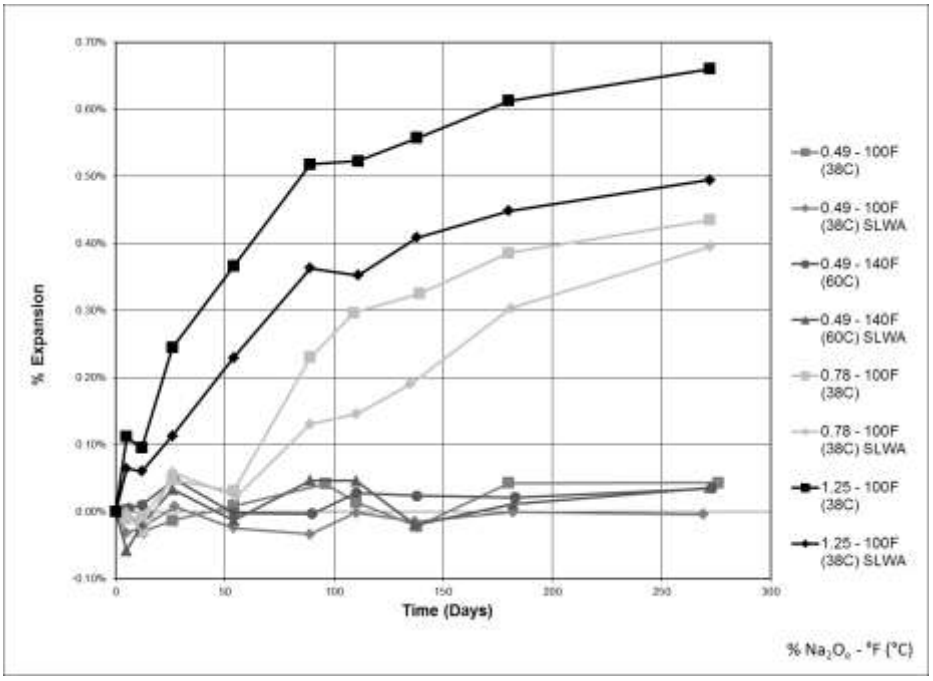

Figure 58: 4 in x 8 in (100 mm x 200 mm) Cylinders with Different Cement Alkalinities

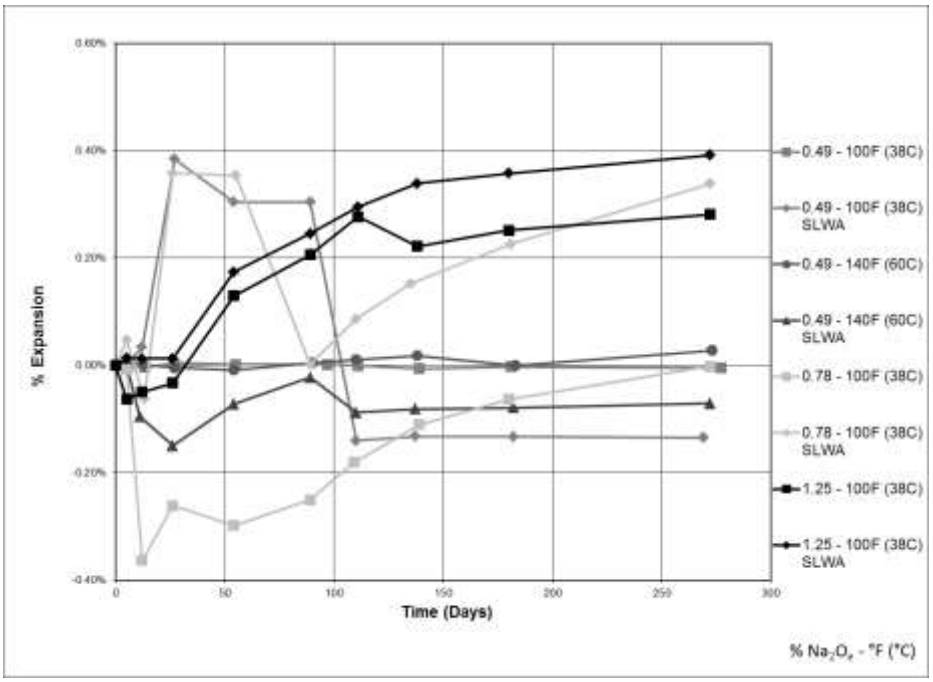

Figure 59: 6 in x 12 in (150 mm x 300 mm) Cylinders with Different Cement Alkalinities

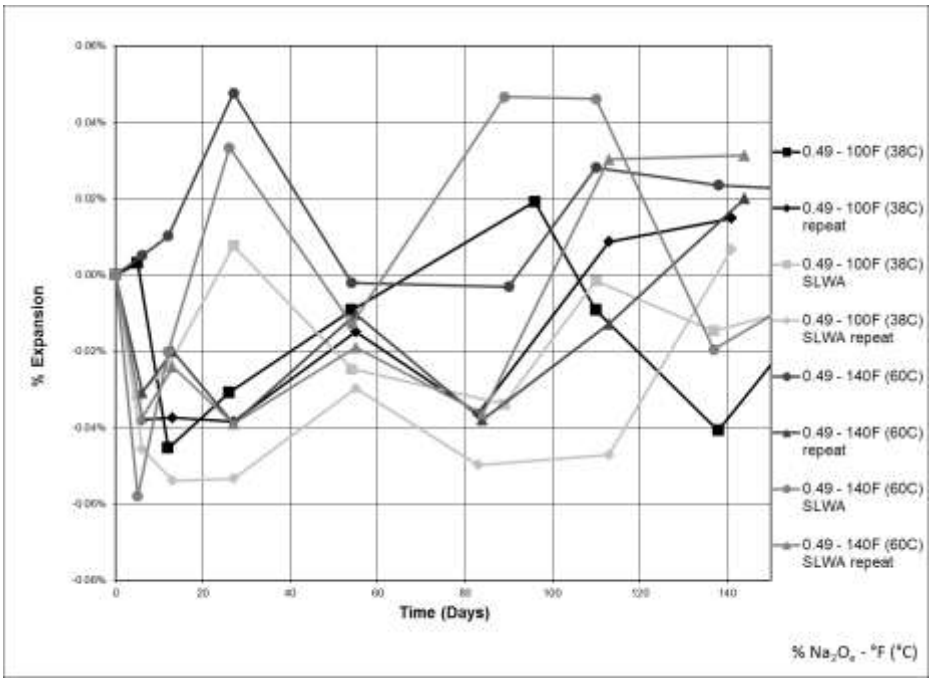

Figure 60: Repeated 4 in x 8 in (100 mm x 200 mm) Cylinders with Silicone Seals and Different Cement Alkalinities

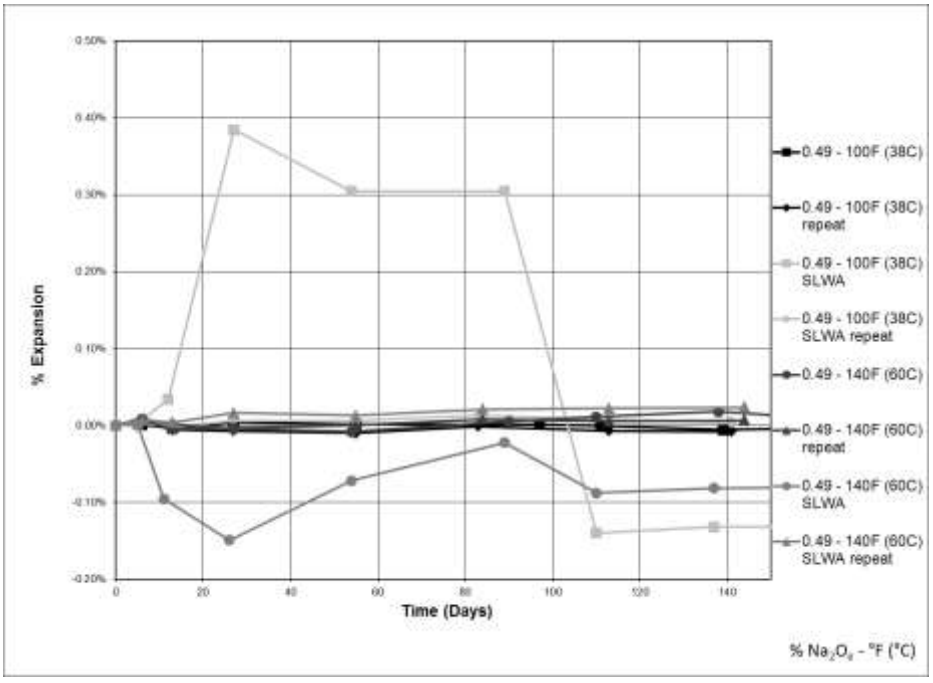

Figure 61: Repeated 6 in x 12 in (150 mm x 300 mm) Cylinders with Silicone Seals and Different Cement Alkalinities

Table 35: Low-Alkali (0.49% Na_2O_e) Concrete Cylinder Expansions

Specimen Dimensions, in. (mm)	SLWA in Mixture	Environmental Condition	Age (days)	Expansion (%)
4 in x 8 in (100 mm x 200 mm)		100°F (38°C)	272	0.023
			141	0.015
		140°F (60°C)	272	0.035
			144	0.02
	X	100°F (38°C)	272	-0.004
	X		141	0.007
	X	140°F (60°C)	272	0.036
	X		144	0.031
6 in x 12 in (150 mm x 300 mm)		100°F (38°C)	272	-0.0005
			141	-0.008
		140°F (60°C)	272	0.028
			144	0.006
	X	100°F (38°C)	272	-0.135
	X		141	0.004
	X	140°F (60°C)	272	-0.071
	X		144	0.024

4.3.3 Comparison with Previous Data

The highly reactive aggregate that was used in this testing regime has been studied in previous projects. TxDOT funded a research project that evaluated this very same very reactive fine aggregate in ASTM C1260, ASTM C1293, and outdoor exposure blocks. The report found that it was not possible to determine alkali thresholds for a given aggregate using ASTM C 1293. Although it was possible to determine alkali thresholds using large outdoor blocks, where exposure conditions are more realistic and the potential for leaching is reduced through the larger sample size (Folliard et al. 2006). The results of ASTM C1293 and exposure block testing for the same highly reactive aggregate that was used in this study is shown in Table 36 and Figure 62. In addition, Figure 63 shows the average expansion of ASTM C1293 prisms cast with varying cement alkalinities and

Figure 64 shows the average expansion of the companion outdoor exposure blocks. The expansion limit for exposure blocks is generally considered to be 0.04%, just like ASTM C1293. From prior ASTM C1293 data in a 140°F (60°C) environment, the 3 in x 3 in x 11.25 in (75 mm x 75 mm x 285 mm) standard-sized prisms tend to have more leaching and the specimens dry out from the increased temperature, therefore ASR does not cause expansion from the lack of alkalis and water in the system. Also, in 60°C (140°F) testing, shrinkage typically occurs early on then it starts to expand. No comparisons between the prior highly reactive aggregate data and the results from this testing regime to date will be made.

Table 36: Highly Reactive Aggregate Previous Testing Summary

Cement Alkalinity, Na_2O_e (%)	Environmental Condition	Expansion (%)
1.25	ASTM C1293 1-Year @ 100°F (38°C)	0.59
1.25	ASTM C1293 1-Year @ 140°F (60°C)	0.59
0.43	exposure block	0.0140 (1435)*
0.49	exposure block	0.0625 (1435)*
0.52	exposure block	0.8800 (1250)*
0.95	exposure block	1.1000 (1250)*
1.25	exposure block	1.0674 (1520)*

* averaged expansion (age in days)

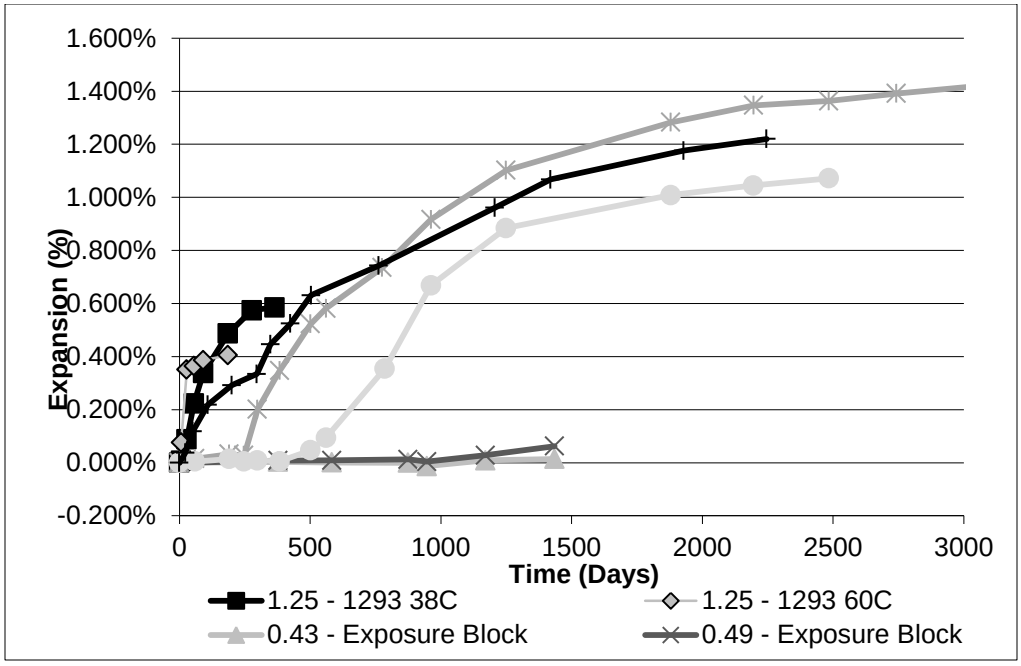

Figure 62: Expansion with Highly Reactive Aggregate

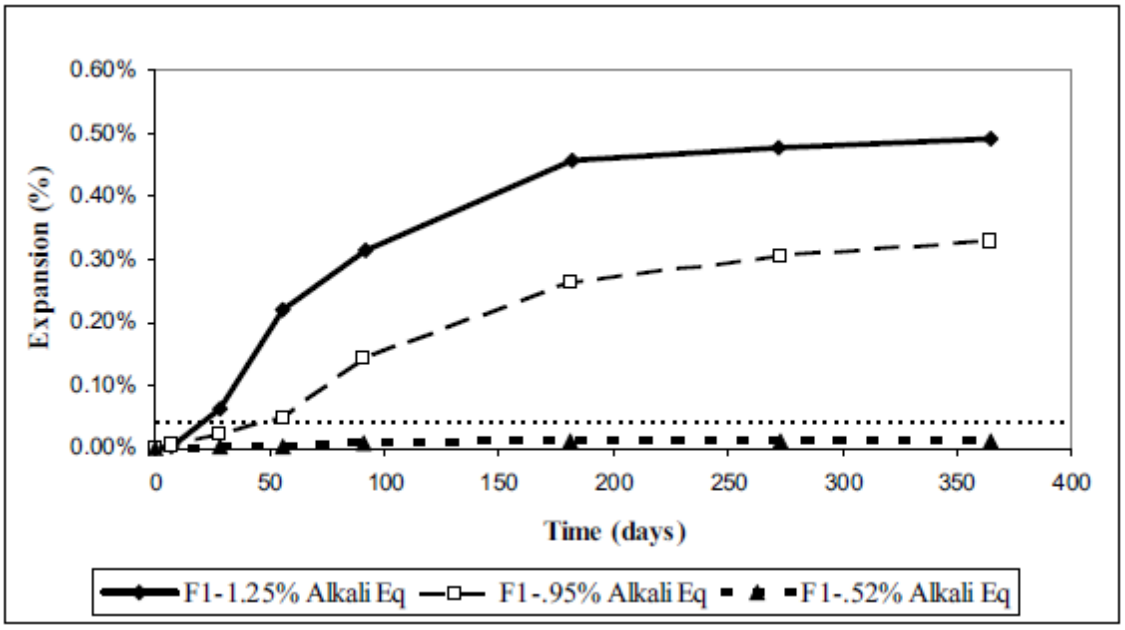

Figure 63: ASTM C1293 Expansion with Different Cement Alkalinities and Highly Reactive Aggregate (Folliard et al. 2006)

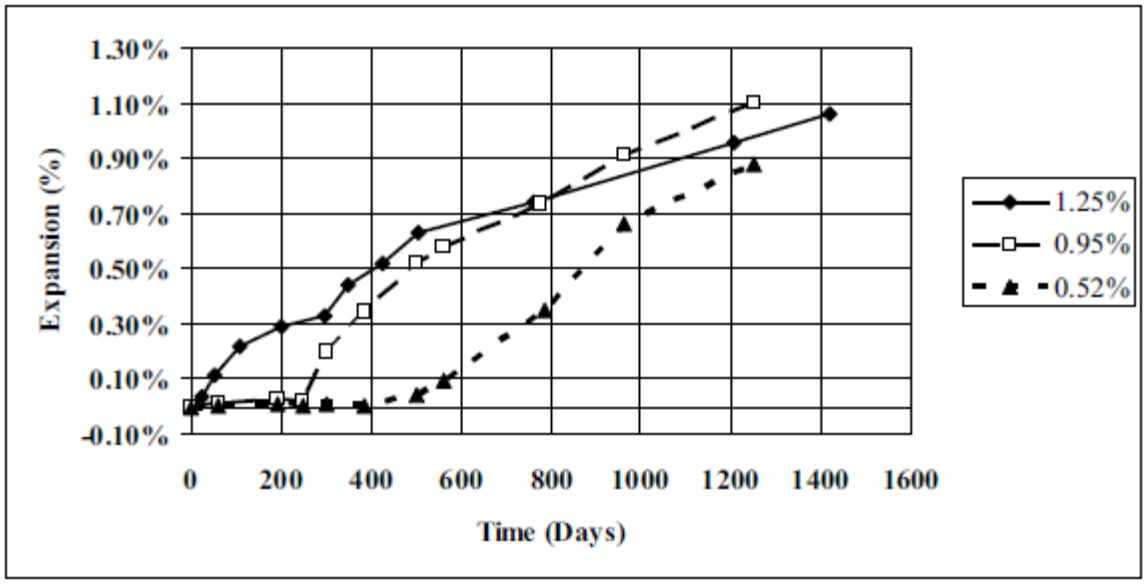

Figure 64: Expansion in Exposure Blocks with Highly Reactive Aggregate and Varying Cement Alkalinities (Folliard et al. 2006)

4.4 SUMMARY

The purpose of this project is to get a low-alkali concrete mixture to fail the 0.04% expansion limit of ASTM C1293 within one year. To date, the concrete cylinders had better performance for the low-alkali concrete specimen types than the concrete prisms did. These results for the low-alkali concrete cylinders were shown in Table 35. It is clear that several of the 4 in x 8 in (100 mm x 200 mm) concrete cylinder mixtures that were stored at 140°F (60°C) are close to the expansion limit and the newer, repeated low-alkali concrete mixtures appear to be approaching this expansion limit at a faster rate. This is most likely due to the improved cylinder sealing that created a better closed system inside the cylinder molds. Alkali leaching is significant in the first month; therefore this improved cylinder sealing method could be preventative enough to result in failed low-alkali concrete mixtures according to the ASTM C1293 0.04% expansion

limit. It would be very interesting to use rigid molds to see if limiting the expansion to one axis would improve the results. The plastic cylinder molds that were used to contain the concrete cylinders are fairly pliable.

In general, the prism mold types appear to have less problems with leaching and resulting increased expansion as the specimen size increases. Currently, the low-alkali concrete mixtures (0.49 Na_2O_e) have minimal expansion activity in all of the concrete prism types. The trends of the varying alkali contents in the prism is expected and systematic between the three specimen sizes. The length change for all the specimens at the varying alkali levels to date is presented in Table 37.

When the testing regime is completed, recommendations will be made on further investigating mold type and setups discussed herein to further quantify low-alkali systems in ASTM C1293. The ASTM C1293 mold type considerations will be:

- Applicability of mold handling
- Ease of modifying and casting mold type
- Strength and ease of pinning molds
- Applicability to jobsite 1293 testing
- Data correlation to exposure blocks
- Length of test to get similar results
- Leaching of samples

Table 37: Modified ASTM C1293 Expansion To Date

Cement Alkalinity, Na_2O_e (%)	Specimen Dimensions, in. (mm)	SLWA in Mixture	Environmental Condition	Age (days)	Expansion
0.49	3x3x11.25 (75x75x285)		100°F (38°C)	277	0.013%
			140°F (60°C)	274	0.014%
	4x4x11.25 (100x100x285)		100°F (38°C)	277	0.002%
			140°F (60°C)	274	-0.003%
	6x6x11.25 (150x150x285)		100°F (38°C)	277	0.003%
			140°F (60°C)	274	-0.018%
	4 in x 8 in (100 mm x 200 mm)		100°F (38°C)	276	0.023%
				141	0.015%
			140°F (60°C)	273	0.035%
				144	0.020%
		X	100°F (38°C)	269	-0.004%
		X		141	0.007%
		X	140°F (60°C)	272	0.036%
		X		144	0.031%
	6 in x 12 in (150 mm x 300 mm)		100°F (38°C)	277	-0.005%
				141	-0.008%
			140°F (60°C)	273	0.028%
				144	0.006%
		X	100°F (38°C)	269	-0.135%
		X		141	0.004%
		X	140°F (60°C)	272	-0.071%
		X		144	0.024%
0.635	3x3x11.25 (75x75x285)		100°F (38°C)	148	0.025%
	4x4x11.25 (100x100x285)			148	0.008%
	6x6x11.25 (150x150x285)			148	0.010%
0.78	3x3x11.25 (75x75x285)			273	0.253%
	4x4x11.25 (100x100x285)			273	0.277%
	6x6x11.25 (150x150x285)			273	0.436%
	4 in x 8 in (100 mm x 200 mm)			272	0.435%
		X		272	0.395%
	6 in x 12 in (150 mm x 300 mm)			272	-0.002%
		X		272	0.339%
1.25	3x3x11.25 (75x75x285)			273	0.471%
	4x4x11.25 (100x100x285)			273	0.501%
	6x6x11.25 (150x150x285)			273	0.477%
	4 in x 8 in (100 mm x 200 mm)			272	0.660%
		X		272	0.495%
	6 in x 12 in (150 mm x 300 mm)			272	0.281%
		X		272	0.392%

4.5 FUTURE TEST IMPROVEMENTS

One test improvement could be to fully quantify the leaching of the different sized specimens. To do this, one could replace the standing water at the bottom of the ASTM C1293 container at every measurement to find the leaching trend throughout the duration of the test. Also, the felt should be replaced at every measurement, so that the water-soluble alkalis could be determined from the old felt and then the total alkali leaching content could be quantified. Another means to quantify the amount of alkalis being leached to the system would be to measure the internal relative humidity inside the ASTM C1293 container over the duration of the test. When more alkalis are added to the system from leaching of the concrete specimens, the relative humidity fluctuates in a sinusoidal manner and this behavior gets more pronounced as more alkalis are added to the system. This idea of different alkali concentrations' effect on the relative humidity inside the ASTM container was previously demonstrated in Section 4.3 for this chapter.

Furthermore, new mold types could be investigated for improving the ASTM standard for low-alkali systems. For example, a five gallon pail mold could be cast with a strain gauge embedded to measure the expansion of the specimen. The larger size of the specimen may be enough to limit alkali leaching. For these large specimens standing water could be placed on the top surface to provide a water source for ASR. In addition, PVC cylinder molds could be created to provide a rigid body to confine the expansion to one direction. The PVC mold could be sealed with standing water and pinned like in this testing regime to provide a rigid structure to better quantify the expansion occurring. Also, the PVC mold could have a strain gauge embedded in it instead of being pinned to analyze the length change in it. Some Schedule 80 PVC piping has a maximum service temperature of 140°F (60°C), therefore use of this material would be recommended.

The incorporation of a SLWA into the concrete mixture might not be appropriate given the LWFA, because some lightweight aggregates contain glassy, aluminosilicates and may react pozzolanically. Also, using a SLWA could somewhat change the response of a concrete mixture with SCMs or the expansion observed. Since SLWA could give pessimum effects, using saturated polymers as an internal water source for ASR should be investigated.

4.6 WORKS CITED

ASTM C 33, "Standard Specification for Concrete Aggregates," ASTM International, West Conshohocken, PA, 2009.

ASTM C 138, "Standard Test Method for Density (Unit Weight), Yield, and Air Content (Gravimetric) of Concrete," ASTM International, West Conshohocken, PA, 2010.

ASTM C 143, "Standard Test Method for Slump of Hydraulic-Cement Concrete," ASTM International, West Conshohocken, PA, 2010.

ASTM C 150, "Standard Specification for Portland Cement," ASTM International, West Conshohocken, PA, 2009.

ASTM C 192, "Standard Practice for Making and Curing Concrete Test Specimens in the Laboratory," ASTM International, West Conshohocken, PA, 2005.

ASTM C 1260, "Standard Test Method for Potential Alkali Reactivity of Aggregates (Mortar-Bar Method)," ASTM International, West Conshohocken, PA, 2007.

ASTM C 1293, "Standard Test Method for Determination of Length Change of Concrete Due to Alkali-Silica Reaction," ASTM International, West Conshohocken, PA, 2008.

Folliard, K. J., Barborak, R., Drimalas, T., Du, L., Garber, S., Ideker, J., Ley, T., Williams, S., Juenger, M., Thomas, M.D.A., and Fournier, B., "Preventing ASR/DEF in New Concrete: Final Report." The University of Texas at Austin, Center for Transportation Research (CTR), CTR 4085-5, 2006.

Fournier, B., Chevrier, R., de Grosbois, M., Lisells, R., Folliard, K., Ideker, J., Shehata, M., Thomas, M., Baxter, S., "The accelerated concrete prism test (60°C): variability of

the test method and proposed expansion limits," Proc. 12th International Conference on Alkali-Aggregate Reaction in Concrete, Beijing, China, vol. 1, 2004, pp. 314-323.

Henkensiefken, R., Castro, J., Bentz, D., Nantung, T., Weiss, J. "Water absorption in internally cured mortar made with water-filled lightweight aggregate," *Cement and Concrete Research*, Vol. 39, pp. 883-892, 2009a.

Henkensiefken, R., Nantung, T., Bentz, D., Weiss, J. "Volume Change and Cracking in Internally Cured Mixtures made with Saturated Lightweight Aggregate under Sealed and Unsealed Conditions," *Cement and Concrete Composites*, Vol. 31 (7), pp. 427-437, 2009b.

Ideker, J., East, B., Folliard, K., Thomas, M., Fournier, B., "The current state of the accelerated concrete prism test." *Cement and Concrete Research,* Vol. 40 (4), pp. 550-555, 2010.

Stanton, T.E. "Expansion of concrete through reaction between cement and aggregate." *Proceedings of the American Society of Civil Engineers,* Vol. 66, No. 10, pp. 1781-1811., 1940.

Thomas, M. D., Hooton, R. D., & Rogers, C. A. "Prevention of damage due to alkali aggregate reaction (AAR) in concrete construction - Canadian approach." *Cement, Concrete and Aggregates,* Vol. *19* (1), pp. 26-30, 1997.

Thomas, M., Fournier, B., Folliard, K., Ideker, J., & Shehata, M. "Test methods for evaluating preventative measures for controlling expansion due to alkali-silica reaction in concrete." *Cement and Concrete Research,* Vol. *36*, pp. 1842-1856, 2006.

Wehrle, E. *The Effects of Coating and Sealers Used to Mitigate Alkali-Silica Reaction and/or Delayed Ettringite Formation in Hardened Concrete.* Austin, Texas: The University of Texas at Austin, 2010.

Chapter 5: Conclusions and Future Work

The overall conclusions from the two main studies are presented herein and that because of the long-term nature of the testing, firm conclusions are generally not possible. This is the nature of long-term concrete durability testing.

5.1 PHYSICAL SULFATE ATTACK

5.1.1 Conclusions

The most significant findings from the laboratory evaluation of concrete cylinder segments exposed to 30% (by mass of solution) sodium sulfate in both physical and chemical sulfate attack conditions were:

- Physical sulfate attack was found to be more severe and aggressive than chemical sulfate attack, using the testing regimes described herein.
- In cyclical testing, the straight cement mixtures had the highest mass losses, while the concrete mixtures with slag had the least amount of mass loss and distress. Concrete mixtures with a Class F fly ash perform superior in chemical and physical sulfate attack than concrete mixtures with Class C fly ash.
- Overall, the lower w/cm mixtures performed superior in chemical and physical sulfate attack and SCMs improved the durability.
- Generally, the straight cement mixtures had higher permeability than the SCM blended concrete mixtures. If permeability is the overlying mechanism governing the durability of concrete to physical sulfate attack, then the straight cement mixtures should show the most distress.

- General absorption trends observed from lowest to highest initial rate of absorption:
    - 0.40 < 0.45 < 0.50 w/cm
    - high CaO fly ash < low CaO fly ash
    - straight cement < fly ash < slag

Overall, the data showed that physical sulfate attack can be quite damaging. However, it should be noted that the specimens tested in this laboratory program were quite small and the testing regime was very aggressive. To better evaluate more realistic (larger) concrete elements in a more realistic environment, a comprehensive program was launched using the aforementioned outdoor exposure site. Concrete cylinders were exposed to approximately 5% (33,000 ppm) sodium sulfate in an outdoor sulfate exposure site in Austin, TX. The cylinders cast for the study were evaluated with a visual, numerical ranking system for both the concrete's scaling distress and wicking action. The smaller, 4 in x 8 in (100 mm x 200 mm) concrete cylinders were also measured for mass change. Comparisons to the laboratory results from Chapter 2 were reported.

In the field testing, the resistance to the physical sodium sulfate attack mechanism is most likely due to the reduced absorption in the concrete matrix. The lack of additional CaO into the concrete mixtures from a Class C fly ash also appears to improve the durability. The cement type does not play an important role in exposure to physical sulfate distress, although all the Type I cements for a given w/cm are superior to ones with Type V cement. Overall, reducing the w/cm seems to provide the most improved durability to physical sodium sulfate attack. The majority of the concrete mixtures with higher permeability performed moderately in the outdoor testing, however many of these specimens had the least durability in the laboratory testing previously presented in Chapter 2. No correlation to the slag's improved performance in the laboratory testing

could be drawn by their outdoor performances because these mixtures fell sporadically in the outdoor ranked results. In conclusion, mixtures that correspond to suggestive preventative measures from ACI 318-08 performed poorly to the aggressive mechanisms of physical sodium sulfate attack. More research on the mechanisms behind this deterioration is needed in the near future to provide adequate guidelines for practitioners.

5.1.2 Recommendations for Future Work

The sodium sulfate, field exposure site will continue to be monitored. In addition, trips to the gypsum exposure site in West Texas will be commenced to weigh and visually rate the concrete cylinders different concrete mixtures' performance over time. This field exposure site is depicted in Figure 65.

Figure 65: West Texas Gypsum Exposure Site

Several untested 4 in x 8 in (100 mm x 200 mm) cylinder cut segments remain from the laboratory physical sulfate attack study presented in Chapter 2. These cut cylinder segments from the same concrete mixtures that were tested in Chapter 2 could be used for a comparison study between sodium sulfate (Na_2SO_4) and sodium carbonate (Na_2CO_3) physical salt attack. Haynes et al. (2010) observed scaling distress on concrete specimens exposed to alternating temperature and humidity cycles that promoted the formation of thermonatrite ($Na_2CO_3 \cdot H_2O$) and natron ($Na_2CO_3 \cdot 10H_2O$). A solubility study was completed on 10, 20, and 30% concentration of the sodium sulfate and sodium carbonate solutions to find a comparable concentration for comparison between the two salts. It was determined that 30% (by mass of solution) sodium sulfate and 20% (by mass of solution) sodium carbonate concentrations should be used in the study, because at those concentrations the salt solutions crystallize at 41°F (5°C) and the salt ions become almost completely dissolved at 104°F (40°C) in the Phase II temperature cycle that was presented in Figure 4 of Chapter 2. This comparison study was not initiated as a result of mechanical issues with the environmental chamber. Since four 4 in x 8 in (100 mm x 200 mm) cylinder segments remain, they should be used for this comparison study to minimize bias between the results of the two different salt studies. Two section A, one section B, and one section C cut cylinder segments remain for the comparison study. The control cylinder cuts that were stored fully submerged in deionized water, which were presented in Chapter 2 can be re-used for a control on the study since no mass loss occurred during testing in Phase I. These cut cylinder segments that remain were used in the ASTM C1202 and ASTM C1585 testing for determining the concrete mixtures permeability and absorption. One of the section A, cut cylinder segment can be fully submerged in each type of solution to allow direct comparisons between the samples.

To fully quantify and capture the physical distress mechanism by sodium sulfate a long term outdoor exposure testing regime is needed. From the testing regime presented in Chapters 2 and 3, the lower the w/cm the more durable a concrete mixture is to physical sulfate attack. However, when using SCMs the reasoning behind why one concrete mixture performs superior to another concrete mixture can get distorted. This outdoor testing regime should contain a 0.40, 0.50, and 0.70 w/cm for each concrete mixture. Also, Type I and Type V cements should be used in straight cement mixtures and mixtures with fly ash, slag, and silica fume with high and low percentages replacement by mass. The addition of SCMs to the concrete mixtures will allow comparisons between permeability and absorption between the concrete mixtures, as well as give guidance to the concrete mixtures that have the best resistance to physical sulfate attack. In this study, large specimens should be cast to better relate to field performance. Over time the different concrete mixtures should be milled millimeter by millimeter to document the sulfate concentration from the base of the specimen to the top surface of the evaporation front. The sulfate testing would start at the base and progress up the evaporation front until no sulfates were present when tested for each concrete mixture. Then this sulfate concentration test would need to be repeated over all the specimens during a short time period and repeated as distress progressed throughout the concrete mixtures. Sulfate concentration measurements should continue at sufficient time intervals to develop the history of sodium sulfate absorption and subsequent capillary rise due to the permeability of the specimens. In addition, concrete specimens should be cast to analyze the absorption and permeability of the different concrete mixtures with various ASTM testing methods.

5.2 ALKALI-SILICA REACTION: ASTM C1293

5.2.1 Conclusions

The purpose of this project is to get a low-alkali concrete mixture to fail the 0.04% expansion limit of ASTM C1293 within one year. To date, the concrete cylinders had better performance for the low-alkali concrete specimen types than the concrete prisms did. These results for the low-alkali concrete cylinders were shown in Table 35. It is clear that several of the 4 in x 8 in (100 mm x 200 mm) concrete cylinder mixtures that were stored at 140°F (60°C) are close to the expansion limit and the newer, repeated low-alkali concrete mixtures appear to be approaching this expansion limit at a faster rate. This is most likely due to the improved cylinder sealing that created a better closed system inside the cylinder molds. Alkali leaching is significant in the first month; therefore this improved cylinder sealing method could be preventative enough to result in failed low-alkali concrete mixtures according to the ASTM C1293 0.04% expansion limit. It would be very interesting to use rigid molds to see if limiting the expansion to one axis would improve the results. The plastic cylinder molds that were used to contain the concrete cylinders are fairly pliable.

In general, the prism mold types appear to have less problems with leaching and resulting increased expansion as the specimen size increases. Currently, the low-alkali concrete mixtures (0.49 Na_2O_e) have minimal expansion activity in all of the concrete prism types. The trends of the varying alkali contents in the prism is expected and systematic between the three specimen sizes. The length change for all the specimens at the varying alkali levels to date was presented in Table 37.

When the testing regime is completed, recommendations will be made on further investigating mold type and setups discussed herein to further quantify low-alkali systems in ASTM C1293. The ASTM C1293 mold type considerations will be:

- Applicability of mold handling
- Ease of modifying and casting mold type
- Strength and ease of pinning molds
- Applicability to jobsite 1293 testing
- Data correlation to exposure blocks
- Length of test to get similar results
- Leaching of samples

5.2.2 Recommendations for Future Work

One test improvement could be to fully quantify the leaching of the different sized specimens. To do this, one could replace the standing water at the bottom of the ASTM C1293 container at every measurement to find the leaching trend throughout the duration of the test. Also, the felt should be replaced at every measurement, so that the water-soluble alkalis could be determined from the old felt and then the total alkali leaching content could be quantified. Another means to quantify the amount of alkalis being leached to the system would be to measure the internal relative humidity inside the ASTM C1293 container over the duration of the test. When more alkalis are added to the system from leaching of the concrete specimens, the relative humidity fluctuates in a sinusoidal manner and this behavior gets more pronounced as more alkalis are added to the system. This idea of different alkali concentrations' effect on the relative humidity inside the ASTM container was previously demonstrated in Section 4.3.

Furthermore, new mold types could be investigated for improving the ASTM standard for low-alkali systems. For example, a five gallon pail mold could be cast with a strain gauge embedded to measure the expansion of the specimen. The larger size of the specimen may be enough to limit alkali leaching. For these large specimens standing water could be placed on the top surface to provide a water source for ASR. In addition, PVC cylinder molds could be created to provide a rigid body to confine the expansion to one direction. The PVC mold could be sealed with standing water and pinned like in this testing regime to provide a rigid structure to better quantify the expansion occurring. Also, the PVC mold could have a strain gauge embedded in it instead of being pinned to analyze the length change in it. Some Schedule 80 PVC piping has a maximum service temperature of 140°F (60°C), therefore use of this material would be recommended.

The incorporation of a SLWA into the concrete mixture might not be appropriate given the LWFA, because some lightweight aggregates contain glassy, aluminosilicates and may react pozzolanically. Also, using a SLWA could somewhat change the response of a concrete mixture with SCMs or the expansion observed. Since SLWA could give pessimum effects, using saturated polymers as an internal water source for ASR should be investigated.

5.3 WORKS CITED

Haynes, H., O'Neill, R., Neff, M., and Mehta, P. K, "Salt Weathering of Concrete by Sodium Carbonate and Sodium Chloride," *ACI Materials Journal,* V. 107, No. 3, May-June, pp. 258-266, 2010.

Appendix: Laboratory Cyclical 30% (by mass of solution) Sodium Sulfate Specimens at End of Test

Figure A-1: 0.40 – I

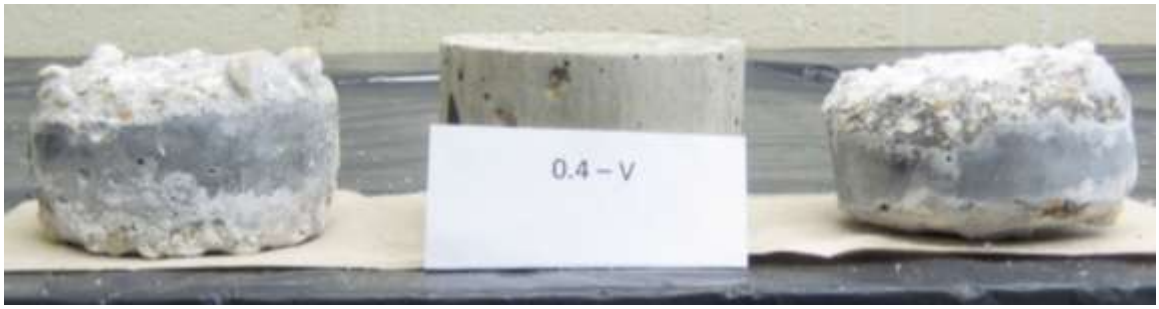

Figure A-2: 0.40 – V

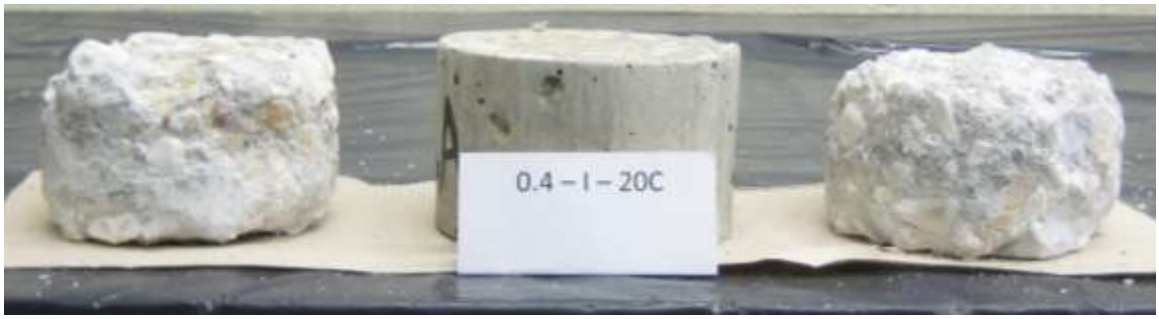

Figure A-3: 0.40 – I – 20C

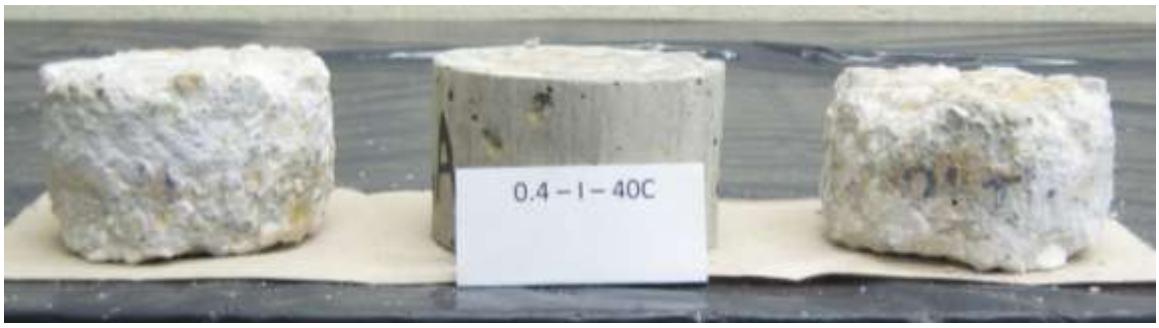

Figure A-4: 0.40 – I – 40C

Figure A-5: 0.40 – I – 20F

Figure A-6: 0.40 – I – 30F

Figure A-7: 0.40 – I – 35S

Figure A-8: 0.40 – I – 50S

Figure A-9: 0.45 – I

Figure A-10: 0.45 – V

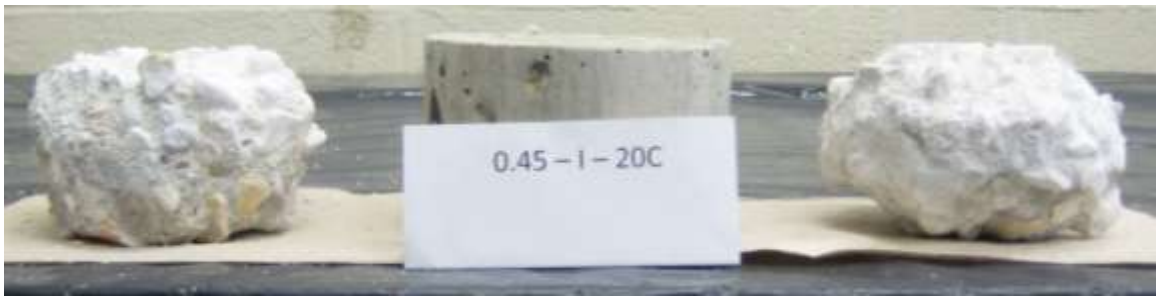

Figure A-11: 0.45 – I – 20C

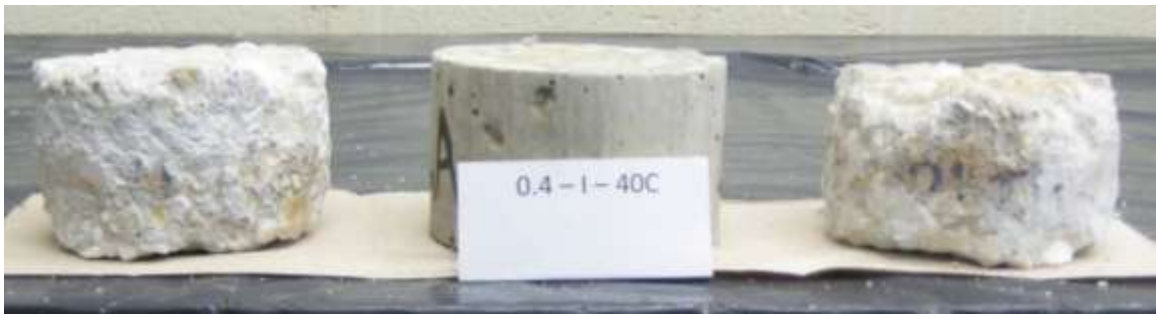

Figure A-12: 0.45 – I – 40C

Figure A-13: 0.45 – I – 20F

Figure A-14: 0.45 – I – 30F

Figure A-15: 0.45 – I – 35S

Figure A-16: 0.45 – I – 50S

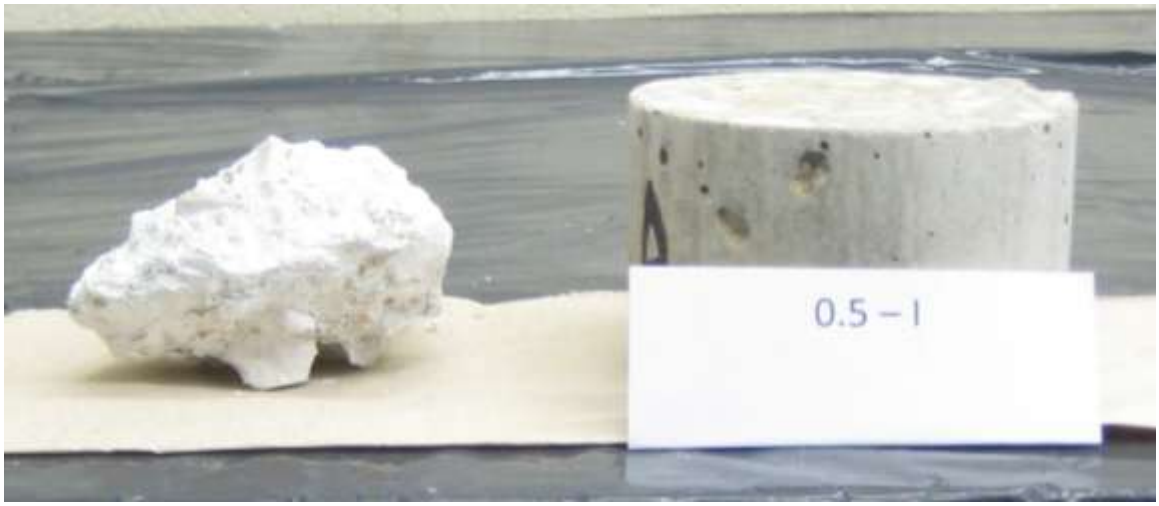

Figure A-17: 0.50 – I

Figure A-18: 0.50 – V

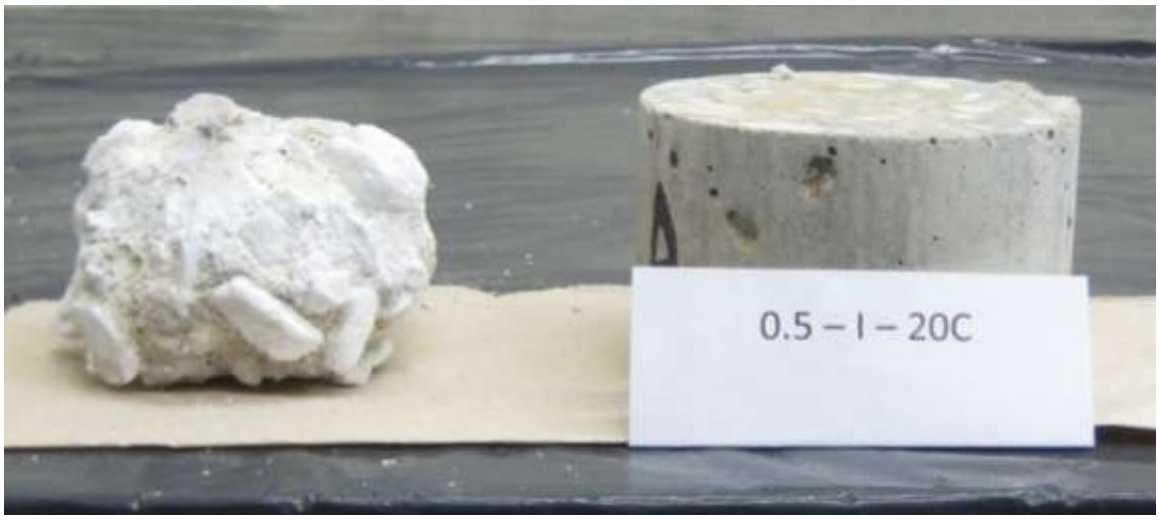

Figure A-19: 0.50 – I – 20C

Figure A-20: 0.50 – I –40C

Figure A-21: 0.50 – I – 20F

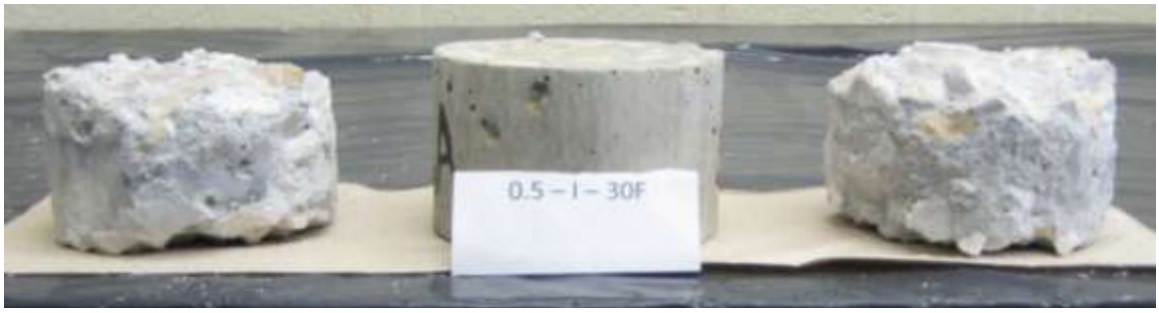

Figure A-22: 0.50 – I –30F

Figure A-23: 0.50 – V –40C

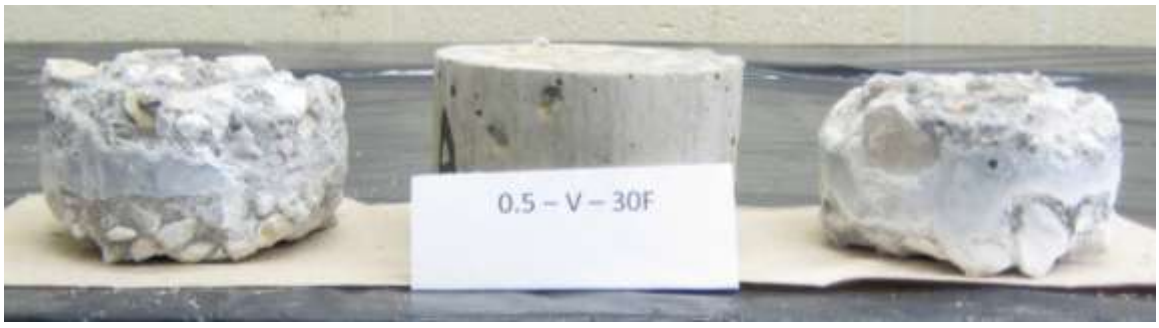

Figure A-24: 0.50 – V –30F

Figure A-25: 0.50 – I – 35S

Figure A-26: 0.50 – I – 50S

Figure A-27: 0.50 – V –50S

Comprehensive Works Cited

ACI 201.2R, "Guide to Durable Concrete." Manual of Concrete Practice, 2001.

ACI 318-08, “Building Code Requirements for Structural Concrete and Commentary” American Concrete Institute. Farmington Hills, MI, 2008.

ASTM C 33, “Standard Specification for Concrete Aggregates,” ASTM International, West Conshohocken, PA, 2009.

ASTM C 138, “Standard Test Method for Density (Unit Weight), Yield, and Air Content (Gravimetric) of Concrete,” ASTM International, West Conshohocken, PA, 2010.

ASTM C 143, “Standard Test Method for Slump of Hydraulic-Cement Concrete,” ASTM International, West Conshohocken, PA, 2010.

ASTM C 150, “Standard Specification for Portland Cement,” ASTM International, West Conshohocken, PA, 2009.

ASTM C 192, “Standard Practice for Making and Curing Concrete Test Specimens in the Laboratory,” ASTM International, West Conshohocken, PA, 2005.

ASTM C 618, “Standard Specification Coal Fly Ash and Raw or Calcined Natural Pozzolan for Use in Concrete,” ASTM International, West Conshohocken, PA, 2008.

ASTM C 672, “Standard Test Method for Scaling Resistance of Concrete Surface Exposed to Deicing Chemicals,” ASTM International, West Conshohocken, PA, 2004.

ASTM C 778, “Standard Specification for Standard Sand,” ASTM International, West Conshohocken, PA, 2006.

ASTM C 1012, “Standard Test Method for Length Change of Hydraulic-Cement Mortars Exposed to a Sulfate Solution,” ASTM International, West Conshohocken, PA, 2004.

ASTM C 1202, “Standard Test Method for Electrical Indication of Concrete’s Ability to Resist Chloride Ion Penetration,” ASTM International, West Conshohocken, PA, 2009.

ASTM C 1240, “Standard Specification for Silica Fume Used in Cementitious Mixtures,” ASTM International, West Conshohocken, PA, 2011.

ASTM C 1260, “Standard Test Method for Potential Alkali Reactivity of Aggregates (Mortar-Bar Method),” ASTM International, West Conshohocken, PA, 2007.

ASTM C 1293, “Standard Test Method for Determination of Length Change of Concrete Due to Alkali-Silica Reaction,” ASTM International, West Conshohocken, PA, 2008.

ASTM C 1585, “Standard Test Method for Measurement of Rate of Absorption of Water by Hydraulic-Measurement of Rate of Absorption of Water by Hydraulic-Cement Concretes,” ASTM International, West Conshohocken, PA, 2004.

Clement, J. C. *Laboratory and Field Evaluations of External Sulfate Attack, Phase II.* Austin, Texas: The University of Texas at Austin, 2009.

Drimalas, T. *Laboratory and Field Evaluations of External Sulfate Attack.* Austin, Texas: The University of Texas at Austin, 2007.

Folliard, K. J., Barborak, R., Drimalas, T., Du, L., Garber, S., Ideker, J., Ley, T., Williams, S., Juenger, M., Thomas, M.D.A., and Fournier, B., “Preventing ASR/DEF in New Concrete: Final Report.” The University of Texas at Austin, Center for Transportation Research (CTR), CTR 4085-5, 2006.

Folliard, K.J. and Sandberg, P., "Mechanisms of Concrete Deterioration by Sodium Sulfate Crystallization," *Proceedings, Third International ACI/CANMET Conference on Concrete Durability*, Nice, France, pp. 933-945, 1994.

Fournier, B., Chevrier, R., de Grosbois, M., Lisells, R., Folliard, K., Ideker, J., Shehata, M., Thomas, M., Baxter, S., “The accelerated concrete prism test (60°C): variability of the test method and proposed expansion limits,” Proc. 12th International Conference on Alkali-Aggregate Reaction in Concrete, Beijing, China, vol. 1, 2004, pp. 314-323.

Haynes, H., O’Neill, R., and Mehta, P.K., “Concrete Deterioration from Physical Attacks by Salts,” *Concrete International*, V.18, No. 1, pp. 63-68, January 1996.

Haynes, H., O’Neill, R., Neff, M., and Mehta, P. K, “Salt Weathering Distress on Concrete Exposed to Sodium Sulfate Environment,” *ACI Materials Journal*, V. 105, No. 1, Jan.-Feb., pp. 35-43, 2008.

Haynes, H., O’Neill, R., Neff, M., and Mehta, P.K., “Salt Weathering of Concrete by Sodium Carbonate and Sodium Chloride,” *ACI Materials Journal*, V. 107, No. 3, May-June, pp. 258-266, 2010.

Hime, W. G., Martinek, R. A., Backus, L. A., and Marusin, S. L. "Salt Hydration Distress." *Concrete International*, V. 23, pp. 43-50, 2001.

Henkensiefken, R., Castro, J., Bentz, D., Nantung, T., Weiss, J. "Water absorption in internally cured mortar made with water-filled lightweight aggregate," *Cement and Concrete Research*, Vol. 39, pp. 883-892, 2009a.

Henkensiefken, R., Nantung, T., Bentz, D., Weiss, J. "Volume Change and Cracking in Internally Cured Mixtures made with Saturated Lightweight Aggregate under Sealed and Unsealed Conditions," *Cement and Concrete Composites*, Vol. 31 (7), pp. 427-437, 2009b.

Ideker, J., East, B., Folliard, K., Thomas, M., Fournier, B., "The current state of the accelerated concrete prism test." *Cement and Concrete Research,* Vol. 40 (4), pp. 550-555, 2010.

Nehdi, M., and Hayek, M., "Behavior of Blended Cement Mortars Exposed to Sulfate Solutions Cycling in Relative Humidity," *Cement and Concrete Research*, V. 35, pp. 731-742, 2005.

Riding, K. A., Poole, J. L., Schindler, A. K., Juenger, M. C., and Folliard, K. J. "Simplified Concrete Resistivity and Rapid Chloride Permeability Test Method." *ACI Materials Journal*, V. 105, No. 4, pp. 390-394, 2008.

Rodriguez-Navarro, C., Doehne, E., and Sebastian, E. "How Does Sodium Sulfate Cyrstallize? Implications for the Decay and Testing of Building Materials." *Cement and Concrete Research*, V. 30, pp. 1527-1534, 2000.

Scherer, G. W. "Stress from Crystallization of Salt." *Cement and Concrete Research*, V. 34, pp. 1611-1624, 2004.

Skalny, J., Marchand, J., and Odler, I. "*Sulfate Attack on Concrete."* London: Spon Press, 2002.

Stark, D., "Longtime Study of Concrete Durability in Sulfate Soils," *Research and Development Bulletin RD086*, Portland Cement Association, Stokie, Ill., p. 13, 1984.

Stark, D., "Durability of Concrete in Sulfate Rich Soils," *Research and Development Bulletin RD 097*, Portland Cement Association, Skokie, Ill., p. 14, 1989.

Stark, D. C. "*Performance of Concrete in Sulfate Environments," RD129.* Skokie, Illinois: Portland Cement Association, 2002.

Stanton, T.E. "Expansion of concrete through reaction between cement and aggregate." *Proceedings of the American Society of Civil Engineers,* Vol. 66, No. 10, pp. 1781-1811., 1940.

Thomas, M. D., Hooton, R. D., & Rogers, C. A. "Prevention of damage due to alkali aggregate reaction (AAR) in concrete construction - Canadian approach." *Cement, Concrete and Aggregates,* Vol. *19* (1), pp. 26-30, 1997.

Thomas, M., Fournier, B., Folliard, K., Ideker, J., & Shehata, M. "Test methods for evaluating preventative measures for controlling expansion due to alkali-silica reaction in concrete." *Cement and Concrete Research,* Vol. *36*, pp. 1842-1856, 2006.

Wehrle, E. *The Effects of Coating and Sealers Used to Mitigate Alkali-Silica Reaction and/or Delayed Ettringite Formation in Hardened Concrete.* Austin, Texas: The University of Texas at Austin, 2010.